A Chemical and Genetic Approach to Study the Polyamine Transport System in Drosophila

2017

Minpei Wang
University of Central Florida

A CHEMICAL AND GENETIC APPROACH TO STUDY THE POLYAMINE TRANSPORT SYSTEM IN *DROSOPHILA*

by

MINPEI WANG

B.S. Sichuan University, 2004

M.S. University of Central Florida, 2010

A dissertation submitted in partial fulfillment of the requirements

for the degree of Doctor of Philosophy in Biomedical Sciences

in the Department of Biology

in the College of Sciences

at the University of Central Florida

Orlando, Florida

Fall Term

2017

Major Professor: Laurence von Kalm

ABSTRACT

Polyamines are small cationic molecules that play important roles in most vital cellular processes including cell growth and proliferation, regulation of chromatin structure, translation and programmed cell death. Cellular polyamine pools are maintained by a balance between biosynthesis and transport (export and import). Increased polyamine biosynthesis activity and an active transport system are characteristics of many cancer cell lines, and polyamine depletion has been shown to be a viable anticancer strategy. Polyamine levels can be depleted by α-difluoromethylornithine (DFMO), an inhibitor of the key polyamine biosynthesis enzyme ornithine decarboxylase. However, malignant cells often circumvent DFMO therapy by up-regulating polyamine import; therefore, there is a need to develop compounds that inhibit polyamine transport. Collectively, DFMO and polyamine transport inhibitors provide the basis for a combination therapy leading to effective intracellular polyamine depletion. Using a *Drosophila* leg imaginal disc model for polyamine transport, I studied three candidate transport inhibitors (Ant444, Trimer44 and Triamide44) for their ability to inhibit transport in the *Drosophila* model. Ant444 and Trimer44 effectively inhibited the uptake of the toxic polyamine analog Ant44 that gains entry to cells via the polyamine transport system. Ant444 and Trimer44 were also able to inhibit the import of exogenous polyamines into DFMO-treated imaginal discs. Triamide44 was an ineffective inhibitor, however a structurally redesigned compound, Triamide444, showed a 50-fold increase in transport inhibition and was comparable to Ant444 and Trimer44. Ant444 and Trimer44 showed differences in their relative abilities to block import of specific polyamines, and I therefore asked if a cocktail of these inhibitors would

be more effective than either alone. My data show that a cocktail of polyamine transport inhibitors is more effective than single inhibitors when used in combination with DFMO, and suggests the existence of multiple polyamine transport systems.

To further the development of effective transport inhibitors it is important to identify components of the transport system. The mechanism of polyamine transport in multicellular organisms including mammals is still unknown. Our laboratory has developed a simple assay to detect components of the transport system using RNAi knockdown and over-expression of candidate genes. However, the assay requires that animals live until the pupal stage of development. Pleiotropic effects of individual gene products following over-expression or knockdown may result in early developmental lethality for reasons unrelated to polyamine transport. Our assay is based on the GAL4/UAS system and involves the use of enhancers driving GAL4 expression (GAL4 driver). GAL4 in turn determines the expression level of UAS-candidate gene constructs (UAS responder). I reasoned that in some cases it might be possible to bypass early lethality by judicious choice of drivers that reduce responder expression, thus permitting survival to the pupal phase. To this end, I used five imaginal disc drivers (30A, 71B, 32B, 69B, and T80) as well as a ubiquitously expressed control driver to over-express and knockdown EGFR and components of the Rho signaling pathway. The relative strength of each driver was ranked, and I was able to demonstrate in principle that animals could survive to later stages of development in a manner that correlated with the relative

strength of the driver. The approach I developed is broadly applicable to other studies of *Drosophila* development.

To identify new components of the polyamine transport system I studied the role of proteoglycans in this process. The proteoglycan glypican-1 has been previously implicated in mammalian polyamine transport. In particular, the heparin sulfate side chains of glypican-1 appear to play an important role. In order to extend our knowledge of the role of proteoglycans in polyamine transport, I examined the role of the core proteoglycans perlecan and syndecan as well as genes encoding enzymes in the heparin sulfate and chondroitin sulfate biosynthetic pathways. I was able to confirm a role for glypican-1 in polyamine transport in imaginal discs but not in whole animals. This may indicate that glypican-1 is not required for polyamine uptake through the gut. Studies of genes encoding perlecan, syndecan and enzymes in the heparin sulfate and chondroitin sulfate biosynthetic pathways did not reveal a role for these genes in polyamine transport. These studies were conducted in whole animals and my data may reflect tissue-specific differences between the imaginal disc and gut transport systems where transport in imaginal discs is proteoglycan dependent and transport in the gut is not.

ACKNOWLEDGMENTS

I would like to thank Dr. Laurence von Kalm for his mentorship and guidance. I would like to thank my committee members, Dr. Otto Phanstiel, Dr. Jack Ballantyne, and Dr. Kenneth Teter, for their time and input. I would like to thank David Jenkins of the Department of Biology and Fanchao Yi for the help with statistical analysis. I would also like to thank my friends and family for their continued support.

TABLE OF CONTENTS

LIST OF FIGURES

LIST OF TABLES

CHAPTER ONE: INTRODUCTION

Polyamines are a family of ubiquitous aliphatic polycations containing two to four amine moieties separated by methylene groups. The native polyamines include putrescine, spermidine and spermine (Figure 1), and are widely distributed in both eukaryotic and prokaryotic cells [1].

Polyamines are essential for many cellular processes (reviewed in Miller-Fleming et al., 2015) [2]. Cell proliferation requires access to a cellular polyamine pool and depletion of cellular polyamines following treatment with the polyamine biosynthesis inhibitor Difluoromethylornithine (DFMO) causes cultured cells to become cytostatic [3]. DFMO acts by inhibiting the activity of ornithine decarboxylase (ODC in figure 1) which catalyzes the first step in the biosynthetic pathway. Polyamines also play a role in transcription. Polyamines primarily bind to RNA in cells and regulate various stages of protein synthesis by modulating the secondary structures of mRNA, tRNA and rRNA [4]. Also, polyamines preferably bind to CG-rich regions of DNA and facilitate DNA condensation, which is inhibited by histone hyperacetylation [5, 6]. These results suggest that polyamines act as transcription repressors *in vivo* by binding to DNA. A role for polyamines in translation is well established. Spermidine is necessary for a unique hypusine modification of eIF5A (eukaryotic initiation factor 5A), a key factor for translation and RNA processing [7]. Programmed cell death is also regulated by polyamines. In several cell lines, apoptosis is activated due to spermine depletion [8]. Moreover, polyamines play important roles in cytoskeletal dynamics. Polyamines regulate the activity of RhoGEFs, which are required

for cell shape change and migration [9]. Polyamines are involved in regulation of signal transduction. Spermidine preferentially stimulates the phosphorylation of p42 and p44 of the Ras/MAPK kinase pathway [10]. Polyamines affect signaling transduction by forming an ATP-Mg^{2+}-spermine complex, which can affect the activity of protein kinase by phosphorylation [11].

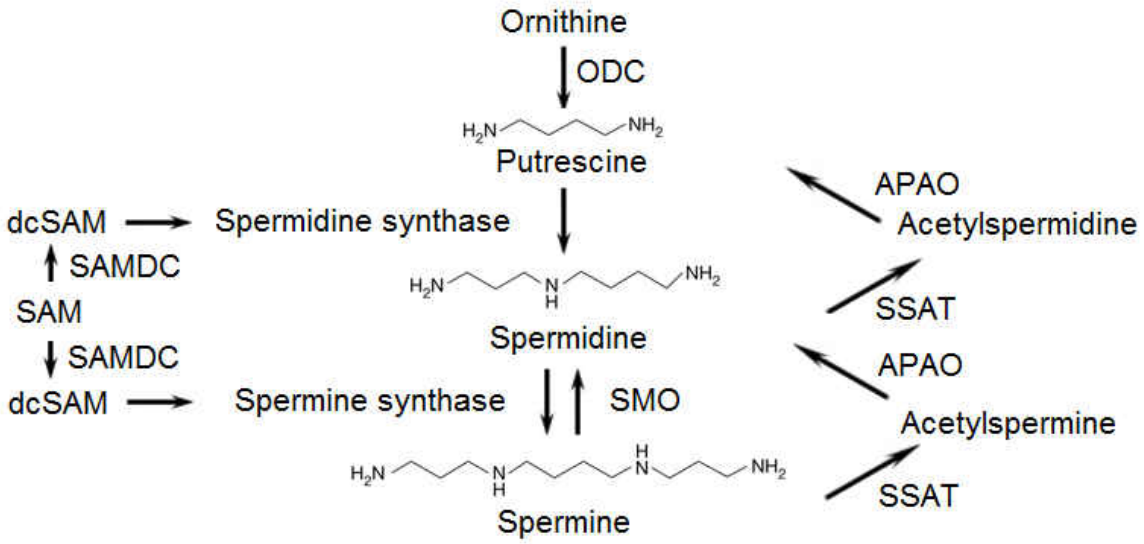

Figure 1 The polyamine biosynthesis and catabolism pathway in eukaryotes (modified from Nowotarski et al., 2013 [12]).

During the first step of polyamine biosynthesis, putrescine is synthesized from ornithine by ornithine decarboxylase (ODC). Then spermidine and spermine are synthesized by spermidine synthase and spermine synthase respectively. *S*-adenosylmethionine (SAM) is converted to decarboxylated SAM (dcSAM) by *S*-adenosylmethionine decarboxylase (SAMDC). dcSAM provides the propyl amine component needed to form spermidine and spermine. Spermine and spermidine can be back converted by spermidine/spermine N^1-acetyltransferase (SSAT) and polyamine oxidase (APAO). Also, spermine can be converted to spermidine directly by spermine oxidase, SMO.

Polyamine Biosynthesis and Catabolism

A balance between biosynthesis, catabolism and import/export of polyamines from/into the extracellular environment is required to regulate intracellular polyamine pools [13]. The polyamine biosynthesis and catabolism pathways have been well documented in both eukaryotic and prokaryotic organisms [2]. In contrast, while the mechanisms of import and export are well understood in single cell prokaryotic and eukaryotic organisms, the transport system is poorly understood in multicellular eukaryotes.

The enzymes involved in polyamine biosynthesis and catabolism are typically present in low abundance, have a rapid turnover rate, and are under tight transcriptional and translational regulation [13]. For example, ODC is the rate-limiting enzyme in the biosynthesis pathway (see Figure 1). ODC expression is controlled at multiple levels including transcription, post-transcriptional processing, translation and altered stability of the protein [14, 15]. In addition, ODC is regulated by ornithine decarboxylase antizyme (OAZ), a unique, nonenzymatic, regulatory protein [16, 17]. Antizyme is synthesized in response to high cellular polyamine levels and binds to ODC, which it then recruits to the 26S proteasome for degradation [18]. Interestingly, OAZ inhibits not only ODC, but also polyamine transport activity suggesting a dual role for this important regulator in polyamine hemostasis [19].

Polyamines and Disease

Polyamines are associated with many human diseases and therefore polyamine biosynthesis, catabolism and transport pathways are attractive therapeutic targets. In this study, we focus on polyamine transport, especially the development of transport inhibitors. Effective polyamine transport inhibitors are needed for treating some parasitic related diseases and human cancers.

1. Polyamines and Parasites

In lower eukaryotes such as the parasitic protozoa *Leishmania* and *Treponema*, the polyamine transport system closely resembles that of bacteria [20, 21]. In general, these parasitic eukaryotes are able to biosynthesize sufficient polyamines to meet their needs and do not have a great reliance on polyamine transport. Therefore, effective therapies against these parasites are primarily focused on inhibition of polyamine biosynthesis. The common drug target is the key biosynthetic enzyme ODC (Figure 1). For example, DFMO, which targets ODC, has been used successfully to treat West African sleeping sickness caused by trypanosomes [22].

In contrast to *Leishmania* and *Treponema*, some parasites do depend on polyamine transport mechanisms for survival. For example, *Plasmodium falciparum*, the malaria parasite, responds to DFMO induced polyamine depletion by up-regulating the polyamine transport system of the host erythrocyte in order to increase the cellular levels of

polyamines [23, 24]. This observation illustrates the need for drugs with the ability to target the polyamine transport system.

Chagas disease affects more than six million people mainly in Latin America and causes premature mortality by cardiac and intestinal damage [25]. There is no effective vaccine or drug with acceptable side-effects available for treatment of this disease [25]. The Chagas' disease parasite, *Trypanosoma cruzi*, lacks an ODC gene and cannot synthesize putrescine, which is needed for spermidine and spermine synthesis [26, 27]. Therefore, *T. cruzi* relies on polyamine transport for survival and DFMO is not useful in treating this disease [28, 29]. In addition, the human SAMDC inhibitor, methylglyoxal-bis (guanylhydrazone) (MGBG), is a poor inhibitor of the *T. cruzi* SAMDC enzyme [30]. Collectively these observations further emphasize the need for effective drugs that target the transport system.

2. Polyamines and Cancer

Polyamines are necessary to sustain rapid cell growth. Many cancer cell types, such as breast, colon, prostate and skin cancer, show elevated intracellular polyamine levels due to up-regulated polyamine biosynthesis and transport [31-34]. Genes in the polyamine metabolic pathway are positively regulated by oncogenes such as c-Myc and Ras, whose expression is frequently altered in cancer [35-38]. These studies suggest that the polyamine biosynthesis and transport pathways are attractive chemotherapeutic targets.

The primary mechanisms malignant cells utilize to increase intracellular polyamine levels are accelerated biosynthesis and active transport of exogenous polyamines into the cell by polyamine transporters [39-42]. Reduction of cellular polyamine content (inhibiting biosynthesis/transport) results in cancer cell growth attenuation [40, 43]. It has been known for more than 40 years that DFMO is a potent inhibitor of polyamine biosynthesis. DFMO has been shown to irreversibly inactivate ODC by formation of enzyme-inhibitor complexes [44] and DFMO has been approved as a chemotherapeutic agent to treat a number of epithelial malignancies [45, 46]. However, cancer cells treated with DFMO frequently circumvent polyamine depletion therapy by upregulating transporter activity several fold to increase import of polyamines from the extracellular environment [47-49]. While the mechanism for transport upregulation is still unknown, the increase of polyamine transport activity is more likely due to an increase of abundance of polyamine transporters than a decrease in the inhibition of transport by antizyme [49-51]. Therefore, a combination treatment simultaneously targeting polyamine biosynthesis and transport is needed to effectively deplete polyamine levels in cancer cells. Although lead compounds that target the transport system have been developed [52-55], the lack of a clear understanding of the molecular nature of the transporter in multicellular eukaryotes is a roadblock to rational drug design. Thus, it is very important to identify the genes and gene products involved in polyamine transport and to determine the mechanism of transport in multicellular cells.

Polyamine Transport

The mechanism of polyamine transport has been studied in different species and cell-types and these studies have established the foundations of polyamine transport as a specific, protein-mediated activity [51, 56]. Polyamine transport has been well characterized in unicellular organisms, such as *Escherichia coli* [57, 58], yeast [59, 60], *Leishmania* [20] and *Treponema* [21]. However, the polyamine transport components in *E. coli* and yeast do not have orthologs in animal cells. In addition, the transport components identified in *Leishmania* and *Treponema* are more related to transporters found in vascular plants [61]. Only a few polyamine transport system (PTS) components have been identified in multicellular eukaryotes [62-65], and it is still unknown how these components interact, or whether they comprise one or more transport systems.

Components of the Mammalian Transport System

1. Glypican-1

Glypican-1 was the first transport-related protein linked to polyamine transport in mammalian cells [62]. Glypican-1 is a core proteoglycan protein and a member of a small family of glycosylphosphatidyl-inositol-anchored cell surface heparan sulfate proteoglycans (HSPG; [66]). In Chinese Hamster Ovary (CHO) cells, polyamines bind with high affinity to heparan sulfate (HS) glycosaminoglycan side-chains [67]. Treatment

of CHO cells with an anti-HS antibody decreases polyamine uptake and attenuates polyamine-dependent cell proliferation [68]. In addition, recycled Glypican-1 is co-localized with spermine, and reduction of Glypican-1 levels inhibits spermine uptake and intracellular delivery of spermine [62]. Collectively, these data indicate that polyamines bind to heparan sulfate glycosaminoglycan side-chains and are then co-transported with Glypican-1 into mammalian cells.

2. Caveolin

Recent work indicates that a dynamin- and caveolae- dependent process is involved in polyamine transport in mammals [63]. In the human colon cancer derived cell line HCT-116, caveolin-1 knock down by antisense RNA leads to significantly increased polyamine uptake suggesting that caveolin-1 is a negative regulator of the transport system. In these colon cells, K-Ras positively regulates polyamine transport by inducing caveolin-1 phosphorylation, which inhibits caveolin-1 leading to an increase in caveolar endocytosis and polyamine transport [63].

3. Solute Carrier Transporter Superfamily Members

The solute carrier (SLC) transporter superfamily comprises 384 members and is the second largest group of membrane proteins in the human genome [69]. So far, seven members of the SLC family have been implicated in polyamine transport (Table 1).

Table 1 SLC superfamily members involved in polyamine transport

Gene	Substrate	Reference
SLC7A1	Put and Spd	Sharpe and Seidel 2005 [64]
SLC12A8	Put, Spd and Spm Amino acids	Daigle et al., 2009 [70]
SLC22A16	PA and BLM-A_5	Aouida et al., 2010 [71]
SLC22A1	Spd and Spm Spd conjugate Agm	Busch et al., 1996 [72] Abdulhussein and Wallace, unpublished work Gründmann et al., 2003; Winter et al., 2011 [73, 74]
SLC22A2	Agm and Put Spd	Winter et al., 2011 [74] Sala-Rabanal et al., 2013 [75]
SLC22A3	Agm Spd	Grundmann et al., 2003 [73] Sala-Rabanal et al., 2013 [75]
SLC3A2	Put	Uemura et al., 2008, 2010 [76, 77]

(Modified from Abdulhussein and Wallace, 2014) [78]. PA: polyamines not specified by author(s), Put: putrescine, Spd: spermidine, Spm: spermine, Agm: agmatine, BLM-A_5: bleomycin A_5.

In rat intestinal epithelial cells, polyamine transport has been linked to the y^+ amino acid uptake pathway [79, 80]. N-ethylmalemide, an inhibitor of the y^+ lysine transport system decreases both lysine and putrescine transport [64]. In this system lysine and putrescine transport is mediated by SCL7A1 (formerly CAT-1), a y^+ transporter [64]. Biochemically the SLC7A1 transporter has similar properties to the general PTS including Na^+ independent and electronegativity dependent activities. However, overexpression of SLC7A1 in a polyamine transport deficient Chinese Hamster Ovary cell line (CHO-MG) is unable to restore polyamine transport activity in this cell line [64]. Therefore, the role of SLC7A1 in polyamine transport remains unclear.

SLC12A8 (also called CCC9A, a variant of CCC9) is a member of the cation-Cl^- cotransporter family and has been proposed to have a role in polyamine transport in human HEK-293 cells [70]. Transport activity is specific to spermidine and spermine with much lower putrescine transport observed. SLC12A8 activity is inhibited by pentamidine, and MGBG, but not paraquat, all of which are potent inhibitors of transport activity [70]. Biochemically, the polyamine transport activity of SLC12A8 in human cells is Na^+, K^+, and Cl^- ion independent, and stimulated by uptake of amino acids such as glutamate and aspartate.

SLC22A16, a member of the SLC22 subfamily (also called OCT/ OAT transporters) has been identified as another potential component of the PTS [71]. SLC22A16 shows high affinity and saturable polyamine transport activity. SLC22A16 recognizes large polyamine

conjugates such as bleomycin A_5, a clinically approved anti-cancer drug. Also, SLC22A16 is able to transport quaternary amino acids, like L-carnitine. As SLC22A16 exhibits a restricted pattern of tissue distribution, it may be required in specific tissues and serve as a backup system for human polyamine transport. Three additional members of the SLC22 family, SLC22A1, SLC22A2 and SLC22A3, show spermidine transport activity [75]. SLC22A2 is also a bidirectional transporter of putrescine [74].

SLC3A2 is reported to be a putrescine exporter in CHO cells [76]. In human cells reduced expression of SLC3A2 is associated with increased putrescine uptake and decreased arginine uptake activity. Additional studies have shown that SLC3A2 can also import putrescine when intracellular polyamine levels are low [77] indicating that SLC3A2 is a bidirectional putrescine transporter. Expression of SLC3A2 is negatively regulated by K-Ras, which actives polyamine transport by facilitating caveolar endocytosis [63]. Moreover, SLC3A2 co-localizes with spermidine/ spermine N^1- acetyltransferase (SAT1) and therefore may be involved in excretion of acetylated polyamines [76].

4. Non- Mammalian Components of the Polyamine Transport System

In *Arabidopsis*, the LAT (L-type amino acid transporter) family is responsible for polyamine transport. There are at least five LAT family members in *Arabidopsis* and three of them are involved in polyamine transport [81]. The RMV1/AtLAT1/AtPUT3 protein is the polyamine transporter on the plasma membrane [82]. AtLAT3/AtPUT1 and PAR1/AtLAT4/AtPUT2 are involved in polyamine transport in the endoplasmic reticulum

and golgi apparatus respectively [83]. An RMV1 knockout mutant showed no change on polyamine uptake suggesting that in addition to RMV1/AtLAT1, there are other unknown polyamine transporters on the plasma membrane [82].

A forward genetic analysis for genes in *C. elegans* encoding resistance to the toxic effects of norspermidine has revealed an additional component of a multicellular PTS [65]. In this study, genetic analysis showed that resistance to norspermidine and uptake of a toxic fluorescent polyamine-conjugate were dependent on the transport protein CATP-5. CATP-5 is a P_{5B}-type ATPase associated with the plasma membrane and is expressed in the apical membrane of intestinal and excretory cells. *C. elegans* double mutants for CATP-5 and ODC show greatly reduced levels of putrescine and spermidine compared to single mutants and wild type animals. Double mutants also show reduced brood size, shortened life span and small body size, consistent with a key role in the PTS. Recently, my lab has identified a P_{5B}-type ATPase as a polyamine transport component in *Drosophila* (Barnett, Brown and von Kalm unpublished data). Whole animals expressing RNAi targeting this P_{5B}-type ATPase have reduced viability when treated with DFMO and exogenous polyamines indicating that the transport system is impaired in these animals. In contrast, DFMO inhibition of development was fully rescued by exogenous polyamine in the control animals. These data suggest that this P_{5B}-type ATPase is required for polyamine transport in *Drosophila*. The human ortholog of CATP-5 is ATP13A3. The protein expression level of ATP13A3 is increased in the presence of DFMO. siRNA against ATP13A3 in DFMO treated L3.6pl human pancreatic cancer cells, is associated with significantly reduced ability to be rescued by exogenous spermidine [84] suggesting

that ATP13A3 plays a role in polyamine import. In addition, cells with high expression of ATP13A3 have high polyamine uptake activity. Another human P_{5B}-type ATPase, ATP13A2, has also been shown to have a role in spermidine uptake [85].

Models for Polyamine Transport

Poulin summarized the main published studies of polyamine transport and proposed three models to explain them (Figure 2) [61]. While connections between the models have not been established it is quite possible that they are not mutually exclusive. A common theme emerging from all three models is that polyamine transport in multicellular organisms can be divided into two steps: binding and transport on the membrane followed by intracellular sorting and transport.

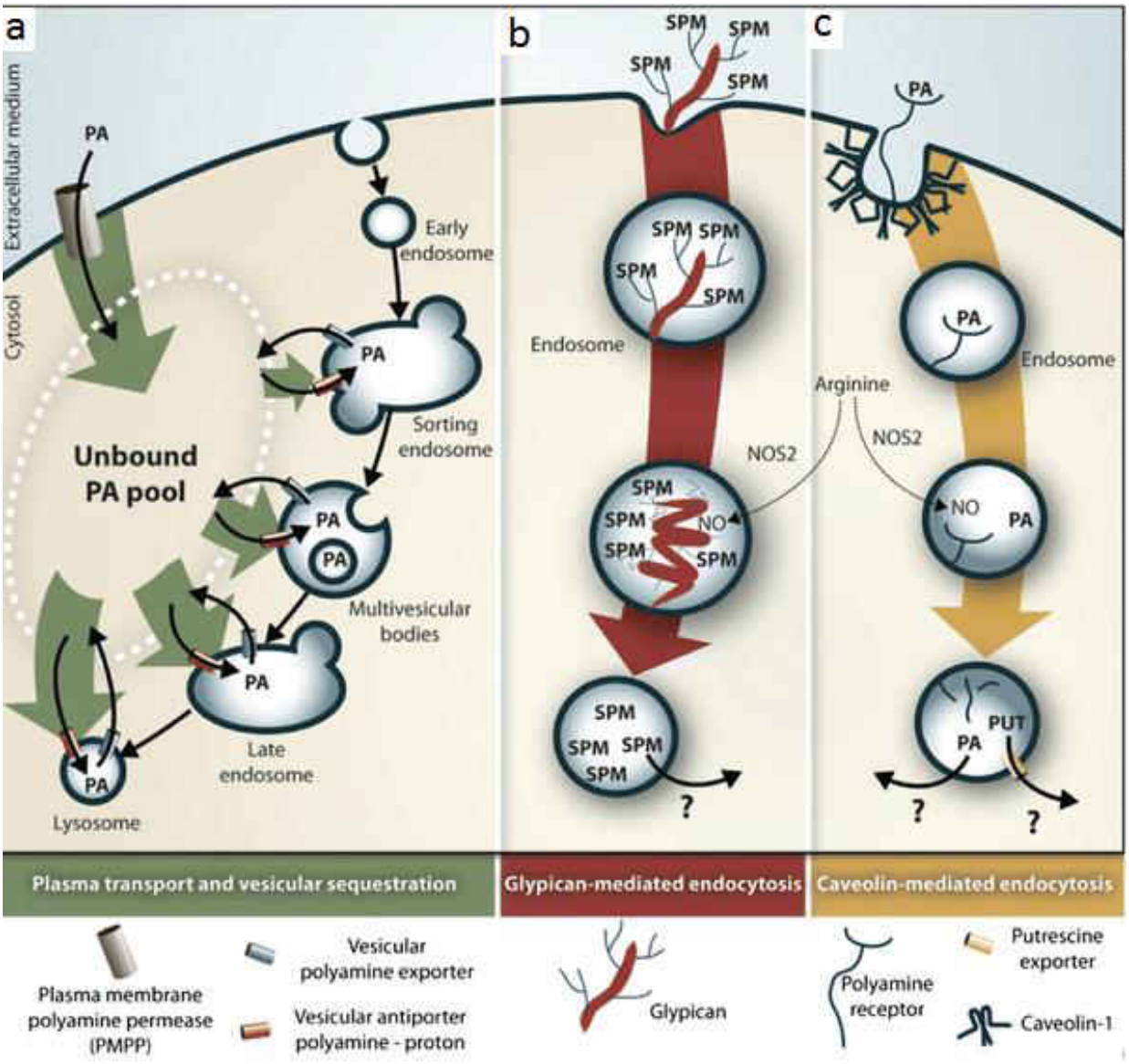

Figure 2 Putative polyamine transport models in mammalian cells (Modified from Poulin et al 2012) [61].

a: model based on Soulet et al. 2004 [86]. b: model based on Belting et al. 2003 [62]. c: model based on Uemura et al. 2010 [77].

NOS2: nitric oxide synthase-2, PA: polyamines, PUT: putrescine, SPM: spermine.

The model in figure 2a is based on the work of Soulet and colleagues who studied the uptake of fluorescently labeled polyamine analogues with specificity for the PTS [86]. In this model polyamines are first imported into the cytosol and then rapidly sequestered into polyamine sequestering vesicles (PSVs). Soulet et al. proposed the existence of two types of polyamine transporters with different cellular localizations. The first is located on the cell membrane (plasma membrane polyamine permease (PMPP) in Figure 2a). Transport involving PMPP would be driven by a steep inward polyamine gradient. In addition to cell membrane associated transport Soulet et al. also proposed the existence of a H+-coupled vesicular polyamine exporter/antiporter responsible for sorting free polyamine from the cytosol into small membrane-bound intracellular PSVs utilizing a proton/polyamine exchange mechanism. PSVs are acidic vesicles of the late endocytotic compartment which includes multivesicular bodies, late endosomes and lysosomes.

The second model (Figure 2b) is based on Belting et al., 2003 [62] and is specific to spermine transport. In this model, spermine binds to the heparan sulfate side chain of HSPG with Glypican-1 as core protein. Polyamine uptake was blocked when cells were treated with heparan sulfate antibody [68]. The binding of spermine triggers receptor mediated endocytosis and HSPG is internalized with spermine into the cell. Following release of nitric oxide by Nitric oxide synthase (NOS), the heparan sulfate side chain is cleaved off the core Glypican-1 protein, followed by release of spermine from the heparan sulfate side chain [62]. How spermine is then released from the vesicle is still unknown.

Uemura et al., 2010 [77] proposed a model similar to the HSPG model in which polyamines bind to an unknown receptor on the cell membrane which triggers caveolin-1 mediated endocytosis (Figure 2c). K-Ras positively regulates polyamine transport by inducing the phosphorylation and inhibition of caveolin-1 leading to an increase in caveolar endocytosis and polyamine transport [63]. In the subsequent endocytic sorting process nitric oxide triggers release of polyamines from the receptor. The mechanism of polyamine release from these caveolin-dependent endosomes is unknown. Putrescine export on the plasma membrane is under the control of SLC3A2 [76]. SLC3A2 expression is negatively regulated by K-Ras and suppressed in human HCT116 colon cancer cells [76]. This suggests that when putrescine concentration is high, cells may respond by decreasing caveolin-1 mediated polyamine import and activate putrescine export via inactivation of K-Ras. In contrast, when intracellular putrescine concentration is low, SLC3A2 can import putrescine by an unknown mechanism [77].

Coordination of Polyamine Biosynthesis and Transport

Polyamine transport is tightly regulated, however, the mechanism by which this occurs is largely unknown. As discussed above, polyamine transport activity is regulated by antizyme (OAZ), which also regulates polyamine biosynthesis. Thus, OAZ may play a critical role in the balance between biosynthesis and transport of polyamines to maintain cellular polyamine homeostasis. OAZs are phylogenetically widespread occurring in organisms ranging from fungi to metazoans. All three of the OAZ genes found in

mammals have similar activities in that they repress ODC activity and polyamine transport [87, 88]. The mechanism of OAZ regulation of polyamine transport is currently unknown.

Antizyme inhibitors (AZIN) have also been reported. AZINs have high binding affinity for OAZs and are activators of polyamine transport [87]. AZINs are also able to induce ODC activity [87]. In the Paju cell line (a human neural-crest-derived tumor cell line) AZINs are localized to the trans-Golgi network where they are involved in vesicular membrane trafficking, the proposed pathway for polyamine internalization [89]. Both OAZ and AZIN proteins have short half-lives allowing the regulatory system to adapt quickly to necessary adjustments in intracellular polyamine concentration.

Using *Drosophila* as a Model for Polyamine Transport

Although a few components of the mammalian PTS have been identified, it is currently unclear how the different components interact if at all, or how many different polyamine pathways are involved. In order to obtain a clearer idea of the molecular nature of the PTS, additional components of a multicellular eukaryotic transporter must be identified. *Drosophila* is a good model system in which to address this problem. Studies in *Drosophila* have been the foundation for characterization of numerous mammalian signaling pathways such as Wnt, Hedgehog and Notch signaling pathways [90-92]. Polyamine transport is active in *Drosophila* S2 cells [93], and our own work has demonstrated that polyamine transport into an intact developing *Drosophila* epithelium is similar to that observed in mammalian CHO and L1210 cells [94]. In the latter experiments

a leg imaginal disc epithelium with all cell-cell contacts and extracellular matrix intact was incubated in *in vitro* culture with a series of polyamine-drug conjugates that exhibit varying degrees of ligand specificity for the polyamine transporter. The profile of sensitivity of *Drosophila* leg imaginal discs to the polyamine-drug conjugates was very similar to that observed in mammalian cells. Thus, the imaginal disc assay is useful for further characterization of compounds that target the transporter in an intact epithelial tissue, and can be used to identify novel components of the transport process. An improved understanding of the PTS in *Drosophila* will further our understanding of the polyamine transport mechanism in mammals, and contribute to rationale design of drugs that target the PTS in malignant cells.

Drosophila Imaginal Discs

One of the most intriguing events in the development of *Drosophila* is metamorphosis [95]. During this process, most larval tissues undergo programmed cell death and adult tissue/structures and organs form from imaginal discs. Imaginal discs are clusters of cells set aside in the embryo that are pre-destined to form specific adult epithelial structures such as wings, legs, eyes and internal organs (Figure 3). Imaginal discs grow by cell division during larval development. Mature imaginal discs in late larvae are single cell thick sac-like epithelial organs. In response to appearance of the steroid hormone 20-hydroxyecdysone which signals the onset of metamorphosis, imaginal discs begin development into adult structures and organs while larval tissues undergo programmed cell death.

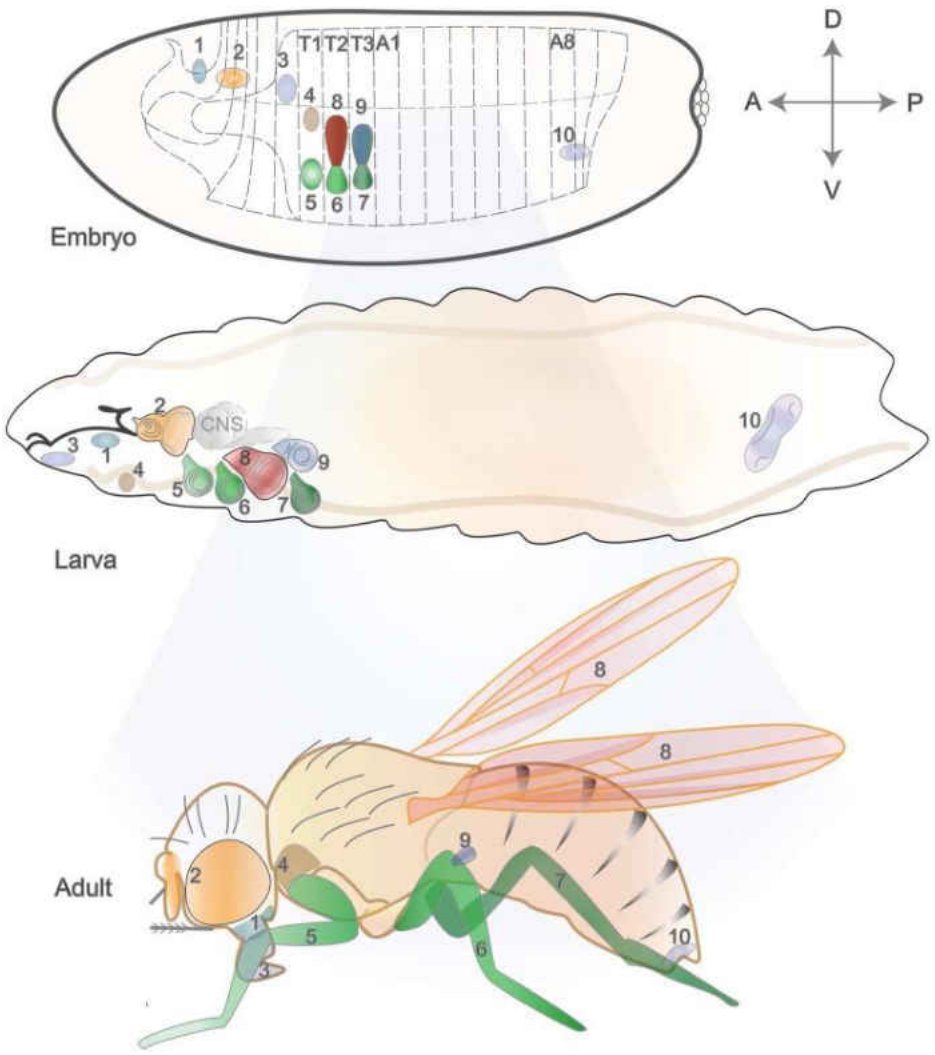

Figure 3 Related imaginal disc primordia in the *Drosophila* embryo and larva and their respective fates in the adult [96].

Top: related primordia of imaginal discs in the embryo. Middle: imaginal discs in larva. Bottom: structures derived from imaginal discs in the adult. Imaginal discs: clypeolabral discs (1); eye-antennal discs (2); labial discs (3); prothoracic discs (4); leg discs (5-7); wing discs (8); haltere discs (9); genital disc (10).

Drosophila leg imaginal discs are well suited for use in this study. The genetics and cell biology of their development is well understood [97]. Leg imaginal discs can be dissected

from late larvae and cultured *in vitro* where, in the presence of 20-hydroxyecdysone, they develop into rudimentary legs (Figures 4a, b). Leg imaginal discs can be used to study the behavior of polyamine transporter ligands (e.g. Tsen et al., 2008 [94]; Figure 4c) and polyamine transport inhibitors (this study). A major advantage of the leg imaginal disc system over mammalian cell culture is that cells are studied in their natural environment with cell-cell contacts preserved and surrounded by extracellular matrix. In addition, the imaginal disc system provides an inexpensive approach to early testing of promising lead compounds and can be used to identify genes involved in polyamine transport.

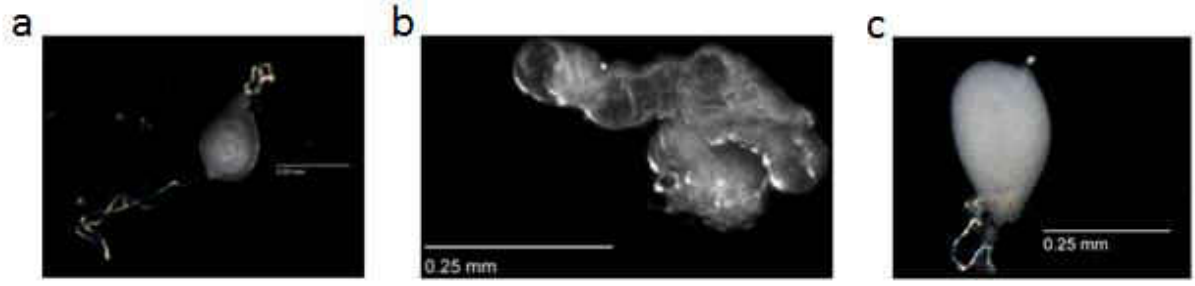

Figure 4 Leg imaginal discs cultured *in vitro*.

a. dissected, undeveloped leg imaginal disc; b. developed leg imaginal disc after treatment with 20-hydroxyecdysone for 18 hours. c. undeveloped leg imaginal disc after treatment with 20-hydroxyecdysone and the toxic polyamine analog Ant44 for 18 hours. Ant44 enters cells via the PTS [94]. All figures were taken under regular light.

Aims of This Dissertation

Depletion of cellular polyamine content results in cancer cell growth attenuation. A combination drug therapy that simultaneously targets polyamine biosynthesis and

transport is desirable. Even though DFMO is a potent inhibitor of polyamine biosynthesis, cancer cells treated with DFMO frequently circumvent polyamine depletion therapy by elevating transporter activity to increase import of polyamines from the extracellular environment. To address this need to develop compounds that inhibit polyamine transport, we have developed a *Drosophila* assay that can be used for early testing of potential transport inhibitors. Specifically, the *Drosophila* imaginal disc assay is useful for characterization of compounds that target the transporter in an intact epithelial tissue, and can be used to identify novel components of the transport process. In this dissertation, several putative polyamine transport inhibitors were successfully tested in *Drosophila* imaginal discs. Also, I attempted to identify additional polyamine transport components in *Drosophila* to further our understanding of the polyamine transport mechanism in mammals.

Aim 1: Early Stage Animal Model Testing of Inhibitors Targeting Polyamine Transport.

Small molecules that inhibit polyamine transport in a *Drosophila* multicellular system were assayed. The work led to the identification of two new polyamine transport inhibitors. A major finding was that the inhibitors have different specificity profiles for the native polyamines putrescine, spermidine and spermine suggesting the existence of multiple transport systems. This conclusion is reinforced by the observation that a cocktail of polyamine transport inhibitors is more effective at inhibiting transport than individual compounds alone.

Aim 2: A Tool Kit for Expressing and Identifying Genes Required for Polyamine Transport.

In order to identify genes required for polyamine transport, it is necessary to knock down and overexpress vital genes which may lead to lethality. A set of reagents was developed that can be used to avoid lethality when performing knock down and overexpression of vital genes. The reagents are broadly applicable to studies of development in *Drosophila*.

Aim 3: Genetic Characterization of the Role of Proteoglycans in Polyamine Transport.

I hypothesize that heparan sulfate proteoglycans (HSPG) are required for polyamine transport in *Drosophila*. Mutation or RNAi knockdown of genes encoding proteoglycan core proteins (glypican, syndecan, and perlecan) and enzymes involved in HSPG biosynthesis were tested for involvement of polyamine transport in imaginal discs and intact animals. The results suggest tissue-specific differences in the polyamine transport system.

CHAPTER TWO: EVALUATION OF POLYAMINE TRANSPORT INHIBITORS IN A *DROSOPHILA* EPIPHILIAL MODEL SUGGESTS THE EXISTENCE OF MULTIPLE TRANSPOR SYSTEMS

This chapter has been previously published in Medical Sciences on November 14th, 2017.

Author names: Minpei Wang, Otto Phanstiel, Laurence von Kalm.

Abstract

Increased polyamine biosynthesis activity and an active polyamine transport system are characteristics of many cancer cell lines and polyamine depletion has been shown to be a viable anticancer strategy. Polyamine levels can be depleted by difluoromethylornithine (DFMO), an inhibitor of the key polyamine biosynthesis enzyme ornithine decarboxylase (ODC). However, malignant cells frequently circumvent DFMO therapy by up-regulating polyamine import. Therefore, there is a need to develop compounds that inhibit polyamine transport. Collectively, DFMO and a polyamine transport inhibitor (PTI) provide the basis for a combination therapy leading to effective intracellular polyamine depletion. We have previously shown that the pattern of uptake of a series of polyamine analogues in a *Drosophila* model epithelium shares many characteristics with mammalian cells, indicating a high degree of similarity between the mammalian and *Drosophila* polyamine transport systems. In this report, we focused on the utility of the *Drosophila* epithelial model to identify and characterize polyamine transport inhibitors. We show that a previously identified inhibitor of transport in mammalian cells has a similar activity profile

in *Drosophila*. The *Drosophila* model was also used to evaluate two additional transport inhibitors. We further demonstrate that a cocktail of polyamine transport inhibitors is more effective than individual inhibitors, suggesting the existence of multiple transport systems in *Drosophila*. Our findings reinforce the similarity between the *Drosophila* and mammalian transport systems and the value of the *Drosophila* model to provide inexpensive early screening of molecules targeting the transport system.

Introduction

The common native polyamines (putrescine **1**, spermidine **2** and spermine **3**; Figure 5) are a family of ubiquitous low molecular weight organic polycations containing two to four amine moieties separated by methylene groups. In eukaryotes, polyamines are essential for a variety of cellular processes including cell proliferation, transcription, translation, apoptosis and cytoskeletal dynamics [4, 35, 98, 99]. Polyamines can also bind to intracellular polyanions including nucleic acids and ATP, as well as specific proteins such as N-methyl-d-aspartate receptors and inward rectifier potassium ion channels to regulate their functions [5, 100-102].

A balance between biosynthesis, degradation and transport of polyamines is required to maintain polyamine homeostasis [13, 51, 103, 104] and an increased intracellular polyamine content due to increased biosynthesis and transport activity is a hallmark of

many types of malignant cells [3, 46, 105]. Difluoromethylornithine (DFMO **4**; Figure 5) is an inhibitor of polyamine biosynthesis and has been used in the treatment of several cancers [3, 46]. DFMO binds irreversibly to ornithine decarboxylase (ODC), the rate limiting enzyme of the polyamine biosynthetic pathway, resulting in the proteasomal degradation of ODC [105]. The clinical effectiveness of DFMO, however, is often limited due to the up-regulation of the polyamine transport system (PTS) to access polyamines from the extracellular milieu [106, 107]. To this end, there is a need to develop compounds that inhibit polyamine import. Use of polyamine transport inhibitor compounds with DFMO should simultaneously inhibit biosynthesis and transport, and efficiently deplete polyamine pools in malignant cells.

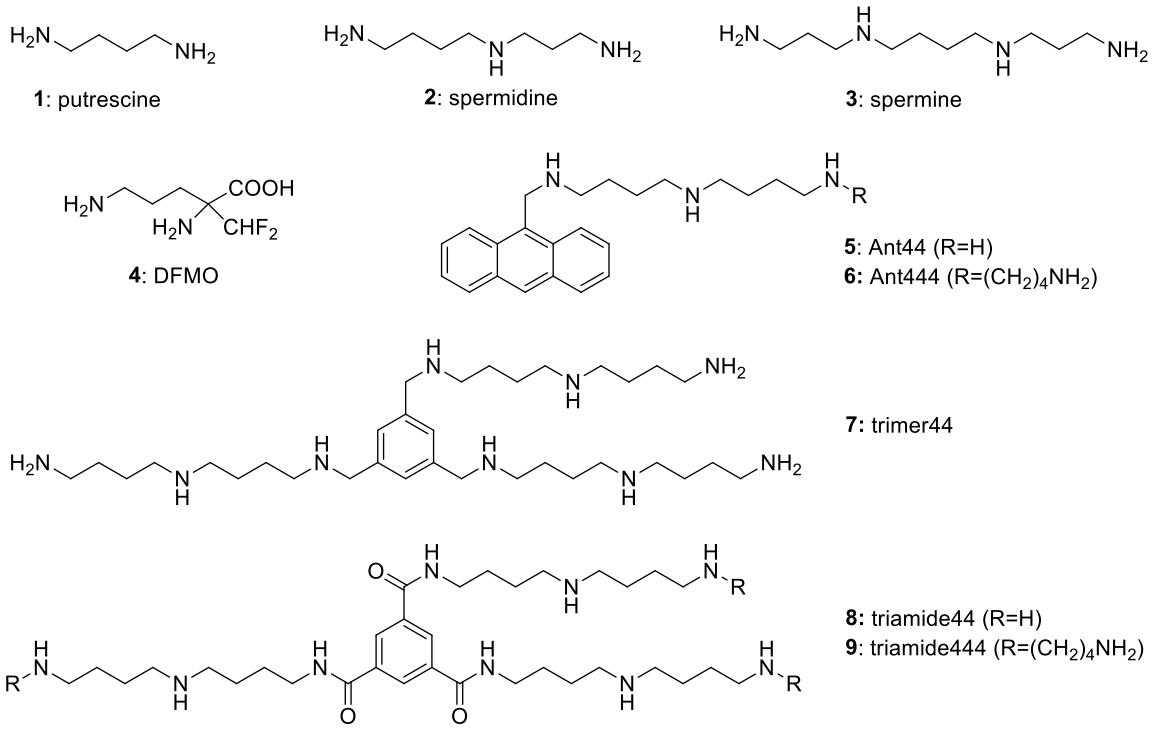

Figure 5 Structures of the native polyamines (**1**–**3**), difluoromethylornithine (DFMO) (**4**), polyamine analogue (**5**) and candidate polyamine transport inhibitors (PTIs; **6**–**9**).

The mechanism of polyamine transport has been well characterized in unicellular organisms, such as *Escherichia coli* [57, 58], yeast [59, 60], *Leishmania* [20] and *Treponema* [21]. In contrast, in multicellular animals only a few PTS components have been identified [62-65, 71, 76, 108-111] and it is not understood how these components interact, or whether they comprise one or more transport systems. The current understanding has been reviewed by Poulin et al., where evidence for three models is presented [61]. In one model, cell surface glypican-1-anchored heparan sulfate proteoglycans capture extracellular polyamines and these complexes are then endocytosed into endosomes [62]. A second model involves caveolin-mediated endocytosis of polyamines via an unknown receptor [77]. In both the glypican-1 and caveolin-mediated models the sequestration of polyamines into endosomes is followed by nitric oxide-mediated release of polyamines from these vesicles. A third model proposes that an energy-dependent cell-surface transporter/channel allows entry of free polyamines into the cytosol and that these are rapidly sequestered into the endosomal sorting pathway, where they are stored or trafficked to specific cellular locations as needed [86]. In reality, none of these models are mutually exclusive and the PTS may well be a combination of all three.

In previous work, we reported a novel assay to study polyamine transport in *Drosophila* leg imaginal discs [94]. Leg imaginal discs are the embryonic and larval precursors of adult legs. In the larval stage prior to adult development, imaginal discs exist as a single-cell-thick folded epithelium. In response to exposure to the steroid hormone ecdysone at

the onset of metamorphosis, they rapidly develop into rudimentary legs (see Figure 6) [97]. Using the *Drosophila* assay we directly compared a series of toxic polyamine ligands for their PTS selectivity in *Drosophila* and mammalian cells. The behavior of the polyamine compounds in imaginal discs was very similar to their behavior in mammalian cell culture, suggesting broad similarities between the PTS of *Drosophila* and mammals. A major advantage of the leg imaginal disc assay is that compounds that access cells through the PTS or inhibit transport can be studied in an environment where cells exhibit normal adhesion properties and are surrounded by extracellular matrix. Thus, the *Drosophila* assay potentially provides an inexpensive animal model for early testing of compounds targeting the PTS.

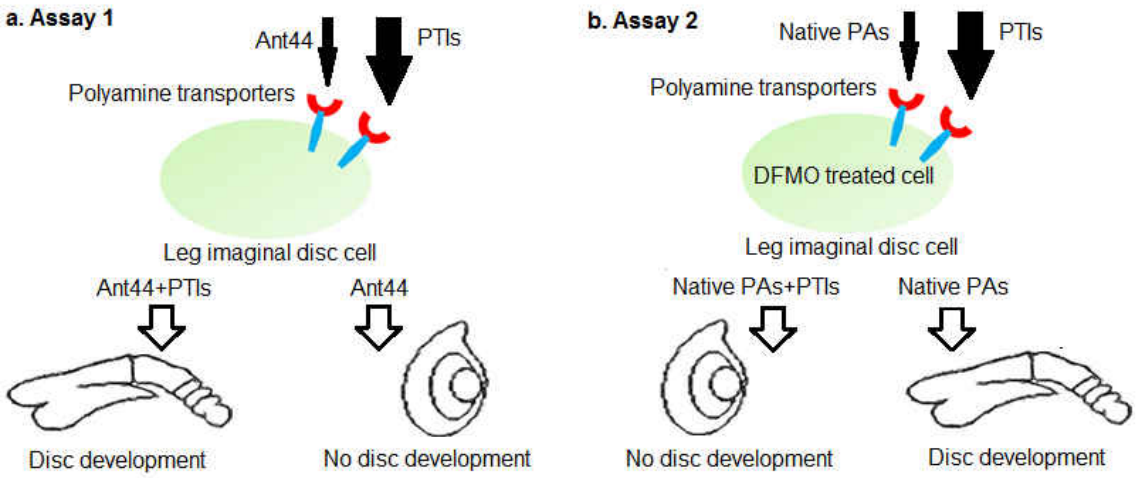

Figure 6 *Drosophila* assays used to characterize polyamine transport inhibitors. Native PAs: native polyamines; PTIs: polyamine transport inhibitors.

a. Assay 1: undeveloped leg imaginal discs were incubated with ecdysone to promote development. In the presence of Ant44 (**5**), a toxic polyamine analog that targets the transport system, leg imaginal discs will not develop. The ability of candidate PTIs to rescue development of imaginal discs treated with Ant44 (**5**) was then assayed by

monitoring and scoring the leg development process. b. Assay 2: leg imaginal discs treated with DFMO fail to develop in the presence of ecdysone. Uptake of exogenous native polyamines can rescue DFMO inhibition of disc development. The ability of candidate PTIs to block rescue of disc development in the presence of DFMO and native polyamines was tested.

In this study, we identified and characterized two compounds that act as polyamine transport inhibitors in *Drosophila*. We also demonstrated that a cocktail of polyamine transport inhibitors was more effective than individual inhibitors, suggesting the existence of multiple transport systems in *Drosophila*.

Results

In order to identify PTIs using the *Drosophila* assay, we selected four compounds for study. Ant444 (**6** in Figure 5) is a N1-anthracenylmethyl substituted polyamine that binds tightly to the surface of mammalian A375 cells with high affinity for the PTS, which suggests that it could be an effective transport inhibitor [52]. However, the ability of this compound to inhibit polyamine transport has never been directly demonstrated. We also tested Triamide444 (**9** in Figure 5), a compound with relatively high toxicity in Chinese Hamster Ovary (CHO) and human pancreatic cancer L3.6pl cells, which precluded an analysis of its transport inhibitory properties in these cell lines. Trimer44 (**7** in Figure 5) has been previously shown to be an effective inhibitor of spermidine uptake in the presence of DFMO in mammalian L3.6pl cells [112, 113]. Triamide44 (**8** in Figure 5) was previously shown to be a poor transport inhibitor [113]. We, therefore, used the transport inhibition properties of Trimer44 (**7**) and Triamide44 (**8**) as a baseline for comparison to

Ant444 (**6**) and Triamide444 (**9**). Armed with these molecular tools, we assessed their ability to perform as PTIs in the *Drosophila* model.

1. *Compounds Ant444 (**6**) and Triamide444 (**9**) Block the Toxicity of the Polyamine Analog Ant44 (**5**) that Gains Entry to Cells via the PTS.*

In the first experiments, all compounds were tested in two different *Drosophila* assays. In Assay 1, these compounds were tested for their ability to block toxicity of a polyamine analogue, Ant44 (**5**, Figure 5), which gains access to leg imaginal disc cells via the polyamine transport system (Figure 6a) [52, 94]. At the concentrations of Ant44 (**5**) used in our experiments (40-50 μM), fewer than 10% of imaginal discs develop. We hypothesized that an effective PTI would inhibit Ant44 uptake or release, and thus reduce the toxicity of Ant44 (**5**) and permit development of leg imaginal discs. A potential caveat of this approach is that a toxic PTI compound would generate a false negative result in this assay. Therefore, it was critical that we first determine the highest dose of PTI compound that could be used without toxicity to avoid biasing the results.

Addition of Ant444 (**6**) and Triamide444 (**9**) at non-toxic concentrations to the assay showed significant rescue of imaginal disc development in the presence of Ant44 (**5**) (Figure 7 a, b). Their effectiveness as PTIs was ranked via determination of EC_{50} values. The EC_{50} value was defined as the effective concentration of the compound which

decreased the inhibition of disc development by Ant44 (**5**) to 50% of the untreated control value (i.e., 50% inhibited). For both Ant444 (**6**) and Triamide444 (**9**) the EC_{50} values (3.6 and 2.8 μM, respectively) were 10 to 15-fold lower than the concentration of Ant44 (**5**, e.g., 40-50 μM) used in the assays. Maximum protection from Ant44 was observed at 10 μM **6** and 5 μM **9**, respectively. These activity profiles are similar to Trimer44 (**7**) which is an effective transport inhibitor in mammalian Chinese Hamster Ovary (CHO) and L3.6pl cells (Figure 7c) [113]. In contrast, Triamide44 (**8**) was a less effective PTI in the *Drosophila* model with an EC_{50} of 144 μM and gave maximum protection at 300 μM (Figure 7d). These observations are consistent with similar findings in mammalian L3.6pl cells [113].

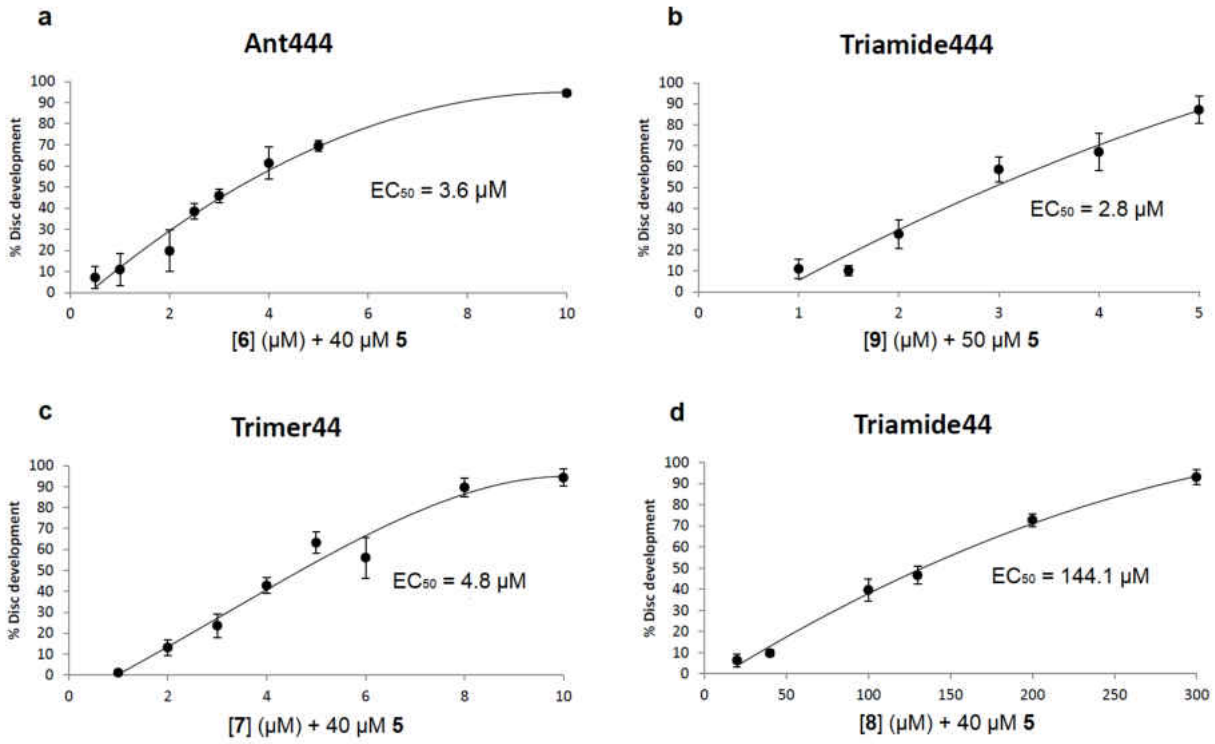

Figure 7 Compounds Ant444 (**6**) and Trimer444 (**9**) are effective PTIs whereas Triamide44 is not.

Candidate PTIs Ant444 (**6**) and Triamide444 (**9**) were tested in the presence of a toxic concentration of Ant44 (**5**) that by itself permitted the development of fewer than 10% of imaginal discs. The percentage of imaginal discs that developed was determined for each PTI concentration tested. All assays were repeated at least in triplicate. Error bars reflect the standard error of the mean (SEM). a-d. Respective dose-response curves of a. Ant444 (**6**), b. Triamide444 (**9**), c. Trimer44 (**7**) and d. Triamide44 (**8**) in blocking the inhibitory effect of Ant44 (**5**) on imaginal disc development. Note: the EC_{50} value is the concentration of the compound needed to block 50% of the inhibitory effect of Ant44 (**5**) on imaginal disc development.

2. *Ant444 (**6**) and Triamide444 (**9**) Are More Effective Than the Native Polyamines in Inhibiting the Toxicity of Ant44 (**5**) in Imaginal Discs*

Compounds containing recognizable polyamine sequences should be able to compete for access to the polyamine receptor on the cell surface. Our previous work has shown

that spermidine is able to inhibit the toxicity of Ant44 (**5**) on mammalian cells and *Drosophila* leg imaginal discs by competing for binding and transport via the PTS [94]. In the present study, the efficiencies of the native polyamines (spermidine and spermine) in rescuing disc development from a toxic concentration of Ant44 (**5**) were evaluated in Assay 1 (Figures 6a and 8a, b). As shown in Figure 8a, the EC_{50} of spermidine was 43.6 μM and complete rescue of imaginal disc development was observed at 80 μM. In contrast, the EC_{50} values of Ant444 (**6**) and Triamide444 (**9**) are 3.6 μM and 2.8 μM, respectively (Figure 7a, b). In short, compounds **6** and **9** were approximately 12-15 times better than spermidine in inhibiting the toxicity of Ant44 (**5**).

Spermine - a native tetraamine - was more effective than spermidine in blocking Ant44 (**5**) inhibition of imaginal disc development with an EC_{50} value of 19.7 μM and afforded complete protection at 40 μM (Figure 8b). The EC_{50} values of Ant444 (**6**) and Triamide444 (**9**) were 5-fold and 7-fold lower than spermine respectively, demonstrating that these compounds are more efficient at competing for access to the PTS than either of the native polyamines spermidine or spermine. The data for Ant444 (**6**) and Triamide444 (**9**) are similar to Trimer44 (**7**). In contrast, Triamide44 (**8**) (EC_{50} 144 μM; Figure 7d) was 3-fold *less* effective than spermidine and 7-fold *less* effective than spermine in inhibiting the toxicity of Ant44 (**5**).

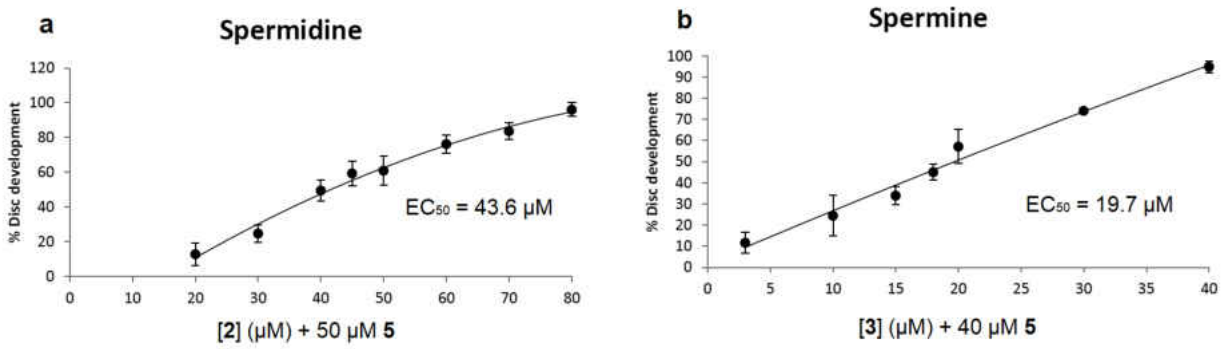

Figure 8 Spermidine and spermine block the inhibitory effect of Ant44 (**5**) on imaginal disc development.

Spermidine (**2**) and spermine (**3**) were tested at different concentrations in the presence of Ant44 (**5**) and the percentage of imaginal disc development was recorded for each concentration. a. Effective concentration of spermidine in blocking the inhibitory effect of Ant44 (**5**) on imaginal disc development; b. Effective concentration of spermine in blocking the inhibitory effect of Ant44 (**5**) on imaginal disc development. Every data point was repeated at least in triplicate. Error bars reflect the standard error of the mean (SEM). Note: the EC_{50} value is the concentration of the polyamine needed to block 50% of the inhibitory effect of Ant44 (**5**) on imaginal disc development.

In contrast to spermidine and spermine, the native diamine, putrescine, was unable to rescue the inhibition of Ant44 (**5**) in imaginal discs. Concentrations of up to 1 mM putrescine had no effect on the inhibition of imaginal disc development by Ant44 (**5**) (Figure 9). One interpretation of these observations is that the diamine putrescine presents fewer charges to the cell surface receptors than Ant44 (**5**), which is a triamine analogue. Therefore, the inability of putrescine to rescue cells from Ant44 (**5**) could be due to differences in relative binding affinity. An alternative interpretation is that Ant44 (**5**) is imported into the cell via a polyamine transporter which does not recognize putrescine. Indeed, the existence of multiple polyamine transporters with different affinities and selectivity for the native polyamines has been suggested in mammalian cells [56] and also in this study (see Section 4).

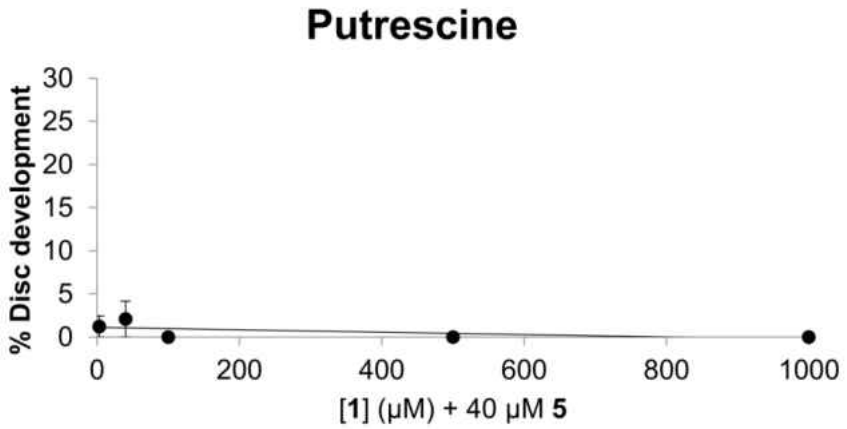

Figure 9 Putrescine fails to block the inhibitory effect of Ant44 (**5**) on imaginal disc development.

Putrescine (**1**) was tested at different concentrations in the presence of Ant44 (**5**) and the percentage of imaginal disc development was recorded for each concentration. Error bars reflect the standard error of the mean (SEM). Note: the EC_{50} value is the concentration of the polyamine needed to block 50% of the inhibitory effect of Ant44 (**5**) on imaginal disc development. An EC_{50} value was not calculated as putrescine was unable to block the inhibitory effect of Ant44 (**5**) on imaginal disc development.

In conclusion, Ant444 (**6**), Trimer44 (**7**) and Triamide444 (**9**) are all considerably more effective than either of the native polyamines spermidine or spermine in competing with Ant44 (**5**) for access to the PTS. Because putrescine could not rescue Ant44 (**5**) toxicity in disc development, no comparisons can be made for this native diamine.

3. *Ant444 (**6**) and Triamide444 (**9**) Effectively Prevent Rescue by Native Polyamines of DFMO-Treated Imaginal Discs*

Assay 1 tested the ability of candidate PTIs to block the toxicity of Ant44 (**5**), which accessed cells via the PTS (Figure 6a). Assay 2 tests the ability of each candidate PTI to

block the uptake of exogenous polyamines into DFMO-treated imaginal discs (Figure 6b). Since DFMO inhibits polyamine biosynthesis [114], intracellular polyamine levels are depleted and cell viability is decreased. The effect of DFMO in mammalian cell culture is dose-dependent and typically cytostatic and this inhibition can be reversed by the addition of native polyamines to the cell culture medium [3, 106]. Therefore, we investigated if DFMO inhibits imaginal disc development and if the compounds Ant444 (**6**), Trimer44 (**7**), Triamide44 (**8**) and Triamide444 (**9**) could prevent the rescue of DFMO-treated imaginal disc development by exogenous native polyamines. Essentially, we asked if these compounds could effectively compete with native polyamines for access to the PTS in DFMO-treated imaginal discs.

When imaginal discs are cultured in the presence of 10 mM DFMO greater than 95% of the discs fail to develop (Figure 10). As in mammalian cell culture, DFMO inhibition of disc development was dose-dependent. As shown in Figure 10, the 18 h IC_{50} value of DFMO on imaginal disc development was 4.4 mM, a value similar to that reported for CHO cells at 48h and L3.6pl cells at 72h [113]. Here the 18 h IC_{50} value is defined as the concentration of DFMO required to inhibit 50% of leg development after 18 h of incubation.

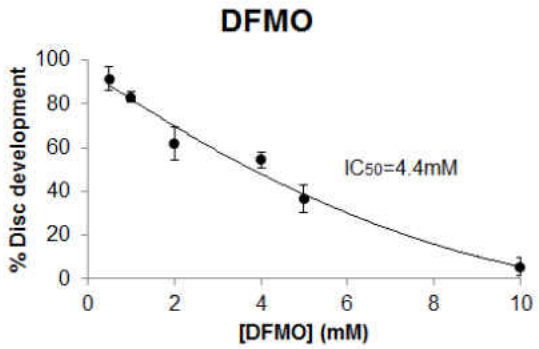

Figure 10 DFMO inhibits imaginal disc development.

DFMO (**4**) was tested at different concentrations and the percentage of disc development was determined for each concentration after 18 h of incubation. All data points were repeated at least in triplicate and error bars reflect the standard error of the mean (SEM). The IC_{50} value corresponds to the concentration of DFMO needed to inhibit 50% of discs from developing into rudimentary legs.

In the presence of exogenous polyamines, polyamines from outside the cell should enter into imaginal disc cells to rescue inhibition of development by DFMO. In contrast, in the presence of DFMO and an effective PTI, exogenous polyamines are expected to be unable to gain access to the cell resulting in inhibition of development. DFMO was used at 10 mM in all experiments because at this dose imaginal discs showed little development and retained the same shape as controls treated with culture medium only (i.e., with no steroid hormone to stimulate development). Data for these experiments are shown in Figures 11 and 12.

Each of the three native polyamines were evaluated for their ability to rescue the development of leg discs treated with DFMO. Addition of 500 µM putrescine to the culture

medium resulted in a significant increase (5% to 59%, Figure 11a; 4% to 66%, Figure 12a) in imaginal disc development compared to DFMO alone (compare blue and green columns in both Figures). Similarly, addition of 200 μM spermidine or spermine to DFMO-treated leg discs also significantly increased imaginal disc development (see Figures 11 and 12). Thus, each of the native polyamines was able to rescue imaginal disc development in the presence of DFMO (10 mM). These results mirror the ability of DFMO-treated mammalian cells to be rescued by each of the native polyamines. We note that the concentrations of native polyamines needed to rescue inhibition by DFMO in the *Drosophila* model assay were much higher (200-500 μM) than those observed in mammalian cells (around 1 μM). The higher doses are likely due to the fact that unlike cell culture, imaginal discs are an intact epithelial tissue surrounded by extracellular matrix, which may impede polyamine access to the PTS.

As with Assay 1, it was important to use a non-toxic dose of each PTI compound because in Assay 2 a toxic PTI would generate a false positive. To avoid introducing this bias, non-toxic concentrations of the PTI compounds were determined and used in both assays. In a series of control experiments, Ant444 (**6**), Trimer44 (**7**) and Triamide444 (**9**) were each found to be non-toxic to imaginal disc development at 100 μM, whereas Triamide 44 (**8**) was non-toxic at 300 μM.

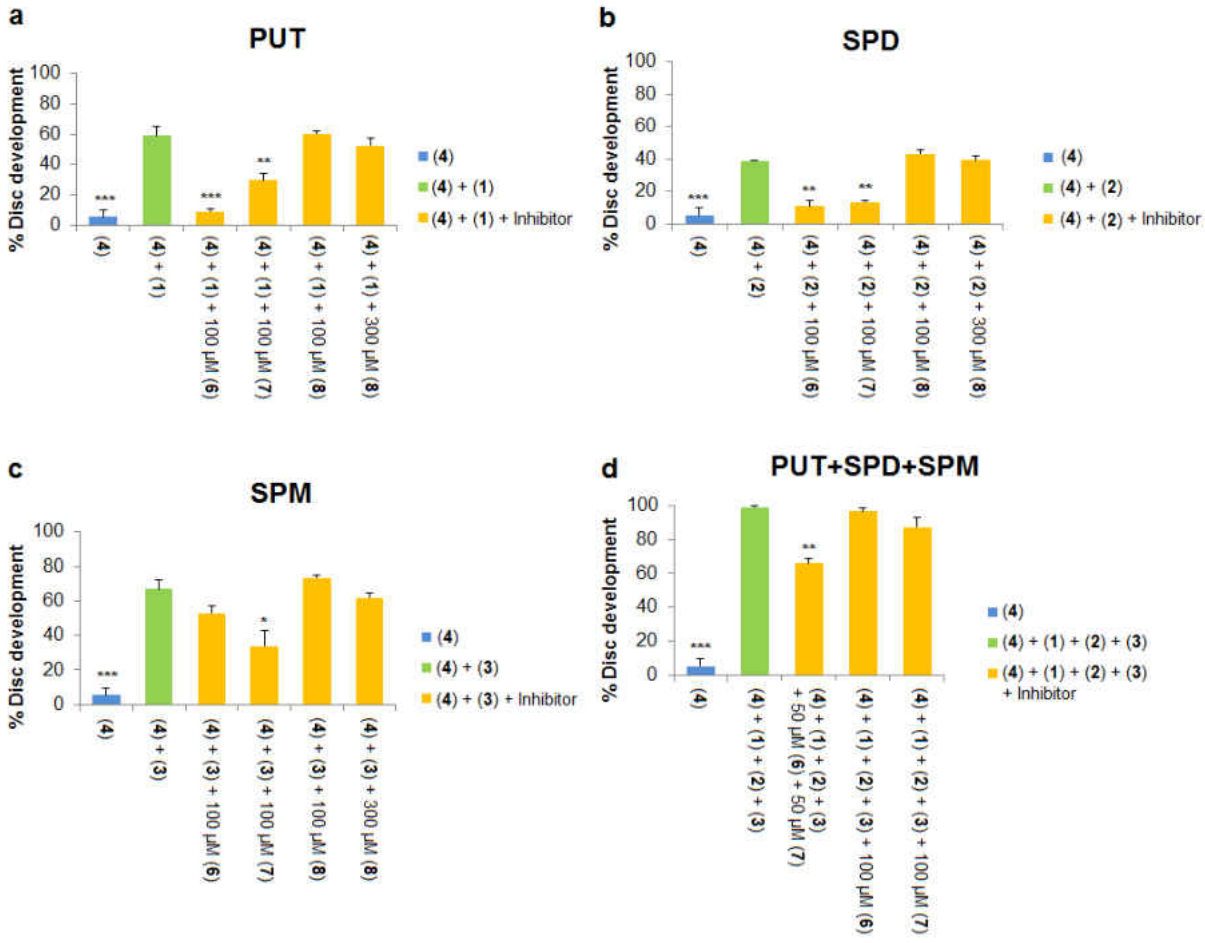

Figure 11 Candidate PTIs prevent native polyamine rescue of imaginal discs treated with DFMO.

Polyamine transport inhibitors at the indicated concentrations were used to block the rescue of DFMO treated imaginal discs (10 mM) by the native polyamines putrescine (PUT; **1**), spermidine (SPD; **2**) and spermine (SPM; **3**). DFMO alone (10 mM) results in approximately 5% imaginal disc development. Native polyamines were tested at the following concentrations (putrescine **1**: 500 µM; spermidine **2**: 200 µM; spermine **3**: 200 µM). Polyamines and PTIs were individually tested in the absence of DFMO to ensure there was no inhibition of imaginal disc development at the concentrations used. In addition, polyamines and PTIs were tested in combination for possible negative synergy on imaginal disc development and none was observed at the concentrations used. Compounds are numbered as described in Figure 5. All data points were repeated at least in triplicate and error bars reflect the SEM. Significant differences * $p < 0.05$; ** $p < 0.01$; *** $p < 0.001$ from treatment with DFMO and native polyamine alone are indicated. a. Ability of PTIs to prevent rescue of DFMO treated imaginal discs with putrescine; b. Ability of PTIs to prevent rescue of DFMO treated imaginal discs with spermidine; c. Ability

of PTIs to prevent rescue of DFMO treated imaginal discs with spermine; d. Ability of PTIs to prevent rescue of DFMO treated imaginal discs with a cocktail containing all three native polyamines (putrescine, spermidine and spermine).

We next asked if non-toxic concentrations of PTIs could block the developmental rescue of DFMO-treated imaginal discs by native polyamines. Rescue of DFMO-treated imaginal discs by putrescine was significantly reduced by addition of 100 μM of Ant444 (**6**), Trimer44 (**7**) and Triamide444 (**9**) (Figures 11a and 12a). Imaginal disc development was reduced from 59% (500 μM putrescine, 10 mM DFMO) to 9% in the presence of 100 μM Ant444, 500 μM putrescine and 10 mM DFMO, a result which was similar to the control with DFMO alone (Figure 11a). Likewise, addition of Trimer44 (100 μM) in the presence of putrescine and DFMO reduces imaginal disc development from 59% to 29% (Figure 11a). Addition of 100 μM Triamide444 reduced imaginal disc development from 66% to 18% (Figure 12a). While the decrease in imaginal disc development in the presence of Ant444 (**6**), Trimer44 (**7**) or Triamide444 (**9**) is significant, our data suggest that Trimer44 (**7**) is less effective than Ant444 (**6**) or Triamide444 (**9**) in inhibiting the uptake of putrescine. Consistent with earlier studies, 100 μM or 300 μM Triamide44 (**8**) was unable to compete with putrescine for access to the *Drosophila* PTS (Figure 11a).

Similar results were observed with spermidine. At 100 μM, Ant444 (**6**), Trimer44 (**7**) and Triamide444 (**9**) were all able to significantly inhibit import of spermidine. In the presence of 10 mM DFMO and 200 μM spermidine imaginal disc development decreased from 39% to 11% in the presence of 100 μM Ant444 and to 13% in the presence of 100 μM Trimer44 (Figure 11b). In the presence of 100 μM Triamide444 imaginal disc development

decreased from 70% to 34% (Figure 12b). In contrast, Triamide44 (**8**) failed to inhibit import of spermidine even at 300 µM (Figure 11b).

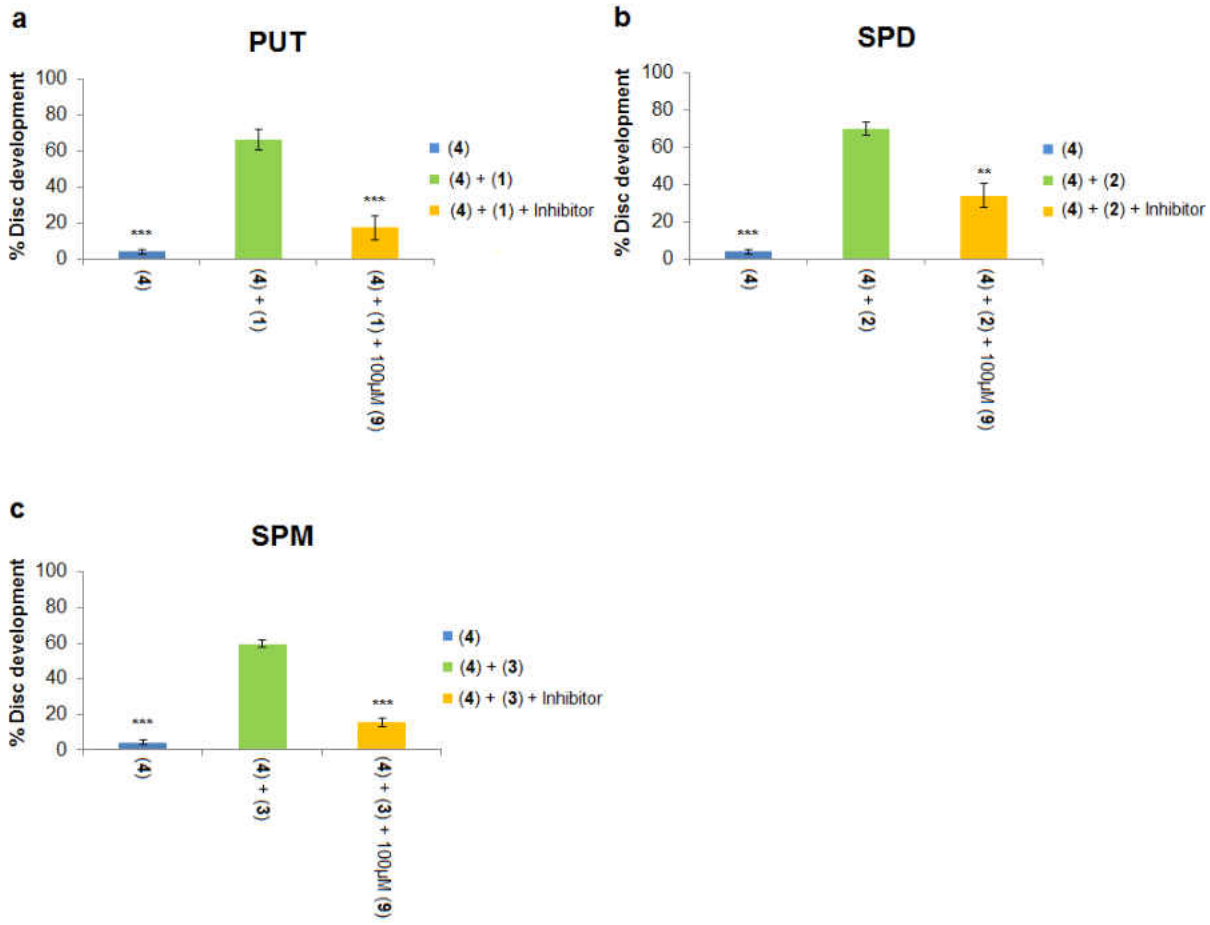

Figure 12 Triamide444 (**9**) is an effective inhibitor of native polyamine uptake.

The ability of 100 µM Triamide444 (**9**) to block the rescue of DFMO **4** treated imaginal discs (10 mM) by native polyamines putrescine (PUT; **1**), spermidine (SPD; **2**) and spermine (SPM; **3**). 10 mM DFMO alone (10 mM) results in approximately 5% disc development. Native polyamines were tested at the following concentrations (putrescine **1**: 500 µM; spermidine **2**: 200 µM; spermine **3**: 200 µM). Triamide444 (**9**) and individual polyamines were tested in the absence of DFMO to ensure there was no inhibition of imaginal disc development at the concentrations used. In addition, Triamide444 and individual polyamines were tested in combination for possible negative synergy on imaginal disc development and none was observed at the concentrations used. All data

points were repeated at least in triplicate and error bars reflect the SEM. Significant differences * $p < 0.05$; ** $p < 0.01$; *** $p < 0.001$ from treatment with DFMO and native polyamine alone are indicated. Ability of Triamide444 (**9**) to prevent rescue of DFMO treated imaginal discs with (a) putrescine; (b) spermidine and (c) spermine.

Finally, we tested the ability of the PTIs to inhibit import of spermine in the presence of 10 mM DFMO and 200 μM spermine. As shown in Figure 11c, 100 μM Ant444 (**6**) did not reduce uptake of spermine, whereas 100 μM Trimer44 (**7**) significantly reduced imaginal disc development from 67% to 34%. Triamide444 (**9**) showed even greater ability to reduce spermine uptake reducing imaginal disc development from 60% to 15% (Figure 12c). Thus, the PTIs can be ranked Triamide444 > Trimer44 > Ant444 with respect to their relative abilities to inhibit spermine uptake. As with the previous assays, Triamide44 (**8**) was unable to inhibit import of spermine even at 300 μM concentration.

In summary, even though Ant444 (**6**), Trimer44 (**7**) and Triamide444 (**9**) have similar EC_{50} values for protection against toxicity of Ant44 (**5**) and a similar concentration of full protection against Ant44 (**5**) (Figure 7a-c), they show different specificities in blocking the uptake of native polyamines into imaginal discs treated with DFMO (Figures 11a-c and 12). Ant444 (**6**) is better at blocking uptake of putrescine, Ant444 (**6**) and Trimer44 (**7**) show similar abilities to block uptake of spermidine and Triamide444 (**9**) is the most potent of the PTIs at blocking spermine uptake. These findings suggest that the PTIs have different specificities for the polyamine transport systems active in the presence of DFMO. In this regard, there may be a basal and DFMO-stimulated PTS in *Drosophila*. The basal PTS is assessed via the Ant44 assay (Assay 1), whereas the DFMO-stimulated PTS is assessed via Assay 2 (Figure 6). The poor performance of triamide44 (**8**) in these assays

is consistent with the inability of this compound to block the toxicity of Ant44 (**5**) (Figure 7d) and suggests that presenting polyamine chains containing only two charges per polyamine arm limits interactions with the putative PTS extracellular receptor (e.g., glypican-1 anchored heparan sulfate proteoglycans [62]).

4. *A Cocktail of Ant444 (**6**) and Trimer44 (**7**) Is More Potent than Either Compound Alone at Inhibiting the Import of Native Polyamines Into DFMO-Treated Imaginal Discs, Suggesting the Existence of Multiple Transport Systems*

In the next experiments, we further examined our finding that the PTIs have different specificities for the PTS. Specifically, we asked if a cocktail of PTIs was more effective than individual PTIs in inhibiting rescue of DFMO-treated imaginal discs in the presence of all three native polyamines. In our prior experiments, we studied the effects of individual native polyamines, however, all three polyamines are present *in vivo*. For example in circulating red blood cells, the levels of putrescine, spermidine and spermine were found to be 3, 55 and 35 pmol/mg protein respectively [115]. Because Ant444 (**6**) and Trimer44 (**7**) are effective PTIs and showed different specificities towards putrescine, spermidine and spermine respectively, a combination of these inhibitors was used to block the rescue of DFMO treated leg discs by a mixture of all of the native polyamines. As shown in Figure 11d, a cocktail of native polyamines (500 μM putrescine, 200 μM spermidine and 200 μM spermine) was able to fully rescue inhibition of leg disc development by DFMO (compare blue and green columns). In contrast to experiments using just one PTI, 100 μM of either Ant444 (**6**) or Trimer44 (**7**) alone was unable to significantly inhibit the rescue of DFMO-

treated discs by the exogenous native polyamine cocktail. In contrast, a combination of 50 μM Ant444 (**6**) and 50 μM Trimer44 (**7**) significantly inhibited rescue by native polyamines even though the amount of each PTI was reduced by half compared to experiments when only one PTI was used. This result suggests that a combination of polyamine transport inhibitors will be more effective in inhibiting the import of all three native polyamines than individual inhibitors dosed alone.

The different selectivity of Ant444 (**6**), Trimer44 (**7**) and Triamide444 (**9**) towards native polyamines and the ability of a cocktail of PTIs to inhibit transport more effectively than individual PTI's suggests the existence of multiple polyamine transport systems in *Drosophila* as has been observed in unicellular organisms [56]. Ant444 (**6**) shows a greater ability to inhibit uptake of putrescine, whereas Trimer44 (**7**) is more effective in inhibiting uptake of spermine (Figures 11a, c) which may be the underlying basis for the improved ability of a cocktail of these compounds to inhibit rescue in the presence of all three native polyamines. Further support for multiple transporters with different specificities for the native polyamines comes from our observation that 500 μM putrescine can rescue inhibition by DFMO (Figure 11a) whereas 1 mM putrescine is unable to rescue the toxicity of 40 μM Ant44 (**5**) (Figure 9), consistent with the notion that putrescine is imported into cells through a transport system different from Ant44. The underlying transport pathway selection may be charge-dependent because unlike the diamine putrescine, Ant44 is a triamine and presents three positive charges to the putative cell surface receptor. In addition, Ant44 is a homospermidine analogue and its toxicity can be rescued by the higher polyamines, spermidine and spermine. An alternative explanation

for our observations is that Ant44 bears both a hydrophobic anthryl substituent along with the hydrophilic polyamine head group and thus its amphiphilic properties may facilitate its uptake via a specific transport system.

Discussion

Our work reinforces the value of the *Drosophila* imaginal disc assay as an early and inexpensive system in which to evaluate compounds targeting the mammalian PTS. There are several advantages to our approach. First, mammalian cell culture is not a natural cellular environment because cells lack cell-cell contacts and extracellular matrix, both of which are factors influencing drug accessibility to cells *in vivo*. In contrast, the imaginal disc assay tests the effects of medicinal compounds on cells in a more natural environment. Second, inexpensive early animal model testing of promising compounds can reduce the time it takes successful compounds to reach the clinic by up to fifty percent. Mice are more expensive to use in the early stages of drug development where most compounds will fail, therefore a cheaper system such as our *Drosophila* assay is useful. Third, experiments in mice can only be performed on a small scale, whereas we can assay relatively large numbers of imaginal discs, typically more than 100 per assay.

Of course, the imaginal disc assay is only useful to understand mammalian transport if the polyamine transport system is similar in *Drosophila* and mammals. Our work suggests that this is the case. In previous work, we compared the uptake of nine polyamine analogs

in mammalian CHO and L1210 cells and *Drosophila* imaginal discs [94]. Two of the compounds tested in those experiments, Ant44 (**5**) and N^1-(3-aminopropyl)-N^4-(anthracen-9-ylmethyl) butane-1,4-diamine (Ant43) gain entry to mammalian cells via the polyamine transport system as evidenced by spermidine competition experiments and greatly reduced uptake in CHO-MG cells, which lack a functional transport system [116]. In imaginal discs, uptake of Ant44 and Ant43 is also greatly reduced in spermidine competition experiments. In contrast, uptake of the other seven polyamine analogs cannot be competed with spermidine in mammalian cells or *Drosophila* imaginal discs, suggesting that they do not utilize the transport system to gain access to cells in either system. In addition, Trimer44 (**7**) has previously been shown to be an effective inhibitor in mammalian cells, whereas Triamide44 (**8**) was not [113] and these results are mirrored in the *Drosophila* assay.

Use of the *Drosophila* imaginal disc assay has added to our knowledge of polyamine transport inhibitors. We show that two compounds that exhibit toxicity in mammalian cell culture, Ant444 (**6**) and Triamide444 (**9**), are non-toxic in the *Drosophila* assay and are effective PTIs with activity profiles similar to that of Trimer44 (**7**). The reduced toxicity of Ant444 and Triamide444 in *Drosophila* may due to a lower effective concentration of these compounds reaching the cell surface due to the presence of intact cell-cell adhesions and extracellular matrix. We also provide activity data for the PTIs against all three native polyamines (putrescine, spermidine, spermine) whereas most mammalian cell culture studies focus on spermidine uptake. This approach revealed differences in the ability of each PTI to inhibit uptake of individual polyamines suggesting the existence

of multiple transport systems. This view is further reinforced by our finding that a mixture of two PTIs is more effective than either PTI alone at inhibiting uptake of a cocktail of all three native polyamines.

In this study, we assayed the ability of PTIs to inhibit the rescue of DFMO treated imaginal discs in the presence of exogenous polyamines. This approach is clinically relevant in that many tumors circumvent DFMO treatment via upregulation of their polyamine transport systems. Our previous work indicates that the PTIs inhibit polyamine uptake. Our data are consistent with the reported K_i values for several of these compounds in terms of competing with ^{3}H-radiolabeled spermidine for the putative cell surface receptors in L1210 murine leukemia cells. The L1210 K_i values for putrescine, spermidine and spermine are 208.2, 2.46 and 1.34 μM, respectively [52]. The L1210 cell K_i values for Ant44 (**5**), Ant444 (**6**) and Trimer44 (**7**) are 1.8 μM, 0.05 μM and 0.49 μM, respectively [52, 112]. Although the K_i value of Triamide44 (**8**) was not determined in L1210 cells, a comparative study of the Trimer44 and Triamide44 compounds in human L3.6pl pancreatic cancer cells revealed K_i values of 36 nM and 398 nM, respectively [113], suggesting a significantly lower affinity of Triamide44 for the putative cell surface receptors of the polyamine transport system.

The low K_i values of Ant44, Ant444 and Trimer44 suggest that these compounds compete with the native polyamines for uptake. For example, Ant44 (a triamine) has a L1210 K_i value of 1.8 μM and provides a fluorescent molecule with similar affinity for the polyamine transport system as the native polyamines spermidine (L1210 K_i = 2.46 μM) and spermine

(L1210 K_i = 1.34 μM). We speculate that in order to be successfully imported, compounds must bind and release from the cell surface receptors. The K_i values of the native polyamines (spermidine and spermine) suggest that K_i values in the low μM range are optimal for these binding and releasing properties. The related Ant444 compound **6** (a tetraamine) has a significantly lower L1210 K_i value (51 nM) indicating high affinity for the cell surface receptors. Using confocal microscopy, we have demonstrated that this higher affinity of Ant444 was observed as a compound which could not be washed off the surface of L1210 cells by phosphate buffered saline (PBS). In contrast, the triamine Ant44 could be readily washed off the surface of L1210 cells by PBS and appeared to have improved uptake past the cell membrane [52]. This data is consistent with the higher toxicity of Ant44 (**5**: 48 h L1210 IC_{50} = 0.3 μM) compared to Ant444 (**6**: 48 h L1210 IC_{50} = 7.5 μM) [52]. In summary, highly charged lipophilic tetraamines like Ant444 tend to stick and not enter, which likely contributes to their ability to act as less toxic PTIs.

Our finding that Ant444 (**6**) and Triamide444 (**9**) are effective PTIs expands our understanding of the chemical rules governing an effective PTI design. Inhibitors presenting diamine arms, like Triamide44 (**8**), are ineffective transport inhibitors. In contrast, compounds containing a higher number of charges in their polyamine arms such as Trimer44 (**7**) and Triamide444 (**9**) are effective PTIs. In this regard, N^1-substituted triamine and tetraamine analogues can be used to design efficient ligands and inhibitors of polyamine transport. Our work and previous studies suggest that presentation of at least three or more positive charges is necessary for efficient competitive binding to the PTS.

A combination therapy using DFMO and a PTI has shown promise in cancer growth inhibition [53, 117]. While the lack of knowledge of the genes and proteins involved in polyamine transport has hampered the development of PTIs, structure-activity relationship studies have nevertheless resulted in the development of effective PTIs. One effective PTI is AMXT-1501 (**11**, Figure 13) [53]. In combination with DFMO, AMXT-1501 inhibits cancer cell growth in several cancer cell lines and mouse models [117]. Recently this compound was also found to reverse immunosuppression in the tumor microenvironment [118]. Structurally the compounds we tested here are different from AMXT-1501, which is a lipophilic palmitic acid–lysine spermine conjugate. Indeed, the hydrophilic compound **12** (Figure 13), which is a N-methylated derivative of Trimer44 (**7**), was recently shown to behave in a similar manner as AMXT-1501 (**11**) both in its ability to shrink tumors *in vivo* as well as to beneficially modulate the immune response [119]. Thus, this report provides alternative three-arm PTI designs and new insights as to how combinations of PTIs can be used to effectively inhibit the import of all three native polyamines. Going forward the *Drosophila* model can be used to pre-screen PTIs prior to more expensive testing in mouse models. Having a cheap model system for early animal testing will reduce the time from conceptual PTI design to future validation in clinical trials.

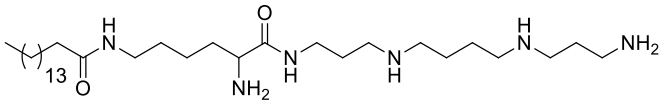

11: AMXT 1501

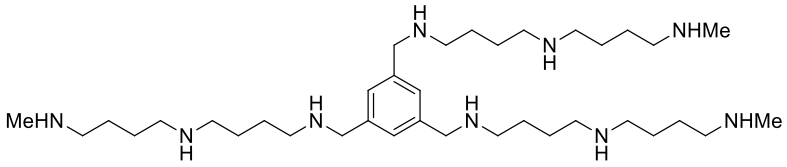

12: trimer44NMe

Figure 13 Structures of PTI compounds **11** and **12**.

Methods

1. Synthesis

The synthesis of the anthracene-polyamine conjugates (**5** and **6**) and the aryl-polyamine conjugates (**7**–**9**) have been described [52, 113].

2. Drosophila Strains and Larval Collections

The Oregon-R variant of *Drosophila melanogaster* was used in all experiments. Larval preparation and staging were performed as previously described [94, 120]. All larvae used in the experiments were synchronized to within 7 h of pupariation, immediately prior to the pulse of 20-hydroxyecdysone that triggers imaginal disc development. Imaginal discs dissected from larvae at this developmental stage develop into rudimentary legs when exposed to 20-hydroxyecdysone in *in vitro* culture.

3. *Imaginal Disc Culture and Scoring*

Leg imaginal discs were dissected at room temperature in Ringer's solution (130 mM NaCl, 5 mM KCl, 15 mM $CaCl_2 \cdot 2H_2O$) containing 0.1% bovine serum albumin (BSA ,w/v), which was added to the Ringer's solution immediately prior to use. Up to 150 discs were dissected in less than 1 h to avoid prolonged storage in Ringer's solution. After dissection, discs were transferred to 12-well plastic culture plates containing Ringer's solution (1 mL). Before the disc culture medium was added, dissected imaginal discs were washed once with 1× minimal Robb's medium (see Section 4). To begin a culture, a solution of 1 mL of 1× minimal Robb's medium (final concentration) containing 20-hydroxyecdysone (1 µg/mL) and each of the compounds to be tested was added to each well. Control experiments lacking polyamine transport inhibitor (PTI) were run in parallel. Imaginal discs were incubated for 18 h at 25 °C. After 18 h, the discs were scored as developed or non-developed. Fully developed discs (the leg is fully extended from the epithelium) and partially developed discs (the leg protrudes from the epithelium but is not fully extended) were scored as developed. Non-developed discs showed no sign of development. For each experiment, the percent development was determined by ([(number of developed discs)/(total number of discs)] × 100.

4. *Robb's Minimal Medium*

2× Minimal Robb's medium consisting of 80 mM KCl, 0.8 mM KH_2PO_4, 80 mM NaCl, 0.8 mM $NaH_2PO_4 \cdot 7H_2O$, 2.4 mM $MgSO_4 \cdot 7H_2O$, 2.4 mM $MgCl_2 \cdot 6H_2O$, 2 mM $CaCl_2 \cdot 2H_2O$, 20

mM glucose, 8.0 mM L-glutamine, 0.32 mM glycine, 1.28 mM L-leucine, 0.64 mM L-proline, 0.32 mM L-serine and 1.28 mM L-valine, pH 7.2 was prepared and stored at −20° C. Immediately prior to use, 20 µL of 10% BSA (w/v) was added to 1 mL of medium [121].

5. Statistical Analysis

Statistical analysis was performed using IBM SPSS Statistics 19 with one-way ANOVA.

CHAPTER THREE: CHOICE OF IMAGINAL DISC GAL4 DRIVER CAN BE USED TO EXPRESS TOXIC UAS RESPONDER CONSTRUCTS THROUGHOUT DEVELOPMENT

Introduction

In order to identify genes involved in polyamine transport our laboratory has developed an RNAi based assay. In this assay animals are grown on media supplemented with DFMO which is lethal at the concentration used (5 mM). Viability of these animals can be rescued by the addition of exogenous polyamines to the media. If the expression of a candidate gene for polyamine transport is reduced by RNAi, viability of the animals cannot be rescued in the presence of DFMO and exogenous polyamines. One drawback to this approach is that genes can exhibit pleiotropic effects leading to early/embryonic death after RNAi knockdown. Such an outcome would exclude the possibility of testing the gene for a role in polyamine transport. I therefore explored the possibility of using the GAL4/UAS system [122] to bypass early developmental lethality following RNAi knockdown.

The GAL4/UAS system is a powerful technique that allows the expression of a target gene in a tissue- and developmental stage- specific manner. The relative strength of a driver is an important factor when attempting to circumvent early developmental lethality caused by overexpression or RNAi knockdown of a particular gene. To test the hypothesis that appropriate choice of GAL4 driver can be used to overcome early developmental

lethality I studied the effects of RNAi knockdown and overexpression of genes encoding components of the Rho1 signaling pathway and EGFR. UAS constructs expressing some of these genes have an embryonic lethal phenotype with commonly used ectodermal drivers such as 69B and T80. To address this problem I determined the expression patterns of five imaginal disc GAL4 drivers (30A, 71B, 32B, 69B, and T80) in late third instar leg, wing and eye antennal discs, ranked their relative strength of expression, and assayed the lethal stage of each driver in the presence of Rho1 pathway and EGFR UAS responder constructs. The five GAL4 drivers fell into three groups according to their expression strength. I also demonstrated that weak drivers are useful to express toxic UAS constructs at later times in development. This study provides useful reference points for choosing the appropriate GAL4 driver to study overexpression and RNAi knockdown of genes required for imaginal disc development and can be adapted for screening for genes involved in polyamine transport.

Results and Discussion

While many GAL4 drivers have been documented and are available in the Bloomington Stock Center, frequently little is known about their temporal or spatial expression patterns or the relative strengths of different GAL4 drivers expressed in the same tissue. The relative strength of a driver can be an important factor when attempting to circumvent early developmental lethality caused by overexpression or RNAi knockdown of a particular gene. Therefore, I determined the expression patterns of five GAL4 drivers (30A,

71B, 32B, 69B, and T80) expressed in late third instar leg, wing and eye antennal imaginal discs, ranked their relative strength of expression, and assayed the lethal stage of each driver in the presence of potentially toxic UAS responder constructs for RNAi knockdown and overexpression of components of the Rho1 signaling pathway and EGFR. A ubiquitous GAL4 driver Tubulin (TubP) were used as a control in all of these studies.

1. *Expression Patterns of GAL4 Drivers in Late Third Instar Imaginal Discs*

To determine the expression pattern of GAL4 lines in imaginal discs, a membrane tethered green fluorescent protein (GFP) fusion molecule that allows rapid *in vivo* imaging as well as the analysis of fixed tissue was used. Each of the GAL4 lines was crossed to UAS-mCD8-GFP [123] and the GFP expression in the progeny was analyzed using a fluorescent microscope. The detailed characterization of these GAL4 lines in imaginal discs identified a variety of interesting and specific expression patterns, which might be of great use in future study. Expression patterns of GAL4 drivers in late third instar imaginal discs, including leg disc, wing disc, eye antennal disc and haltere disc are shown in Figure 14.

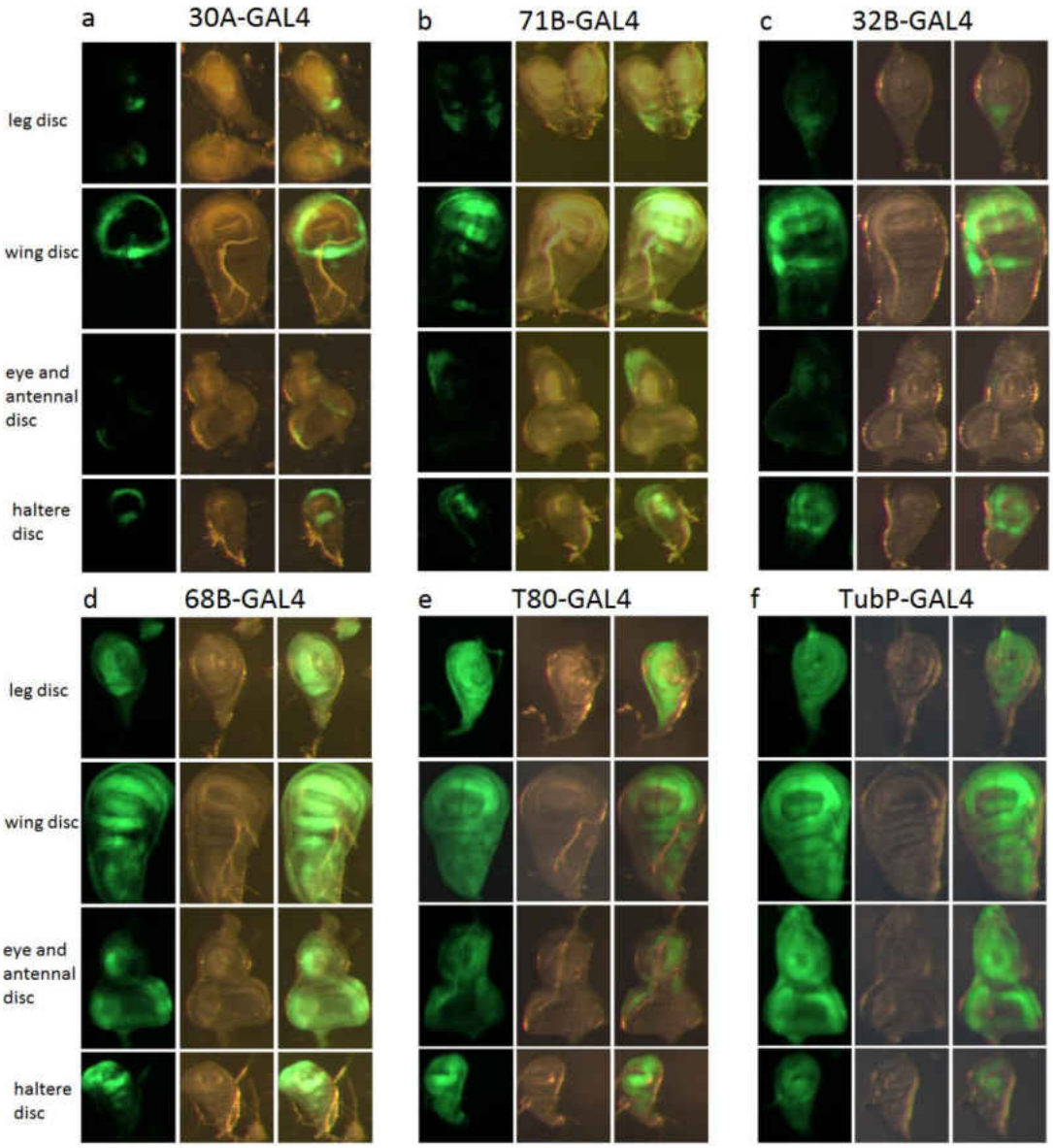

Figure 14 Expression patterns of GAL4 drivers in late third instar imaginal discs.

a: expression pattern of 30A-GAL4 driver; b: expression pattern of 71B-GAL4 driver; c: expression pattern of 32B-GAL4 driver; d: expression pattern of 69B-GAL4 driver; e: expression pattern of T80-GAL4 driver; f: expression pattern of TubP-GAL4 driver. Each set of figures contains three sections (from left to right): fluorescent light only with constant settings; white light only; merge of the first two sections.

As recorded in Flybase, expression of the 30A-GAL4 driver in leg imaginal disc is focused in the dorsal sector [124], however, as shown in Figure 14a, 30A-GAL4 is also expressed in distal regions. The expression of 30A-GAL4 in the wing disc and eye antennal discs are consistent with data reported in Flybase [122]. In the haltere disc expression of 30A-GAL4 is primarily in the hinge region.

The expression pattern of the 71B-GAL4 driver is consistent with the description in Flybase (Figure 14b) [122, 125]. In leg imaginal discs this driver is expressed in two dorsal spots and also in the stalk. In wing imaginal discs expression is observed in part of the dorsal and ventral posterior wing pouch and a similar pattern is observed in haltere discs. Expression in eye antennal imaginal discs is limited except to the stalk region.

Expression of the 32B-GAL4 driver in leg and eye-antennal imaginal disc is weak (Figure 14c). In wing discs, it expresses throughout wing blade region with a similar pattern in haltere discs, which is consistent with data from Flybase [122].

In contrast to the 32B driver, expression of 69B-GAL4 in imaginal discs of late 3rd instar larvae is much stronger (Figure 14d). 69B-GAL4 expression is observed in most parts of leg, wing, eye antennal and haltere discs. This expression pattern is similar to T80-GAL4 and the TubP-GAL4 control driver (Figures 14e, f).

In summary, the imaginal discs drivers tested show different expression patterns and different degrees of expression making them good candidates to test the hypothesis that weak drivers could be used to express toxic UAS constructs. I next asked if the drivers with weaker expression could be used to circumvent early lethality of stronger drivers expressing Rho1 pathway and EGFR UAS constructs.

2. *Use of Weak Imaginal Disc GAL4 Drivers to Express Toxic UAS Responders Results in Viable Adult Offspring*

I assayed the ability of each driver (30A, 71B, 32B, 69B, T80 and TubP) to permit development to the late larval stage and beyond in the presence of potentially toxic UAS responder constructs. The 11 UAS constructs tested either reduced expression of Rho1 signaling pathway components and EGFR by RNAi or overexpressed these genes (Table 2). Where viable adults were observed, leg, wing and eye phenotypes were documented. Also, in each cross the TubP driver was tested as a control for strong and ubiquitous expression (Table 2).

The penetrance and severity of adult leg, wing and eye phenotypes is consistent with the expression pattern shown in Figure 14. For example, the overall expression level of the 30A driver in wing imaginal discs is lower than 71B as shown in Figure 14a and 14b. At the same time, whenever there was detectable adult wing phenotype, in most cases the 71B driver resulted in higher percentage and/or more malformed phenotypes than 30A

driver (Table 2). In contrast, the severity of the malformed leg phenotype was very similar in most cases for the 71B and 30A drivers which was consistent with their similar strength of expression in leg imaginal discs as shown in Figures 14a and 14b.

Table 2 Cross result and phenotypes in leg, wing and eye for all combinations of six GAL4 drivers and eleven UAS responders.

RNAi Responder	Driver	Phenotype			Note
		Mlf-legs	Wing	Eye	
UAS-Rho1 N19	30A-GAL4	Pupae lethal			
	71B-GAL4	Pupae lethal			
	32B-GAL4	Embryonic lethal: food was untouched with dead eggs on top			
	69B-GAL4	Embryonic lethal: food was untouched with dead eggs on top			
	T80-GAL4	Larval lethal: 79.9% larvae hatched from eggs (565/707)			
	TubP-GAL4	Embryonic lethal：0% larvae hatched from eggs (0/337)			
UAS-Rho1$^{Sph1.21}$ (3rd Chromosome)	30A-GAL4	F 18.9% (17/90)	F 12.9% thicker ACV (9/70), 1.4% extra vein material (1/70)	F 0% (0/90)	
		M 19.0% (8/42)	M 17.1% thicker ACV (12/70)	M 0% (0/42)	
	71B-GAL4	F 6.3% (4/63)	F 16.7% thicker ACV (13/78)	F 0% (0/63)	
		M 2.8% (2/71)	M 25.7% thicker ACV (18/70)	M 0% (0/71)	
	32B-GAL4	F 0% (0/3)	F 100% crumpled wings (6/6)	N/A	Reduced viability
		M lethal			
	69B-GAL4	F 78.4% (76/97)	F 23.6% crumpled wings (26/110), 42.7% partial PCV (47/110), 0.9% partial ACV (1/110)	100% rough eye (48/48)	Reduced viability
		M 97.3% (36/37)	M 32.9% crumpled wings (23/70), 30% partial ACV (21/70), 12.9% partial PCV (9/70)	100% rough eye (26/26)	
	T80-GAL4	Pupae lethal			
	TubP-GAL4	Larval lethal：84.5% larvae hatched from eggs （142/168)			

RNAi Responder	Driver	Phenotype			Note
		Mlf-legs	Wing	Eye	
UAS-Rho1 RNAi (BL27727)	30A-GAL4	F 0% (0/4)	F 42.9% crumpled wings with unscorable pattern (3/7), 42.9% unflatten wings with normal pattern (3/7)	F 0% (0/4)	Reduced viability
		M 50% (3/6)	M 66.7% crumpled wings with unscorable pattern (8/12), 16.7% unflatten wings with normal pattern (2/12)	M 0% (0/6)	
	71B-GAL4	Pupae lethal			
	32B-GAL4	Larval lethal			
	69B-GAL4	Larval lethal			
	T80-GAL4	Pupae lethal			
	TubP-GAL4	Larval lethal：94.4% larvae hatched from eggs 168/178)			
UAS-Sb $^{6.1.4\text{-}13A(2)}$	30A-GAL4	F 100% (66/66)	F 16% thicker ACV (16/100)	N/A	
		M 96.1% (49/51)	M 5.6% crumpled wings (3/54)	N/A	
	71B-GAL4	F 95.1% (77/81)	F 32.7% crumpled wings (32/98)	N/A	
		M 98.1% (106/108)	M 43.6% crumpled wings (34/78)	N/A	
	32B-GAL4	Pupae lethal (Only 1 adult eclosed with crumpled wings and mlf-legs)			
	69B-GAL4	F 100% (11/11)	F 40% crumpled wings (8/20)	F 0% (0/11)	Reduced viability
		M 100% (10/10)	M 31.6% crumpled wings (6/19)	M 0% (0/10)	
	T80-GAL4	Larval lethal：93.0% larvae hatched from eggs （304/327)			
	TubP-GAL4	Embryonic lethal			
UAS-Sb RNAi	30A-GAL4	F 0% (0/39)	F 7.4% crumpled wings (5/68)	F 0% (0/39)	

RNAi Responder	Driver	Phenotype			Note
		Mlf-legs	Wing	Eye	
UAS-Sb RNAi	30A-GAL4	M 0% (0/19)	M 0% crumpled wings (0/36)	M 0% (0/19)	
	71B-GAL4	F 0% (0/46)	F 1.2% partial L4 (1/84), 1.2% crumpled wings (1/84)	F 0% (0/46)	
		M 0% (0/40)	M 2.9% crumpled wings (2/70)	M 0% (0/40)	
	32B-GAL4	F 58.7% (27/46)	F 65.8% crumpled wings (50/76)	F 0% (0/46)	
		M 37.1% (13/35)	M 75.8% crumpled wings (47/62)	M 0% (0/35)	
	69B-GAL4	F 100% (43/43)	F 100% crumpled wings (75/75)	F 0% (0/43)	
		M 96.4% (27/28)	M 100% crumpled wings (52/52)	M 0% (0/28)	
	T80-GAL4	F: pupae lethal			Reduced viability
		M 100% (4/4)	M 100% crumpled wings (6/6)	N/A	
	TubP-GAL4	Pupae lethal			
UAS-EGFR1	30A-GAL4	F 27.3% (3/11)	F 100% crumpled wings with normal vein pattern (22/22)	F 0% (0/11)	Reduced viability
		M 0% (0/1)	M N/A	M 0% (0/1)	
	71B-GAL4	F 0% (0/14)	F 7.1% crumpled wings (2/28), 78.6% extra vein material (22/28), 57.1% partial AVC (16/28)	F 0% (0/14)	Reduced viability
		M 0% (0/3)	M 100% extra vein material (6/6), 50% partial AVC (3/6)	M 0% (0/3)	
	32B-GAL4	Pupae lethal			small-sized pupa

RNAi Responder	Driver	Phenotype			Note
		Mlf-legs	Wing	Eye	
UAS-EGFR1	69B-GAL4	Pupae lethal			
	T80-GAL4	Pupae lethal: 65.3% larvae formed pupae (130/199)			
	TubP-GAL4	Larval lethal：73.7% larvae hatched from eggs (160/217)			
UAS-EGFR2	30A-GAL4	F 0% (0/37)	F 100% crumpled wings with normal vein pattern (74/74)	F 0% (0/37)	Reduced viability
		M 0% (0/32)	M 100% crumpled wings with normal vein pattern (60/60)	M 0% (0/32)	
	71B-GAL4	F 4.7% (4/85)	F 17.7% crumpled wings (29/164), 92.1% extra vein material (151/164), 7.9% tumor-like wing (bubble in wing) (13/164), 1.8% partial AVC (3/164)	F 1.2% heart-shape eye (1/85)	Reduced viability, small-sized pupa
		M 0% (0/96)	M 12.1% crumpled wings (23/190), 93.7% extra vein material (178/190), 2.1% tumor-like wing (bubble in wing) (4/190), 3.7% partial AVC (7/190)	M 0% (0/96)	
	32B-GAL4	Pupae lethal			small-sized pupa
	69B-GAL4	Pupae lethal			small-sized pupa
	T80-GAL4	Larval lethal：96.8% larvae hatched from eggs (454/469)			
	TubP-GAL4	Larval lethal：79.9% larvae hatched from eggs (183/229)			
UAS-EGFR RNAi	30A-GAL4	F 0% (0/53)	F 0.9% missing ACV (1/108), 8.3% crumpled wings (9/108)	F 0% (0/53)	
		M 0% (0/38)	M 4.5% crumpled wings (3/66)	M 0% (0/38)	

RNAi Responder	Driver	Phenotype			Note
		Mlf-legs	Wing	Eye	
UAS-EGFR RNAi	71B-GAL4	F 0% (0/33)	F 7.6% crumpled wings (5/66), 3.0% missing PCV (2/66), 92.4% loss/partial L3, L4 and ACV (61/66), 4.5% partial L2 (3/66), 18.2% partial L5 (12/66), 12.1% extra vein material male (8/66)	F 97% mild rough eye (32/33)	Reduced viability
		M 0% (0/34)	M 13.3% crumpled wings (8/60), 3.3% missing PCV (2/60), 88.3% loss/partial L3, L4 and ACV (53/60), 45% partial L2 (27/60), 40% partial L5 (24/60), 33.3% extra vein material male (20/60)	M 64.7% mild rough eye (22/34)	
	32B-GAL4	Pupae lethal			
	69B-GAL4	Pupae lethal			
	T80-GAL4	Pupae lethal			
	TubP-GAL4	Larval lethal：48.1% larvae hatched from eggs （51/106)			
UAS-RhoGEF2	30A-GAL4	F 0% (0/105)	F 0.5% crumpled wings (1/205)	F 0% (0/105)	
		M 0% (0/88)	M 4.6% crumpled wings (8/174)	M 0% (0/88)	
	71B-GAL4	F 0% (0/74)	F 0.7% extra vein (1/146), 3.4% crumpled wings (5/146)	F 0% (0/74)	Reduced viability
		M 0% (0/61)	M 10% crumpled wings (12/120)	M 0% (0/61)	
	32B-GAL4	F 0% (0/54)	F 22.6% crumpled wings (24/106)	F 0% (0/54)	Reduced viability, growth delay
		M 0% (0/29)	M 20.7% crumpled wings (12/58)	M 0% (0/29)	
	69B-GAL4	F 0% (0/70)	F 4.3% crumpled wings (6/140), 20.7% partial PCV (29/140), 2.1% extra vein (3/140), 2.9% curly wings (4/140)	F 0% (0/70)	Reduced viability, growth delay
		M 0% (0/46)	M 6.7% crumpled wings (6/90), 2.2% partial PCV (2/90)	M 0% (0/46)	

RNAi Responder	Driver	Phenotype			Note
		Mlf-legs	Wing	Eye	
UAS-RhoGEF2	T80-GAL4	F 0% (0/10)	F None (0/20)	F 0% (0/10)	Reduced viability
		M 0% (0/8)	M None (0/16)	M 0% (0/8)	
	TubP-GAL4	Embryonic lethal：9.9% larvae hatched from eggs （14/142)			
RhoGEF2 RNAi	30A-GAL4	F 0% (0/63)	F 4.9% crumpled wings (4/82)	F 0% (0/63)	
		M 3% (2/67)	M 7% crumpled wings (9/128)	M: 25% mild rough eye (16/64)	
	71B-GAL4	F 0% (0/124)	F 4.9% extra vein (10/203)	F 0% (0/124)	
		M 0% (0/95)	M 7.6% crumpled wings (12/158), 2.5% extra vein (4/158)	M 0% (0/95)	
	32B-GAL4	Larval lethal (Lots of dead larvae in the food, 1 pupa formed)			
	69B-GAL4	Larval lethal (Lots of dead larvae in the food, 1 pupa formed)			
	T80-GAL4	F 80% (4/5)	F 100% crumpled wings (8/8)	F 0% (0/5)	Reduced viability
		M 100% (2/2)	M 75% crumpled wings (3/4), 25% thicker ACV (1/4)	M 0% (0/2)	
	TubP-GAL4	Larval lethal：86.1% larvae hatched from eggs (149/173)			
UAS-RhoGAP p190	30A-GAL4	F 0% (0/70)	None (0/140)	F 0% (0/70)	
		M 0% (0/63)	None (0/126)	M 0% (0/63)	
	71B-GAL4	F 1.8% (1/57)	F 73.0% extra wing vein material (84/115)	F 0% (0/57)	

RNAi Responder	Driver	Phenotype			Note
		Mlf-legs	Wing	Eye	
UAS-RhoGAP p190	71B-GAL4	M 8.0% (4/50)	M 85.0% extra wing vein material (85/100)	M 0% (0/50)	
	32B-GAL4	F 0% (0/52)	F 88.2% extra wing vein material (90/102)	F 0% (0/52)	
		M 0% (0/41)	M 84.0% extra wing vein material (68/81)	M 0% (0/41)	
	69B-GAL4	F 0% (0/47)	F 100% extra wing vein material (94/94)	F 0% (0/47)	
		M 3.1% (1/32)	M 100% extra wing vein material (62/62)	M 0% (0/32)	
	T80-GAL4	F: 50% (3/6)	F 33.3% crumpled wing (4/12), 58.3% extra wing vein material (7/12)	F: 0% (0/6)	Reduced viability
		M pupae lethal			
	TubP-GAL4	Pupae lethal: 18.5% larvae formed pupae (37/200)			

F: female; M: male; N/A = not available; Mlf-legs: malformed legs.

I also demonstrated that weak drivers are useful to express toxic UAS constructs at later times in development. For example, expression of a dominant negative Rho1N19 construct is embryonic lethal in combination with the 69B or T80 drivers, but in the presence of the 30A and 71B drivers, animals survive until the pupal stage permitting studies of the effects of impaired Rho1 signaling during imaginal disc morphogenesis (Table 2). Also, UAS constructs like UAS-Rho1, UAS-Rho1 RNAi, UAS-RhoGEF2 RNAi, UAS-EGFR1 and UAS-EGFR2 were lethal when crossed to strong drivers, however, when combined with the 30A and 71B drivers they were viable and resulted in a high frequency of leg malformation and wing phenotypes (Table 2). Thus, the 30A and 71B drivers are useful for expression of toxic UAS constructs.

Based on the data in Table 2 the relative strength of expression of each driver was ranked (Figure 15). The 32B, 69B and T80 drivers fell into one group with the strongest relative strength of expression and in general these commonly used drivers are not useful to express toxic UAS constructs. The strength of the 32B, 69B and T80 drivers varied with UAS responder tested. For example, following expression of a dominant negative Rho1N19 construct or Rho1 RNAi, the lethal stage is earlier when in combination with the 69B or 32B drivers than with the T80 driver (Table 2). However, the T80 driver was a stronger driver than 69B or 32B when expressing UAS-Rho1, UAS-Sb, UAS-Sb RNAi and UAS-EGFR2 (Table 2). Meanwhile, these drivers had similar outcomes when expressing UAS-EGFR1 and UAS-EGFR RNAi (Table 2).

3. Data Analysis

The penetrance and severity of leg, wing and eye phenotypes was used to rank GAL4 driver expression strength for all combinations of drivers and responders. Phenotypes were scored from 0 to 40. While treating the rates as the ordinal data, the non-parametric Friedman's test was implemented to compare the strength of drivers. The results indicated four distinct groups from weakest to strongest: 30A-GAL4<71B-GAL4<32B-GAL4, 69B-GAL4, T80-GAL4< TubP-GAL4 (Figure 15). These rankings are consistent with the driver expression patterns showing in Figure 14. A similar ranking was obtained when using Tukey's range test following one-way ANOVA if the rates were treated as the numerical data (data not shown).

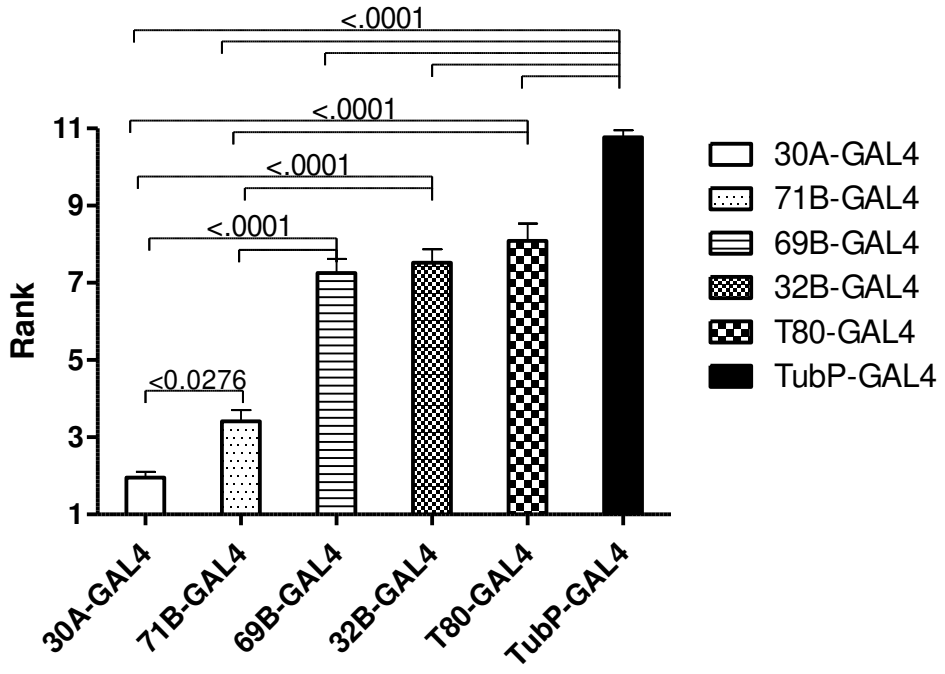

Figure 15 Friedman's test to rank the strength of expression of GAL4 drivers. P values were shown between drivers and expression strength of two GAL4 drivers is significantly different if $p < 0.05$.

Methods

1. *Fly Stocks*

All the fly stocks used in the study are listed in Table 3. If the stock was homozygous viable, homozygotes were used to set up crosses.

Table 3 Stocks used in Chapter 3.

Stock	Chromosome location	Balancer	Source	Note
30A-GAL4	2	CR_2	Lab stock	Homozygous viable
71B-GAL4	3	N/A	BL1747	
32B-GAL4	3	N/A	BL1783	TM3 floating
69B-GAL4	3	N/A	Lab stock	TM6B floating
T80-GAL4	2	CR_2 or Cyo, actGFP	Lab stock	
TubP-GAL4	3	TM3 or TM6B, dfd-EYFP	BL5138	
UAS-Rho1 N19	3	N/A	BL7328	
UAS-Rho1$^{Sph1.21}$	3	N/A	Lab stock	
UAS-Rho1 RNAi	3	N/A	BL27727	
UAS-Sb $^{6.1.4-13A(2)}$	2	CR_2	Lab stock	Homozygous viable
UAS-Sb RNAi	3	TM6B	From V1613	
UAS-EGFR1	3	N/A	BL9532	
UAS-EGFR2	3	N/A	BL9535	
UAS-EGFR RNAi	3	N/A	BL36770	
UAS-RhoGEF2	2	N/A	BL9387	
UAS-RhoGEF2 RNAi	3	N/A	BL34643	
UAS-RhoGAP p190	2	Cyo or Cyo, actGFP	BL6684	Cyo floating
UAS-mCD8:GFP	2	N/A	BL5137	Cyo floating

N/A= not available.

2. GAL4 Driver Expression Pattern

All of the GAL4 drivers were crossed to UAS-mCD8-GFP [123] and late third instar larvae were harvested for dissection. 20 virgin females of the UAS-mCD8-GFP strain were crossed to 5 males of each GAL4 driver in bottles. Crosses were turned over onto fresh media after 2 days. Adults were cleared after 2 days to avoid over-crowding in the culture. The larvae dissected in the experiments were staged to within 7 h of pupariation but have not been exposed to the pulse of 20-hydroxyecdysone that triggers imaginal disc morphogenesis. Bromophenol blue dye (0.1%) was added to the media which allowed for the selection of late third instar larvae based on the light blue color of the gut [120]. The gut of younger animals appeared purple and older animals appeared pale blue or white in color. GFP expressing larvae were selected by fluorescence microscopy. Leg, wing, eye antennal disc and haltere discs were dissected from larvae in Ringer's solution (130mM NaCl, 5mM KCl, 1.5mM $CaCl_2 \cdot 2H_2O$, 0.1% BSA). Freshly dissected imaginal discs were analyzed and pictured live without prior fixation using a Leica MZ16FA fluorescent microscope equipped with a Diagnostic Instruments RTKE spot 7.2 color mosaic camera.

3. Fly Crosses

All crosses were performed at 25ºC. Most of the crosses were set up using female UAS responder and GAL4 driver males except for UAS-Sb and experiments to determine the lethal phase. Progeny from each cross were scored using a light microscope for leg, wing

and eye phonotypes. Initially, crosses were set up in vials with 10 females and 5 males. Parental flies were turned over once after 5 days, and flies in vials were cleared after 5 days. F1 generations were scored for leg, wing and eye phonotypes until 18 days after the crosses were set up. All non-homozygous responders/ GAL4 drivers were rebalanced over florescent balancers (Cyo, actGFP or TM6B, dfd-EYFP). Crosses were set up with 100-150 females per cages (GAL4 driver) and 50 males (UAS responder). The media was changed every 22 hours. Prior to embryo collection the media was changed every two hours for three times. Embryo collections were incubated at 25ºC and fluorescent eggs were removed from the plates after 22 hours. The number of hatched and un-hatched eggs was then scored for 46 hours. For experiments to determine pupal lethality newly hatched larvae were transferred to vials after counting (50 larvae per vial). The vials were then scored for pupal formation for 18 days. In addition, test crosses were set up (e.g. GAL4 drivers X UAS-Rho1 N19) to confirm that the drivers were behaving as expected.

4. Data Analysis

The penetrance and severity of leg, wing and eye phenotypes was used to rank GAL4 expression strength for all combinations of drivers and responders. For non-parametric analysis, scores for each driver were treated as ordinal scale (score from 0-40 as penetrance and severity of phenotypes increases). Embryonic lethality was scored as 40, larval lethality as 35, pupal lethality as 30. Reduced adult viability was scored from 15 to

25 (n >30 as 15, 30≥n>10 as 20, n≤10 as 25) plus severity of leg, wing and eye phenotypes with a full score of 5 (81-100% as 5/3 each, 61-80% as 4/3 each, 41-60% as 3/3 each, 21-40% as 2/3 each, 1-20% as 1/3 each and 0% as 0 each). Crosses showing leg, wing and eye phenotypes with no effect on viability were scored with full score 15 (81-100% as 5 each, 61-80% as 4 each, 41-60% as 3 each, 21-40% as 2 each, 1-20% as 1 each and 0% as 0 each). The resulting scores were ranked using Friedman's non-parametric test.

CHAPTER FOUR: HEPARAN SULFATE PROTEOGLYCANS HAVE A TISSUE-SPECIFIC ROLE IN POLYAMINE TRANSPORT IN *DROSOPHILA*

Abstract

Polyamine transport is a basic biological process found in almost all living organisms. Polyamines have been linked to many human diseases, like cancer, Africa sleeping disease and malaria. Intracellular polyamine content is tightly regulated by polyamine biosynthesis, catabolism and transport. The polyamine biosynthesis pathway has been well studied in both prokaryotes and eukaryotes. However, the mechanism of polyamine transport in multicellular organisms is still largely unknown after decades of studies. Although a few components of the mammalian transporter have been identified, it is currently unclear how many different polyamine transporters are involved, or whether the known transporter components belong to one or more transport systems. Glypican-1 was identified as having a role in polyamine transport in Chinese Hamster Ovary (CHO) cells. In this chapter, I demonstrate that Glypican-1 is required for polyamine transport in *Drosophila* imaginal discs but is apparently not required for transport across the gut. Two additional proteoglycan core proteins, Perlecan and Syndecan, and specific enzymes of the heparan sulfate biosynthesis pathway were tested but their involvement in polyamine transport could not be confirmed. The genes, nitric oxide synthase (Nos), scaffold attachment factor B (SafB) and huntingtin interacting protein 1 (Hip1) were tested in whole animals and do not appear to have a role in polyamine transport in *Drosophila*.

Introduction

Glypican-1 is a member of the core proteins constituting a family of glycosylphosphatidyl-inositol-anchored cell surface heparan sulfate proteoglycans (HSPG) [66]. In Chinese Hamster Ovary (CHO) cells, polyamines bind with high affinity to heparan sulfate (HS) glycosaminoglycan side-chains [67]. Treatment of CHO cells with an anti-HS antibody decreases polyamine uptake and attenuates polyamine-dependent cell proliferation [68]. In addition, recycled Glypican-1 is co-localized with spermine, and reduction of Glypican-1 levels inhibits spermine uptake and intracellular delivery of spermine [62]. Collectively, these data indicate that polyamines bind to heparan sulfate (HS) glycosaminoglycan side-chains and are then co-transported with Glypican-1 into mammalian cells. However, it is unknown if Glypican is the only proteoglycan core protein involved in polyamine transport or if any specific structure of heparan sulfate side chain is necessary for polyamine binding. In this study, I tested three proteoglycan core proteins, glypican, perlecan and syndecan for roles in polyamine transport in *Drosophila*. Heparan sulfate side chain biosynthetic enzymes were also tested.

Our laboratory has shown that a *Drosophila* P_{5B}-Type ATPase is required for polyamine transport (Barnett, Brown and von Kalm unpublished data). Based a high throughput screen for protein-protein interactions I identified two proteins, huntingtin interacting protein 1 (Hip1) and scaffold attachment factor B (SafB), that exhibited high confidence physical interactions with the *Drosophila* P_{5B}-Type ATPase [126]. Hip1 is a clathrin coat

binding protein active in endocytosis, the process through which polyamines enter the cell [86, 127, 128]. Hip1 is overexpressed in a variety of malignancies and lymphomas and is critical for cell survival [129-131]. Interestingly, Hip1 is also a membrane associated protein in sperm and is critical for spermatogenesis, a process involving spermine [127, 132]. SafB is a scaffold protein and interacts physically with a serine/arginine protein kinase, which is an important component of polyamine transport in yeast [133, 134]. In addition, SafB was recently reported to be involved in to breast cancer [135]. Finally, I studied Nitric oxide synthase (Nos) which is required for release of polyamines from HSPG binding in T24 cells and HCT116 colon cancer cells [62].

Results and Discussion

Drosophila has three proteoglycan core proteins: Glypican, Perlecan and Syndecan. In *Drosophila* there are two Glypican genes, dally and dally-like, and one gene for Perlecan and Syndecan respectively. At the Bloomington Stock Center there are 3 stocks targeting 3 unique sequences of the gene dally for RNAi, 4 stocks targeting 3 different sequences of the gene dally-like for RNAi, 3 stocks targeting 3 unique sequences of the gene Perlecan for RNAi, and 1 RNAi stock for Syndecan.

1. *Results of Crossing Six GAL4 Drivers with or Without Dicer Expression to RNAi Lines of Proteoglycan Core Proteins*

To test the involvement of proteoglycan core proteins in polyamine transport using imaginal disc culture, RNAi against proteoglycan core proteins was used. RNAi expression was controlled by crossing these UAS-RNAi lines to different GAL4 drivers. In order to get viable imaginal discs to test in culture, the viability of flies following RNAi expression was verified (Table 4). In Table 4, six GAL4 drivers were crossed to 11 lines expressing RNAi against proteoglycan core proteins. Dicer is a protein involved in RNAi processing, which enhances the RNAi effect in *Drosophila* [136]. Therefore, five GAL4 drivers with added Dicer expression were also tested. Introduction of UAS-Dicer into flies containing the TubP-GAL4 driver caused lethality so this driver-UAS-Dicer combination was not used.

Table 4 Results of six GAL4 drivers with or without Dicer expression crossing to RNAi lines of proteoglycan core proteins at 25°C.

GAL4 driver		Dally RNAi lines			Dally-like RNAi lines				Perlecan RNAi lines			Syndecan RNAi line
		V14136	BL28747	BL33952	V10299	V10298	BL34089	BL34091	V24549	BL29440	BL22642	V13322
-Dcr	30A	P: 6 d E:10 d A: viable	P: 6 d E:10 d A: viable	P: 6 d E:11 d A: viable	P: 6 d E:10 d A: viable	P: 6 d E:10 d A: viable	P: 7 d E:10 d A: viable	P: 7 d E:12 d A: viable	P: 6 d E:10 d A: viable	P: 6 d E:10 d A: viable	N/A	P: 7 d E:11 d A: viable
	71B	P:7 d E:11 d A: viable	P: 6 d E:10 d A: viable	P: 6 d E:11 d A: viable	P: 6 d E:11 d A: viable	P: 6 d E:11 d A: viable	P: 6 d E:10 d A: viable	P: 5 d E:9 d A: viable	P: 6 d E:10 d A: viable	P: 6 d E:11 d A: viable	N/A	P: 7 d E:11 d A: viable
	32B	P: 6 d E:10 d A: viable	P: 6 d E:10 d A: viable	P: 7 d E:11 d A: viable	P: 6 d E:10 d A: viable	P: 6 d E:10 d A: viable	P: 7 d E:11 d A: viable	P: 7 d E:11 d A: viable	P: 6 d E:10 d A: viable	P: 6 d E:10 d A: viable	N/A	P: 7 d E:11 d A: viable

GAL4 driver		Dally RNAi lines			Dally-like RNAi lines				Perlecan RNAi lines			Syndecan RNAi line
		V14136	BL28747	BL33952	V10299	V10298	BL34089	BL34091	V24549	BL29440	BL22642	V13322
-Dcr	69B	P: 6 d E:10 d A: viable	P: 6 d E:10 d A: viable	P: 6 d E:10 d A: viable	P: 6 d E:10 d A: viable	P: 6 d E:11 d A: viable	P: 6 d E:10 d A: viable	P: 7 d E:11 d A: viable	P: 6 d E:10 d A: viable	P: 7 d E:11 d A: viable	N/A	P: 7 d E:11 d A: viable
	T80	P: 7 d E:11 d A: viable	P: 6 d E:10 d A: viable	P: 7 d E:12 d A: viable	P: 7 d E:11 d A: viable	P: 6 d E:11 d A: viable	P: 7 d E:11 d A: viable	P: 6 d E:11 d A: viable	P: 7 d A: pupal lethal	P: 7 d E:11 d A: viable	N/A	P: 7 d E:11 d A: viable
	TubP	P: 6 d E:10 d A: viable	P: 6 d E:10 d A: viable	P: 6 d E:10 d A: viable	P: 7 d E:10 d A: viable	P: 7 d E:11 d A: viable	P: 7 d E:11 d A: reduced viability	P: 7 d E:11 d A: viable	Larval or embryonic lethal	No eclosion	Larval or embryonic lethal	P: 8 d A: pupal lethal

GAL4 driver		Dally RNAi lines			Dally-like RNAi lines				Perlecan RNAi lines			Syndecan RNAi line
		V14136	BL28747	BL33952	V10299	V10298	BL34089	BL34091	V24549	BL29440	BL22642	V13322
+Dcr	30A	P: 7 d E:11 d A: viable	P: 7 d E:12 d A: viable	P: 7 d E:11 d A: viable	P: 7 d E:11 d A: viable	P: 8 or 9 d E:12 d A: viable	P: 7 d E:12 d A: viable	P: 7 d E:12 d A: viable	P: 7 d E:11 d A: viable	P: 7 d E:10 d A: viable	P: 8 d E:12 d A: viable	P: 7 d E:11 d A: viable
	71B	P: 7 d E:11 d A: viable	P: 7 d E:13 d A: viable	P: 9 d E:12 d A: viable	P: 7 d E:12 d A: viable	P: 7 d E:14 d A: viable	P: 8 d E:12 d A: viable	P: 8 d E:12 d A: viable	P: 8 d E:14 d A: viable	P: 8 d E:12 d A: viable	P: 7 d E:12 d A: viable	P: 9 d E:15 d A: reduced viability
	32B	P: 7 d E:11 d A: viable	P: 7 d E:11 d A: viable	P: 7 d E:11 d A: viable	P: 7 d E:12 d A: viable	P: 7 d E:11 d A: viable	P: 7 d E:11 d A: viable	P: 7 d E:12 d A: viable	P: 7 d E:11 d A: reduced viability	P: 7 d E:12 d A: viable	P: 8 d E:12 d A: viable	P: 7 d E:14 d A: reduced viability, malformed wings

GAL4 driver		Dally RNAi lines			Dally-like RNAi lines				Perlecan RNAi lines			Syndecan RNAi line
		V14136	BL28747	BL33952	V10299	V10298	BL34089	BL34091	V24549	BL29440	BL22642	V13322
+Dcr	69B	P: 7 d E:12 d A: viable	P: 7 d E:12 d A: viable	P: 7 d E:12 d A: viable	P: 7 d E:12 d A: viable	P: 7 d E:13 d A: viable	P: 7 d E:11 d A: viable	P: 7 d E:12 d A: viable	P: 7 d E:13 d A: viable	P: 7 d E:11 d A: viable	P: 8 d E:12 d A: viable	P: 8 d E:17 d A: reduced viability, malformed wings
	T80	P: 7 d E:12 d A: viable	P: 7 d E:11 d A: viable	P: 7 d E:11 d A: viable	P: 7 d E:12 d A: reduced viability	P: 7 d E:11 d A: viable	P: 7 d E:13 d A: viable	P: 8 d E:12 d A: viable	P: 7 d A: pupal lethal	No eclosion	P: 7 d A: pupal lethal	Larval or embryonic lethal

Dcr: UAS-Dicer-2D; P: pupa forming day from crosses set up; E: eclosion day from crosses set up; A: adult viability.

As show in Table 4, all RNAi lines were viable when crossed to 30A-GAL4 and 71B-GAL4, which is consistent with my findings in chapter 3 as these two weak drivers are useful to obtain viable animals when expressing of toxic constructs. Introduction of Dicer expression to 30A-GAL4 did not alter viability but did slow down development by 1 to 2 days in some cases. Introduction of Dicer expression to 71B-GAL4 slowed down development but did not change viability except the Syndecan RNAi line. The 32B-GAL4 and 69B-GAL4 drivers, which have stronger expression strength, were also tested. In the absence of Dicer expression, all RNAi lines were viable when crossed to the 32B-GAL4 and 69B-GAL4 drivers. Introduction of Dicer slowed down development and in some cases resulted in reduced viability and malformation of adult wings. T80-GAL4 is a strong driver and is expressed ubiquitously in the *Drosophila* embryo and third instar larval stages [137]. Following crossing to T80-GAL4, all RNAi lines were viable without Dicer expression and introducing Dicer expression resulted in delay of development, viability reduction and in some cases death. Finally, TubP-GAL4 is a driver that expresses strongly and ubiquitously during all stages of development. TubP-GAL4 in the absence of Dicer expression resulted in reduced viability and death in many RNAi lines as shown in Table 4.

2. *Crossing the Actin5-GAL4 Driver with Dicer Expression to RNAi Lines of Proteoglycan Core Proteins*

Our laboratory has developed a simple assay to identify genes involved in polyamine transport *in vivo*. Briefly intact animals or cultured imaginal discs are grown/incubated in the presence of DFMO to block polyamine biosynthesis and induce lethality. Exogenous polyamines are added to the culture medium and if the transport system is functional these polyamines will be taken up and animal/imaginal disc viability will be rescued. However, if RNAi against a particular gene inactivates the transport system, animal/disc viability will not be rescued in the presence of DFMO indicating that the gene is required for polyamine transport. In the experiments employing this assay I used an Actin5-GAL4 driver (with Dicer expression) to drive RNAi expression. The results of RNAi against proteoglycan core proteins are shown in Table 5. For dally RNAi, flies of all 3 lines were viable. However, for dally-like RNAi expression, only 2 of the 4 RNAi lines were fully viable, 1 line showed reduced viability and the other line was pupal lethal. For Perlecan, viabilities of all 3 RNAi lines were reduced. Syndecan RNAi resulted in larval or embryonic death at 25°C.

Table 5 Results of Actin5- GAL4 driver with Dicer expression crossing to RNAi lines of proteoglycan core proteins at 25°C.

GAL4 driver	Dally RNAi lines			Dally-like RNAi lines				Perlecan RNAi lines			Syndecan RNAi line
	V14136	BL28747	BL33952	V10299	V10298	BL34089	BL34091	V24549	BL29440	BL22642	V13322
Actin5 + Dcr	P: 8 d E:12 d A: viable	P: 8 d E:12 d A: viable	P: 8 d E:12 d A: viable	P: 8 d A: pupal lethal	P: 8 d E:12 d A: reduced viability	P: 8 d E:12 d A: viable	P: 8 d E:12 d A: viable	P: 8 d E:13 d A: reduced viability	P: 8 d E:14 d A: reduced viability	P: 8 d E:12 d A: reduced viability	Larval or embryonic lethal

P: pupa forming day from crosses set up; E: eclosion day from crosses set up; A: adult viability.

3. *Glypican-1 Is Required for Polyamine Transport in Imaginal Discs*

After determining the viability of proteoglycan core protein RNAi lines, I asked if these genes were required for polyamine transport in imaginal discs. I used two different assays to test for involvement in polyamine transport. The first approach involved treating RNAi expressing lines with a toxic polyamine analogue Ant44. Ant44 is taken up into imaginal discs via polyamine transport system [94]. I expected to see reduced sensitivity to Ant44 in RNAi lines if the core protein was involved in polyamine transport. The second approach involved testing the ability of native polyamines to rescue DFMO treated imaginal discs. In this case I expect to see inhibition of rescue by the native polyamines in RNAi lines where the core protein is required for transport.

3.1 Ant44 Effect on Glypican RNAi Lines

Ant44 at 50µM was toxic to disc development in wild type animals (Oregon R), resulting in less than 2%-disc development (Figure 16). RNAi expression against the dally or dally-like glypican genes of *Drosophila* reduced Ant44 toxicity and resulted in about 30% and 20%-disc development respectively (Figure 16). Thus, dally and dally-like are likely to be involved in the import of Ant44 into imaginal discs.

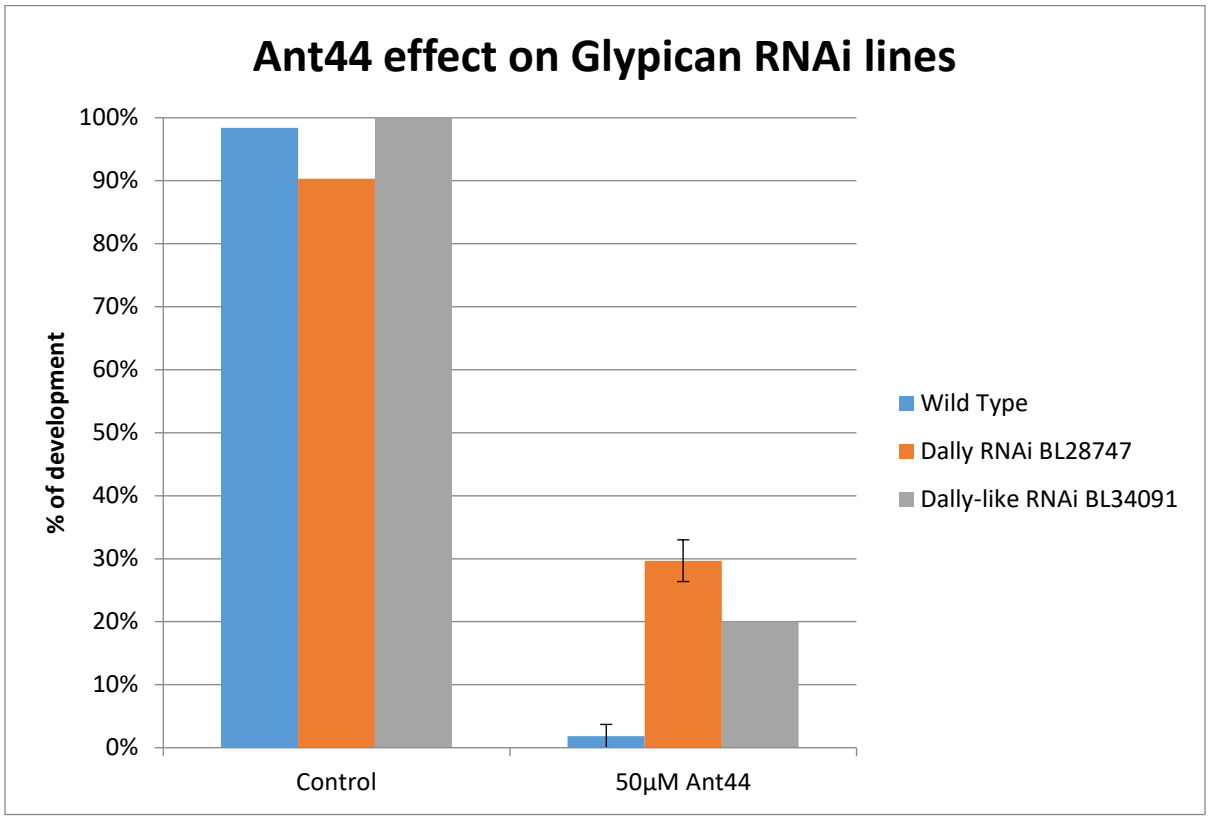

Figure 16 Dally and Dally-like RNAi expressing larvae are less sensitive to Ant44 in imaginal disc culture.

In this graph, 50µM Ant44 treated wild type (Oregon R) data is based on 2 replicates and 50µM Ant44 treated Dally RNAi BL28747 data is based on results of 3 replicates. All other data was calculated from 1 replicate. TubP-GAL4 was used in these experiments to drive RNAi expression.

3.2 Rescuing DFMO Inhibition by Native Polyamines in Dally RNAi Lines

Two dally RNAi lines were tested for their ability to rescue DFMO inhibition when supplemented with native polyamines (Figures 17 and 18). In all the RNAi line experiments, the sibling lines from the same cross were used as control lines in order to get the closest matched genetic background. In Figure 17, one of the dally RNAi lines

(BL33952) was able to block DFMO rescue by exogenous putrescine, spermidine and spermine. The IC_{50} of DFMO inhibition to imaginal disc development was 4mM. Line BL33952 had similar sensitivity to DFMO as the control line at both 10mM and 4mM, indicating that the decreased rescue was not due to increased sensitivity to DFMO in the RNAi expressing line.

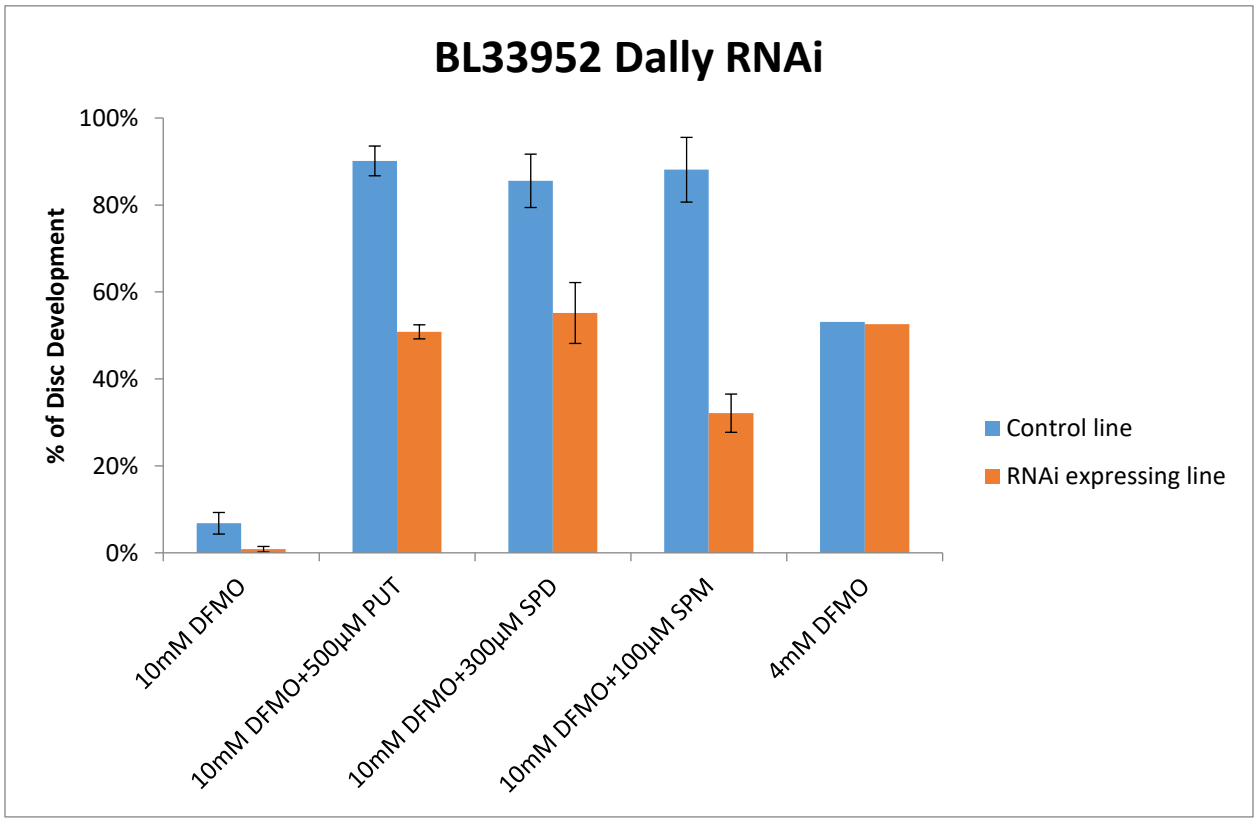

Figure 17 Dally RNAi expression (BL33952) blocked DFMO inhibition rescued by native polyamines.

All experiments were repeated at least 3 times separately except the 4mM DFMO data, which was the result of 1 replicate. The control line was the sibling class from the cross. T80-GAL4 with UAS-Dicer was used in these experiments to drive RNAi expression.

Another dally RNAi line (V14136) was able to block DFMO rescue by putrescine and spermine, but not spermidine at 300µM (Figure 18). Therefore, the concentration of spermidine was titrated to rescue DFMO inhibition in both the control line and the RNAi expressing line. Though only tested once, the control line and the RNAi line showed a big difference in DFMO rescue by spermidine at 100µM and 50µM.

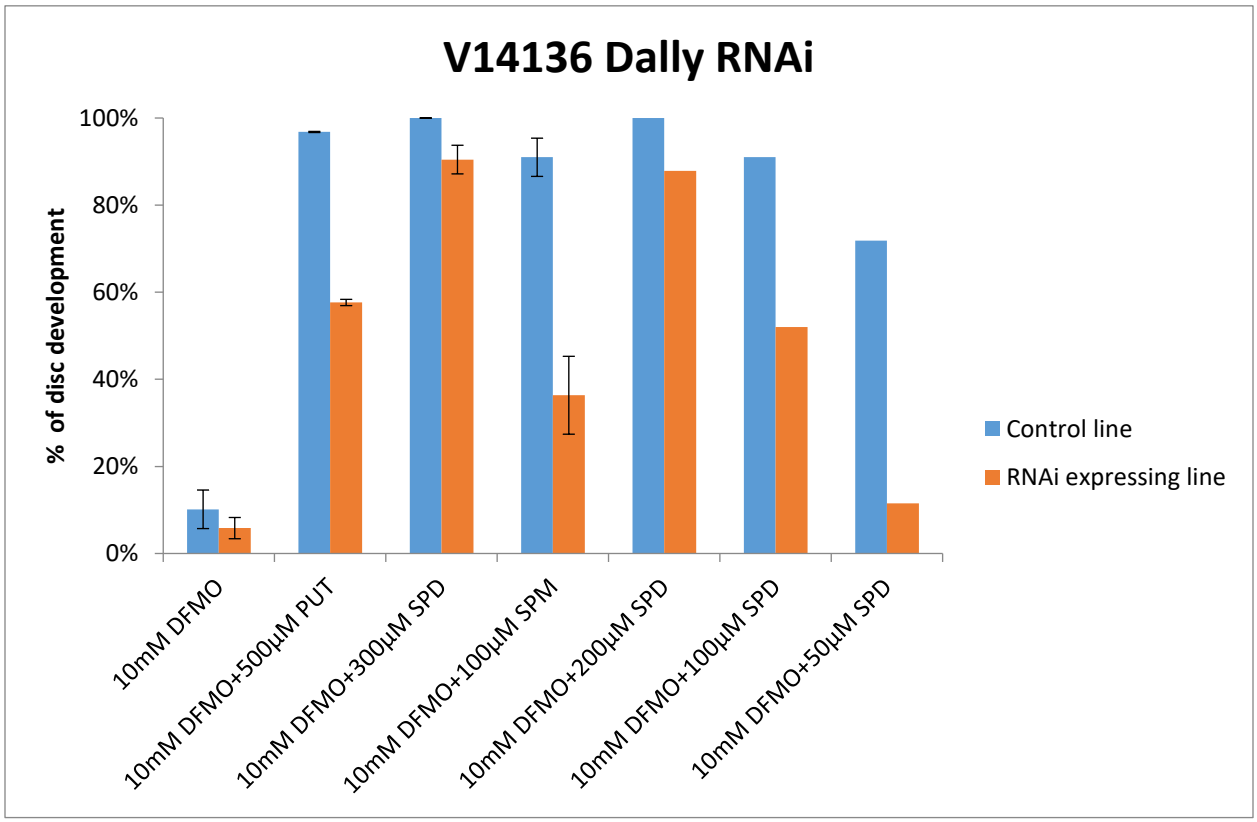

Figure 18 Dally RNAi expression (V14136) blocked DFMO inhibition rescued by native polyamines.

The first 4 sets of data shown in the figure were repeated at least 3 times separately. The rest were results from 1 replicate. The control line was the sibling class from the cross. T80-GAL4 with UAS-Dicer was used in these experiments to drive RNAi expression.

3.3 Rescuing DFMO Inhibition by Putrescine in Dally-like RNAi Line (BL34091)

Rescuing DFMO inhibition in the dally-like RNAi line was tested once using putrescine (Figure 19). Compared to the control line, the ability of putrescine to rescue DFMO inhibition was decreased in the dally-like RNAi expressing line indicating that dally-like is required for polyamine transport.

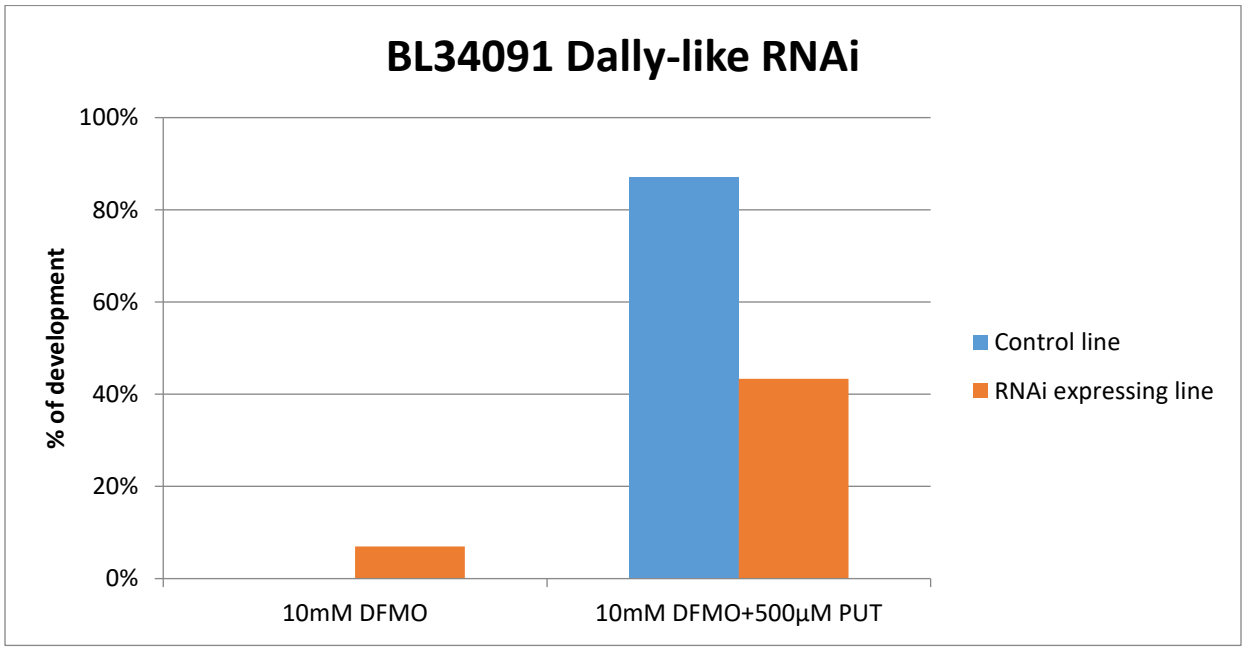

Figure 19 Dally-like RNAi expression (BL34091) blocked DFMO inhibition rescued by putrescine.

All data were results from 1 replicate. Control line was the sibling class from the cross. T80-GAL4 with UAS-Dicer was used in these experiments to drive RNAi expression.

In conclusion, RNAi against both dally and dally-like showed reduced sensitivity to Ant44 and was able to block DFMO inhibition rescued by native polyamines in imaginal disc

culture. Thus, both glypican proteins are required for polyamine transport in imaginal discs.

I did not use the imaginal disc assay for further experiments because it was very difficult to get enough material for dissection. Instead I performed the assay in a whole animal context which essentially assays for uptake through the gut.

4. *Glypican, Perlecan, Syndecan and Enzymes in the Heparan Sulfate Biosynthesis Pathway Are Not Required for Polyamine Transport in Intact Animals*

The whole animal assay described above has been successfully used to identify a component of the polyamine transport in *Drosophila* (Barnett, Brown and von Kalm unpublished data). In this study, the involvement of HSPG (including core proteins and biosynthetic enzymes of the heparan sulfate side chain) and some other genes (Nos, Hip1 and SafB) were tested for a role in polyamine transport by using RNAi, mutants or overexpression of candidate genes. A summary of genes tested is shown in Table 6.

Table 6 Summary of genes tested in whole animals for involvement in polyamine transport in *Drosophila*

Name of Genes			Stocks	Results	Note
Heparan Sulfate Proteoglycan	Core proteins	Dally (Glypican)	3 RNAi lines	No effect	
		Dally-like (Glypican)	4 RNAi lines	No effect	2 stocks have reduced viability following RNAi
		Perlecan	2 RNAi lines	No effect	Reduced viability
		Syndecan	1 RNAi line 4 mutants 1 overexpression line	No effect	Reduced viability (RNAi and overexpression)
		Dally/Dally-like double knockdown	2 RNAi lines	No effect	Reduced viability
		Dally/Syndecan double knockdown	1 RNAi line	No effect	Increased viability than Sdc RNAi alone at 18 °C
	Biosynthetic enzymes	Sugarless	1 RNAi line	No effect	Reduced viability
		Slalom (PAPS)	2 RNAi lines	No effect	Both stocks have reduced viability
		Tout velu	1 RNAi line	No effect	Reduced viability
		Brother of Tout velu	1 RNAi line	No effect	Reduced viability

Name of Genes			Stocks	Results	Note
Heparan Sulfate Proteoglycan	Biosynthetic enzymes	Fringe Connection (GlcAT)	2 RNAi lines	No effect	
		Sulfateless (NDST)	2 RNAi lines	No effect	Reduced viability
		Hsepi	1 mutant	No effect	
Other genes		Nitric Oxide Synthase (Nos)	1 RNAi line 1 mutant	No effect	Reduced viability
		Scaffold attachment factor B (SafB)	1 mutant	No effect	
		Huntingtin interacting protein (Hip1)	1 RNAi line 1 mutant	No effect	

4.1 Testing Involvement of Heparan Sulfate Proteoglycans (HSPG) in Polyamine Transport Using Intact Animals

Heparan sulfate proteoglycans (HSPG) are required for polyamine transport in vertebrate cells [62, 67]. One of the core proteins, Glypican-1 has been identified as a component in polyamine transport and is required for spermine uptake into mammalian cells. Moreover, the heparan sulfate (HS) glycosaminoglycan side-chains of HSPG are required for polyamine transport into CHO cells [67]. Polyamines bind to HS side-chains and are co-transported with Glypican-1 into the cell following HS side-chain cleavage [62, 68]. Therefore, I asked if Glypican and HS side-chain biosynthetic enzymes are required for polyamine transport into the *Drosophila* gut. Also, I expanded this study by looking at the involvement of other core proteins (Perlecan and Syndecan) in polyamine transport.

i. Testing Involvement of Core Proteins of HSPG in Polyamine Transport

Three proteoglycan core proteins were studied for polyamine transport using the whole animal method. A summary is shown in Table 6 and details were shown in Appendix Figures 20-40.

Dally: Three dally RNAi lines were tested (Appendix Figure 20-24). One of these RNAi lines was from the Vienna Stock Center and the other two were from the Transgenic RNAi Project. These RNAi lines target different sequences of the gene and had different genetic

backgrounds. When using the Actin5-GAL4 driver for RNAi expression, none of these stocks showed reduced viability (Table 5). However, none of them showed inhibition of polyamine rescue in the presence of DFMO, which indicated polyamine transport was functioning in these RNAi lines. Similar results were obtained using the T80-GAL4 and TubP-GAL4 as drivers for RNAi expression (data not shown).

Since glypican 1 was expected to be involved in polyamine import, these results with RNAi against glypican 1, contradicted prior cell culture data and the results obtained with the imaginal disc assay. One possible explanation may be that in the whole animal method the primary affected tissue of the animals is the gut and dally is not required for polyamine transport in this specific tissue. Another explanation is the possible redundancy of the transport system in whole animals compared to cell culture or imaginal discs of *Drosophila,* which are isolated cells or tissues.

Dally-like: Four dally-like RNAi lines were tested (Appendix Figures 25-29). Two of them were from the Vienna Stock Center targeting the same sequences of the gene and the other two were from the Transgenic RNAi Project targeting different sequences of the gene. When driven with Actin5-GAL4, the two lines from the Vienna Stock Center could not form viable adults (Table 5), which indicated RNAi expression was working properly. However, none of them showed the ability to inhibit polyamine rescue in the presence of DFMO, which indicated polyamine transport was functioning in these RNAi lines. Some

of these experiments were repeated using the T80-GAL4 and TubP-GAL4 drivers with similar results (data not shown).

Perlecan: Two perlecan RNAi lines were tested (Appendix Figures 30-31). One of them was from the Vienna Stock Center and the other one was from the Transgenic RNAi Project. Each of them targeted different sequences of the gene. When driving with Actin5-GAL4, neither line could form viable adults (Table 5), which indicated RNAi expression was working properly. However, neither of the lines showed the ability to block polyamine rescue in the presence of DFMO suggesting that perlecan is not involved in polyamine transport in the presence of DFMO.

Syndecan: One RNAi line, one overexpression line and four mutants were tested for involvement of syndecan in polyamine transport in *Drosophila* (Appendix Figures 32-37). When driving with Actin5-GAL4, the RNAi line was larval lethal at 25^0C (Table 5), therefore, this experiment was performed at 18^0C to reduce GAL4 expression. The overexpression line driven by Actin5-GAL4 could not form viable adults. However, neither RNAi expression or the over-expression line had an ability to inhibit polyamine rescue in the presence of DFMO (Appendix Figures 32-33). Homozygous unviable mutants were tested as heterozygotes (Appendix Figures 34-37), however, none showed the ability to inhibit polyamine rescue in the presence of DFMO.

Double knockdown: In order to see if redundancy was the reason for the inability to block polyamine rescue in the presence of DFMO, double knockdown stocks of dally/dally-like and dally/syndecan were made and tested using the whole animal method (Appendix Figures 38-40). However, none of these lines showed an ability to inhibit polyamine rescue in the presence of DFMO.

In conclusion, we could not confirm the involvement of glypican (dally and dally-like), Perlecan or Syndecan in polyamine transport using the whole animal method. While redundancy of the polyamine transport system in the whole animal context provides one explanation, the double knockdown experiments above suggest otherwise. Another explanation of our failure to see the desired phenotype (inhibition of polyamine rescue in the presence of DFMO) is that the primary tissue affected in the whole animal method is the gut and the core proteoglycan proteins may not be required for polyamine transport in this specific tissue.

ii. Testing Involvement of Biosynthetic Enzymes of HSPG in Polyamine Transport

The biosynthetic enzymes required for constructing the heparan sulfate side chain were tested using RNAi lines as a way to assess the requirement of specific heparan structures in polyamine transport. The following enzymes were evaluated for their role in polyamine transport: Sugarless, Slalom, Tout velu (Ttv), Brother of Tout velu (Botv), Fringe

Connection, Sulfateless, Hsepi. None of the lines were able to form viable adults following RNAi expression (Appendix Figures 41-52). In addition, none of the RNAi experiments showed the ability to inhibit polyamine rescue in the presence of DFMO.

In conclusion, we could not confirm the involvement of Heparan sulfate biosynthetic enzymes in polyamine transport.

4.2 Involvement of Genes that Interact Physically with Polyamine Transporters Using Whole Animal Method

For Nos, one RNAi line and one mutant were tested for inhibition of polyamine rescue in the presence of DFMO (Appendix Figures 53-54). For the RNAi line, no viable adults eclosed from the RNAi expressing class, which indicated the RNAi was functioning. The mutant was a transposon insertion in intron 5, therefore, it is not sure if gene function was disrupted in the mutant. Neither the RNAi line or mutant inhibited rescue by polyamines in the presence of DFMO.

For Hip1, two RNAi lines and one mutant were tested for their ability to inhibit polyamine import in the presence of DFMO (Appendix Figures 55-57). The insertion site of the mutant tested in this studied was in the second to last exon. In both RNAi lines, no reduction of viability was observed when crossing to Actin5-GAL4 for RNAi expression.

However, these stocks could be rescued by supplementing polyamines in the presence of DFMO, which suggested that polyamine transport was functioning.

For SafB there was only one mutant available to test (Appendix Figure 58). The insertion site of the mutant tested in this study was in the 5' UTR. Similar as to what was found with Nos and Hip1, no block of rescue by polyamines in the presence of DFMO was observed.

In conclusion, we could not confirm the involvement of Nos, Hip1 or SafB in polyamine transport in *Drosophila* using this whole animal method.

Materials and Methods

1. *Stocks Information*

Table 7 and Table 8.

Table 7 Information of RNAi, mutant and overexpression lines used in experiments.

Targeting Gene	Stock	Chromosome location	Balancer	Source	Note
Dally-like RNAi	V10298	3	TM6B, Tb, Sb, EYFP	Vienna	These two stocks target the same sequence of the gene
	V10299	3	N/A	Vienna	
	BL34089	3	N/A	Trip	V20
	BL34091	3	N/A	Trip	V20
Dally RNAi	V14136	3	N/A	Vienna	
	BL33952	3	N/A	Trip	V20
	BL28747	3	N/A	Trip	V10
Perlecan RNAi	V24549	2	N/A	Vienna	
	BL29440	3	TM6B, Tb, Sb, EYFP	Trip	V10, w floating
Syndecan RNAi	V13322	3	N/A	Vienna	
Syndecan overexpression	BL8564	3	N/A	Bloomington	
Syndecan mutants	BL23972	2	N/A	Bloomington	Transposon was inserted in intron 1
	BL19695	2	Cyo	Bloomington	Testing heterozygous, transposon was inserted in the last intron

Targeting Gene	Stock	Chromosome location	Balancer	Source	Note
Syndecan mutants	BL36954	2	SM6a	Bloomington	Testing heterozygous, transposon was inserted in intron 4
	BL37444	2	SM6a	Bloomington	Testing heterozygous, transposon was inserted in intron 4
Sulfateless RNAi	V5070	3	N/A	Vienna	
	BL34601	3	N/A	Trip	V20
Tout velu RNAi	V4871	3	N/A	Vienna	
Brother of Tout velu RNAi	V37185	2	N/A	Vienna	
Fringe Connection RNAi	V47542	2	Cyo, dfd-EYFP	Vienna	
	V47543	3	N/A	Vienna	
Slalom RNAi	V12148	3	N/A	Vienna	
	V12149	3	TM6B, Tb, Sb, EYFP	Vienna	
Sugarless RNAi	V29434	2	N/A	Vienna	
Nitric Oxide Synthase RNAi	BL28792	3	N/A	Trip	V10

Targeting Gene	Stock	Chromosome location	Balancer	Source	Note
Nitric Oxide Synthase mutant	BL18555	2	N/A	Bloomington	Transposon was inserted in intron 5
Hsepi mutant	BL13498	2	N/A	Bloomington	Cyo, ry floating, transposon was inserted in exon 3, in the 5' UTR
Hip1 RNAi	BL38377	2	N/A	Trip	V20, Sc, Cyo floating
	BL32504	3	N/A	Trip	V20
Hip1 mutant	BL42355	3	N/A	Bloomington	TM3, Sb^1, Ser^1 floating, transposon was inserted in the 2^{nd} last exon
SafB mutant	BL32026	3	N/A	Bloomington	TM6C floating, transposon was inserted in exon 1, in 5' UTR
CG32000 mutant	BL23396	4	N/A	Bloomington	
	BL16262	4	N/A	Bloomington	

Table 8 GAL4 driver information

GAL4 drivers	Stock number	Chromosome location	Balancer	Source	Note
Act5-GAL4	BL25708	2	Cyo, dfd-EYFP	Trip	Including UAS-Dcr2 on the 1st chromosome
TubP-GAL4	BL5138	3	TM6B, Tb, Sb, EYFP	Bloomington	
T80-GAL4	BL1878	2	Cyo, dfd-EYFP	Bloomington	With/ without UAS-Dcr2 on the 3rd chromosome
30A-GAL4	BL1795	2	Cyo, dfd-EYFP	Bloomington	With/ without UAS-Dcr2 on the 3rd chromosome; homozygous viable
71B-GAL4	BL1747	3	N/A	Bloomington	With/ without UAS-Dcr2 on the 2nd chromosome
69B-GAL4	Lab stock	3	N/A	Bloomington	With/ without UAS-Dcr2 on the 2nd chromosome
32B-GAL4	BL1782	3	N/A	Bloomington	With/ without UAS-Dcr2 on the 2nd chromosome

2. *Crossing GAL4 Drivers with or Without Dicer Expression to RNAi Lines of Proteoglycan Core Proteins*

Crosses were set up using 5 males and 5 females in each vial. Vials were turned over into a second vial 4 days after setup. Flies in the second vial were cleared after 4 days. In all crosses, GAL4 drivers were virgin females except for one of the perlecan RNAi lines (BL22642). Crosses using this perlecan RNAi line (BL22642) were set up with virgin females of the RNAi line instead. GAL4 drivers used in all crosses were tested by crossing to UAS-RhoN19. No adult progeny survived in these test crosses, which indicated that the drivers were functioning properly. All the crosses were cultured at 25^0C.

3. *Crossing the Actin5-GAL4 Driver with Dicer Expression to RNAi Lines of Proteoglycan Core Proteins*

Crosses were set up using 5 males and 5 females in each vial. Vials were turned over into a second vial 5 days after setup. Flies in the second vial were cleared after 5 days. In all crosses, virgin females were Actin5-GAL4 driver. The Actin5-GAL4 driver was tested by crossing to UAS-RhoN19. No adult progeny survived which indicated the driver was functioning properly. All the crosses were cultured at 25^0C.

4. Larval Collections for Imaginal Disc Culture

The larvae used in the experiments were within 7 h of pupariation but have not been exposed to the pulse of 20-hydroxyecdysone that triggers imaginal disc morphogenesis. Bromophenol blue dye (0.1%) was added to the fly food and allowed for the selection of the late third instar larvae based on the light blue color of the larvae's gut [120]. The gut of younger animals appeared purple and older animals appeared pale blue or white in color. Imaginal discs dissected from larvae at this developmental stage are able to develop when exposed to 20-hydroxyecdysone in *in vitro* culture. For RNAi expression lines, crosses were set up in bottles using 20 female virgins and 5 males. RNAi expressing larvae were selected using a fluorescent microscope, where RNAi expressing lines were not fluorescent and the control sibling classes were fluorescent.

5. Imaginal Disc Culture and Scoring

Late 3rd instar larvae were selected for leg imaginal disc dissection via the blue food approach described above. Leg imaginal discs were dissected at room temperature in Ringer's solution (130 mM NaCl, 5mM KCl, 15 mM $CaCl_2 \cdot 2H_2O$) containing 0.1% BSA (w/v), which was added to the Ringer's solution immediately prior to use. The dissection was finished in approximately one hour so that the dissected leg imaginal discs would not be exposed to the Ringer's solution for too long, which may affect disc eversion. After dissection, discs were transferred to 12-well plastic culture plates containing Ringer's solution (1 mL). Before the disc culture medium was added, dissected leg imaginal discs

were washed once with 1× minimal Robb's medium. To begin cultures, a solution of 1 mL of 1× minimal Robb's medium (final concentration) containing 20-hydroxyecdysone (1µg/mL) and the tested compound was added to each well. A control experiment without added any tested compound was run in parallel. Imaginal discs were incubated for 18 h at 25°C. After 18 h, the discs were scored as developed or non-developed. Fully developed discs (the leg is fully extended from the epithelium) and partially developed discs (the leg protrudes from the epithelium but is not fully extended) were scored as developed. Non-developed discs showed no sign of development. For each experiment, the percent development was determined by ([(number of developed discs)/(total number of discs)] × 100).

6. Robb's Minimal Medium

2× Minimal Robb's medium consisting of 80 mM KCl, 0.8 mM KH_2PO_4, 80 mM NaCl, 0.8 mM $NaH_2PO_4 \cdot 7H_2O$, 2.4 mM $MgSO_4 \cdot 7H_2O$, 2.4 mM $MgCl_2 \cdot 6H_2O$, 2 mM $CaCl_2 \cdot 2H_2O$, 20 mM glucose, 8.0 mM L-glutamine, 0.32 mM glycine, 1.28 mM L-leucine, 0.64 mM L-proline, 0.32 mM L-serine, and 1.28 mM L-valine, pH 7.2) was prepared using a standard protocol and stored at -20° C. Immediately prior to use, 20 *µ*L of 10% BSA (w/v) was added to 1 mL of medium.

7. Whole Animal Experiments

Crosses or mutants were set up in cages with about 200 virgin females and 50 males. Grape plates attaching to the cage were changed every 22 hours. Newly hatched larvae (less than 4 h after hatching) with the right genotype were picked and transferred to freshly made instant food (Jazz Mix, from Fisher Scientific) with or without treatment added. Newly hatched larva were picked and cultured in food with or without treatment. Then the survival rate was scored. In every experiment, eight different conditions were tested. Four controls were used: no DFMO and no polyamine supplemented in the food; putrescine only; spermidine only and spermine only. Four treatment conditions were used: DFMO only; DFMO plus putrescine; DFMO plus spermidine and DFMO plus spermine. A previous study showed that 5mM DFMO was sufficient to knockdown survival rate to less than 5% in wild type flies (Oregon R). Also, in wild type Oregon R flies, neither putrescine, spermidine nor spermine showed any toxicity up to 1 mM and at this concentration all three types of native polyamines could rescue adult survival to untreated levels in the presence of 5 mM DFMO (unpublished data). Dilution experiments showed that 0.4 mM putrescine/ 0.2 mM spermidine/ 0.2 mM spermine were the minimum concentrations needed to rescue 5mM DFMO to untreated levels in wild type flies. Therefore, experiments were performed using these minimum concentrations as mentioned in the figures. Instant food preparation was done in the standard way as described in the manufacturer's instructions. Compounds were dissolved in water and added to instant food when it was at 50^0C. The total volume of instant food was 6 mL per vial and fifty of the selected larvae were added per vial. Experiments were kept at 25^0C (or 18^0C as

mentioned). The number of adult eclosed was recorded every day until no eclosion occurred for 3 consecutive days or 25 days after the start of the experiment. If there was no or low numbers of adults, pupae were scored. In each experiment, 3 replicates vials for each treatment were set up in the same week on 3 different days.

8. Statistical Analysis

Statistical analysis was performed using IBM SPSS Statistics 19 with one-way ANOVA.

CHAPTER FIVE: GENERAL DISCUSSION

Cellular polyamine content is tightly regulated by a combination of biosynthesis, biodegradation, import and export [13]. Polyamine levels are elevated in many cancer cell types by upregulated biosynthesis and import activity, and depletion of cellular polyamine content results in cancer cell growth attenuation [40, 43]. Therefore, polyamine depletion is an attractive chemotherapeutic target. Polyamine biosynthesis can be inhibited by α-difluoromethylornithine (DFMO), an inhibitor of the key polyamine biosynthesis enzyme ornithine decarboxylase [44]. However, malignant cells frequently circumvent DFMO therapy by up-regulating polyamine import and thus a combination drug therapy that simultaneously targets polyamine biosynthesis and transport is desirable [47-49]. To this end there is a need to identify compounds that inhibit polyamine transport, however the development of novel polyamine transport inhibitors (PTIs) is hindered by a poor understanding of the polyamine transport system in multicellular organisms.

This dissertation has two objectives. The first objective is to characterize polyamine transporter inhibitors. Four candidate polyamine transport inhibitors were assayed for their ability to inhibit transport in *Drosophila*. Three of the compounds effectively inhibited the uptake of a toxic polyamine analog Ant44 that gains entry to cells via the polyamine transport system, and were also able to inhibit the import of exogenous polyamines. In addition, a cocktail of polyamine transport inhibitors was found to be more effective than individual inhibitors at blocking transport.

The second objective was to identify new components of the polyamine transport system, which will help with transport inhibitor development. In this study, core proteins of the heparan sulfate proteoglycans and biosynthesis enzymes of the heparan sulfate side chain were tested for involvement in polyamine transport. Glypican-1 was demonstrated to be involved in polyamine transport in *Drosophila* imaginal discs confirming reports in mammalian cell culture.

Drosophila as a Model to Study Polyamine Transport

Drosophila is an excellent model system in which to study polyamine transport and many genes in *Drosophila* are functionally conserved in mammals. Studies in *Drosophila* have been the foundation for the characterization of numerous mammalian signaling pathways, including the Wnt, Hedgehog and Notch signaling pathways [90-92]. In addition, *Drosophila* has a polyamine transporter with properties similar to those observed in mammalian cells. Polyamine transport is active in *Drosophila* S2 cells [93] and our own work has demonstrated that polyamine transport into imaginal discs is similar to that observed in CHO and L1210 cells [94, 138].

In these studies, I used *Drosophila* leg imaginal discs to investigate polyamine transport. A major advantage of the leg imaginal disc assay is that compounds that access cells through the PTS or inhibit transport can be studied in an environment where cells exhibit

normal adhesion properties and are surrounded by extracellular matrix [97]. This environment is more reflective than cell culture of the environment candidate drugs will encounter *in vivo*. I have shown that the *Drosophila* model is a robust indicator of the effectiveness of PTIs in mammalian systems, and in the future it will be possible to pre-screen PTIs in *Drosophila* prior to conducting more expensive testing in mouse models. Having a cheap model system for early animal testing will greatly reduce to time from conceptual design of PTIs to validation in clinical trials.

Evidence for Multiple Polyamine Transporters

In this study, I have shown that 1 mM putrescine is unable to rescue the toxicity of 40 µM Ant44 (Chapter 2, Figure 9). This result is consistent with the notion that putrescine and Ant44 utilize different transporters to gain entry to cells. The choice of transporter may be charge-dependent because unlike the diamine putrescine, Ant44 is a triamine and presents three positive charges to the putative cell surface receptor. Consistent with these observations, Ant44 is a homospermidine analogue and its toxicity can be rescued by the higher polyamines SPD and SPM.

Interestingly, even though Ant444 and Trimer44 have similar EC_{50} values for protection against Ant44 toxicity, and similar profiles for full protection against Ant44 (Chapter 2, Figure 7a, c), they show different specificities in blocking the uptake of native polyamines

in DFMO treated imaginal discs. Ant444 is more effective than Trimer44 in inhibiting the import of putrescine, whereas Trimer44 is more effective in inhibiting the import of spermine (Chapter 2, Figures 11a, c). The differential selectivity of Ant444 and Trimer44 may be the underlying basis for the improved ability of a cocktail of these compounds to inhibit rescue in the presence of all three native polyamines (Chapter 2, Figure 11d). This difference in selectivity is consistent with the existence of multiple polyamine transport systems in *Drosophila* similar to those observed in the unicellular organisms *E. coli* and yeast.

E. coli contains putrescine and spermidine, but not spermine. It has a spermidine-preferential uptake system (PotABCD), putrescine transporter (PotE) and a putrescine-specific uptake system (PotFGHI) [57, 58, 139]. The Km values for spermidine and putrescine with these transporters are different [56], which further illustrates the diversity of polyamine transporters existing in *E.coli*.

Polyamine uptake in yeast is energy-dependent. There are a least 10 proteins involved in polyamine transport in yeast. In the plasma membrane, four transmembrane proteins have been identified as polyamine transport components: Dur3, Sam3, Agp2 and Gap1 [60, 140, 141]. Also, UGA4, which is a transporter of 4-aminobutyric acid on the vacuolar membrane can take up putrescine [142]. A general transporter of amino acids on the plasma membrane called GAP1 can transport putrescine and spermidine [60]. A polyamine export system is known in yeast. TOP1 and TOP4 are exporters for putrescine,

spermidine and spermine. TOP2 and TOP3 are spermine-specific exporters [143, 144]. Both uptake and export of polyamines in yeast are regulated by phosphorylation and dephosphorylation [56]. However, the known polyamine transport components in *E. coli* and yeast do not have close orthologs in animal cells.

In multicellular organisms, a few polyamine transport system (PTS) components have been identified [62, 63, 65, 76]. It is still unknown how these components interact, or whether they comprise one or more transport systems. However, our data support the existence of multiple polyamine transport systems.

Rational Design of Compounds Inhibiting Polyamine Transport

The polyamine transport system shows relatively high substrate tolerance. Many polyamine analogues are imported into cells via the polyamine transport system and the notion was explored that polyamine uptake could provide selective targeting of cancer cells via their upregulated polyamine transport activity. As a result, numerous polyamine analogues were developed as anti-tumor agents starting in the mid-1980s [145]. However, these analogues had off-target effects (including neurotoxicity and nephrotoxicity), which were dose limiting.

In our study, Triamide44 could not inhibit the uptake of either Ant44 or the import of exogenous polyamines. By increasing the chain length and the number of amine groups on the arms of the Triamide44, this compound was converted into a good PTI. Therefore, the PTI efficiency of Triamide444 was tested to evaluate how a PTI with tetraamine arms performed vs the triamine arms present inTriamide44.

The EC_{50} of Triamide444 (2.8 µM) was comparable to Ant444 (3.6 µM) and Trimer44 (4.8 µM) and showed a 50-fold improvement in potency compared to Triamide44 (144 µM) (Chapter 2, Figure 7). Triamide444 effectively blocks the rescue of DFMO by PUT (Figure 12a), SPD (Figure 12b) and SPM (Figure 12c). Triamide444 appeared to be a more effective PTI than Ant444, which was unable to inhibit SPM uptake at 100 µM, and in general showed an improved ability to inhibit SPM than either Ant444 or Trimer44 (Chapter 2, Figure 11). Therefore, the structure activity relationships explored here demonstrate that it is possible to use *Drosophila* models to develop improved polyamine transport inhibitors.

Feasibility of a Combination Drug Therapy Targeting Both Polyamine Biosynthesis Pathway and the Transport System

A combination therapy using DFMO and a PTI has shown promise in cancer growth inhibition. While the lack of knowledge of the genes and proteins involved in polyamine

transport has hampered the development of PTIs, SAR studies have nevertheless resulted in the development of several effective PTIs.

The HIV-Tat transduction peptide is a cationic peptide (GRKKRRQRRRPPQC). It can bind to heparin sulfate of proteoglycans with high affinity and is well known to carry large cargo (e.g., nuclear acids and proteins) across the cell membrane into the cytoplasm and nuclear compartment of mammalian cells [146, 147]. Previous studies showed that HIV-Tat competitively inhibited the uptake of polyamines in human bladder carcinoma T24 cells in the presence of DFMO [55]. Spermine transport was facilitated by heparan sulfate binding and HIV-Tat may share the same binding receptor on the cell surface. In a mouse model, HIV-Tat was able to inhibit T24 carcinoma-cell tumor growth in the presence of DFMO, and no serious side effects were noticed [55]. Therefore, HIV-Tat in combination with DFMO is a feasible treatment for tumor growth. However, no further studies have been published concerning HIV-Tat in tumor treatment. Off-target effects are a major problem of Tat cell-penetrating peptides and it is not clear if this off-target problem exists with the specific HIV-Tat transduction peptide used.

One of the most effective PTIs is AMXT-1501. It is relatively non-toxic (IC_{50} value of 62μM in MDA-231 cells) and facilitated oral delivery [53]. In combination with DFMO, AMXT-1501 inhibits cancer cell growth in several cancer cell lines and mouse models [53, 117]. Recently this compound was found to reverse immunosuppression in the tumor

microenvironment. In combination with DFMO, AMXT-1501 blocked tumor growth in immunocompetent mice but not in athymic nude mice lacking T cells. This combined treatment prevented immune escape by tumors [118].

Together, a combination drug therapy targeting both the polyamine biosynthesis pathway and the transport system is feasible. Combining with DFMO, polyamine transport inhibitors can inhibit cancer growth by blocking polyamine import and can result in sustained intracellular polyamine depletion. Structurally the compounds we developed and tested are different from AMXT-1501 which is a lipophilic lysine spermine conjugate. Our more hydrophilic designs will likely have different absorption and excretion profiles which may provide a clinical benefit.

Use of A Combination of Polyamine Transport Inhibitors May Be More Effective Than Individual Inhibitors Alone

A combination of Ant444 and Trimer44 was shown to be more effective at blocking DFMO rescue by native polyamines than either inhibitor alone (Figures 11d). This is the first time a cocktail of PTIs has been used in combination with DFMO to target both polyamine transport and biosynthesis in cells. The different selectivity of Ant444 and Trimer44 may be the underlying basis for the improved ability of a cocktail of these compounds to inhibit rescue in the presence of all three native polyamines. Rational design of PTIs with

different selectivity to polyamine transporters may further improve PTI efficiency in inhibiting rescue in the presence of native polyamines.

Future Directions

Polyamine content is elevated in malignant cells as compared with normal tissues. In combination with DFMO, AMXT-1501 blocked tumor growth in a T cell-dependent manner [118]. This suggests that polyamine blockade promotes antitumor immunity [148]. In future studies, Ant444, Trimer44 and Triamide444 can be used to test them to induce antitumor immunity in combination with DFMO. However, these compounds will need to be tested in systems other than *Drosophila*, because of *Drosophila*'s lack of an adaptive immune system.

My work suggests that multiple polyamine transport systems exist in multicellular organisms like *Drosophila*. These transport systems may have different affinity for each of the three native polyamines as has been observed in unicellular organisms. Rational design of PTIs with different selectivity to polyamine transporters may further improve PTI efficiency.

While the lack of knowledge of the genes and proteins involved in polyamine transport has hampered the development of PTIs, polyamine transporter characterization is still

one of the most important tasks in this area in the future. Moreover, future studies are needed to test how these known transport components interact, or whether they comprise one or more transport systems.

REFERENCES

1. Gerner, E.W. and F.L. Meyskens Jr, *Polyamine and cancer: old molecules, new understanding.* Nature Review Cancer, 2004. **4**: p. 781-792.
2. Miller-Fleming, L., et al., *Remaining mysteries of molecular biology: the role of polyamines in the cell.* Journal of Molecular Biology, 2015. **427**(21): p. 3389-3406.
3. Meyskens Jr, F.L. and E.W. Gerner, *Development of difluoromethylornithine (DFMO) as a chemoprevention agent.* Clinical Cancer Research, 1999. **5**(5): p. 945-951.
4. Igarashi, K. and K. Kashiwagi, *Polyamines: mysterious modulators of cellular functions.* Biochemical and Biophysical Research Communications, 2000. **271**(3): p. 559-564.
5. Watanabe, S., et al., *Estimation of polyamine binding to macromolecules and ATP in bovine lymphocytes and rat livers.* Journal of Biological Chemistry, 1991. **266**: p. 20803-20809.
6. Pollard, K.J., et al., *Functional interaction between GCN5 and polyamines: a new role for core histone acetylation.* The EMBO Journal, 1999. **18**(20): p. 5622-5633.
7. Cooper, H.L., et al., *Identification of the hypusine-containing protein hy+ as translation initiation factor eIF-4D.* Proceedings of the National Academy of Sciences, 1983. **80**(7): p. 1854-1857.
8. Brüne, B., et al., *Spermine prevents endonuclease activation and apoptosis in thymocytes.* Exp Cell Res, 1991. **195**(2): p. 323–329.

9. Ray, R.M., et al., *Activation of Dbl restores migration in polyamine-depleted intestinal epithelial cells via Rho-GTPases.* American Journal of Physiology - Gastrointestinal and Liver Physiology, 2011. **300**(6): p. G988-G997.

10. Flamigni, F., et al., *p44/42 mitogen-activated protein kinase is involved in the expression of ornithine decarboxylase in leukaemia L1210 cells.* Biochemical Journal, 1999. **341**(Pt 2): p. 363-369.

11. Meksuriyen, D., et al., *Formation of a complex containing ATP, Mg2+, and spermine: structural evidence and biological significance.* Journal of Biological Chemistry, 1998. **273**(47): p. 30939-30944.

12. Nowotarski, S.L., P.M. Woster, and R.A. Casero, *Polyamines and cancer: implications for chemoprevention and chemotherapy.* Expert reviews in molecular medicine, 2013. **15**: p. e3.

13. Wallace, H.M., A.V. Fraser, and A. Hughes, *A perspective of polyamine metabolism.* Biochemical Journal, 2003. **376**: p. 1-14.

14. Nowotarski, S.L. and L.M. Shantz, *Cytoplasmic accumulation of the RNA-binding protein HuR stabilizes the ornithine decarboxylase transcript in a murine nonmelanoma skin cancer model.* Journal of Biological Chemistry, 2010. **285**(41): p. 31885-31894.

15. Pegg, A.E., *Regulation of ornithine decarboxylase.* Journal of Biological Chemistry, 2006. **281**(21): p. 14529-14532.

16. Murakami, Y., et al., *Antizyme, a protein induced by polyamines, accelerates the degradation of ornithine decarboxylase in Chinese-hamster ovary-cell extracts.* Biochemical Journal, 1992. **283**(Pt 3): p. 661-664.

17. Murakami, Y., et al., *Destabilization of ornithine decarboxylase by transfected antizyme gene expression in hepatoma tissue culture cells.* Journal of Biological Chemistry, 1992. **267**(19): p. 13138-13141.

18. Murakami, Y., et al., *Ornithine decarboxylase is degraded by the 26S proteasome without ubiquitination.* Nature, 1992. **360**(6404): p. 597-599.

19. Mitchell, J.L., et al., *Feedback repression of polyamine transport is mediated by antizyme in mammalian tissue-culture cells.* Biochemical Journal, 1994. **299**(Pt 1): p. 19-22.

20. Marie-Pierre, H. and U. Buddy, *Identification and characterization of polyamine permease from the protozoan parasite Leishmania major.* Journal of Biological Chemistry, 2005. **208**: p. 15188-15194.

21. Machius, M., et al., *Structural and biochemical basis for polyamine binding to the Tp0655 lipoprotein of Treponema pallidum: putative role for Tp0655 (TpPotD) as a polyamine receptor.* Journal of Molecular Biology, 2007. **373**(3): p. 681-694.

22. Wang, C., *Molecular mechanisms and therapeutic approaches to the treatment of African Trypanosomiasis.* Annual Review of Pharmacology and Toxicology, 1995. **35**(1): p. 93-127.

23. Assaraf, Y.G., et al., *Effect of polyamine depletion on macromolecular synthesis of the malarial parasite, Plasmodium falciparum, cultured in human erythrocytes.* Biochemical Journal, 1987. **242**(1): p. 221-226.

24. Mishra, M., *Arginine uptake by mouse erythrocytes infected with Plasmodium yoelii nigeriensis.* J. Parasitic Dis., 1995. **19**: p. 55-58.

25. Malik, L.H., G.D. Singh, and E.A. Amsterdam, *Chagas heart disease: an update.* The American Journal of Medicine, 2017. **128**(11): p. 1251.e7-1251.e9.

26. Gonzalez, N.S., C. Ceriani, and I.D. Algranati, *Differential regulation of putrescine uptake in trypanosoma cruzi and other trypanosomatids.* Biochemical and Biophysical Research Communications, 1992. **188**(1): p. 120-128.

27. Hunter, K.J., S.A.L. Quesne, and A.H. Fairlamb, *Identification and biosynthesis of N1,N9-Bis(Glutathionyl)Aminopropylcadaverine (Homotrypanothione) in Trypanosoma cruzi.* European Journal of Biochemistry, 1994. **226**(3): p. 1019-1027.

28. Schwarcz de Tarlovsky, M., et al., *Polyamines in Trypanosoma cruzi.* Biochem Mol Biol Int., 1993. **30**(3): p. 547-558.

29. Carrillo, C., et al., *Trypanosoma cruzi epimastigotes lack ornithine decarboxylase but can express a foreign gene encoding this enzyme.* FEBS Letters, 1999. **454**(3): p. 192-196.

30. Persson, K., et al., *Trypanosoma cruzi has not lost its S-adenosylmethionine decarboxylase: characterization of the gene and the encoded enzyme.* Biochem. J. , 1998. **333**: p. 527–537.

31. Manni, A., et al., *Involvement of the polyamine pathway in breast cancer progression.* Cancer Letters, 1995. **92**(1): p. 49-57.

32. Upp, J.R., et al., *Polyamine levels and gastrin receptors in colon cancers.* Annals of Surgery, 1988. **207**(6): p. 662-669.

33. Gupta, S., et al., *Chemoprevention of prostate carcinogenesis by α-Difluoromethylornithine in TRAMP Mice.* Cancer Research, 2000. **60**(18): p. 5125-5133.

34. Gilmour, S.K., *Polyamines and nonmelanoma skin cancer.* Toxicology and Applied Pharmacology, 2007. **224**(3): p. 249-256.

35. Packham, G. and J.L. Cleveland, *Ornithine decarboxylase is a mediator of c-Myc-induced apoptosis.* Molecular and Cellular Biology, 1994. **14**(9): p. 5741-5747.

36. Shantz, L.M. and A.E. Pegg, *Ornithine decarboxylase induction in transformation by H-Ras and RhoA.* Cancer Research, 1998. **58**(13): p. 2748-2753.

37. K Kelly, a. and U. Siebenlist, *The regulation and expression of c-myc in normal and malignant cells.* Annual Review of Immunology, 1986. **4**(1): p. 317-338.

38. Fernández-Medarde, A. and E. Santos, *Ras in cancer and developmental diseases.* Genes & Cancer, 2011. **2**(3): p. 344-358.

39. Russell, D.H., et al., *Urinary polyamines in cancer patients.* Cancer Res, 1971. **31**(11): p. 1555-1558.

40. Pegg, A.E., *Polyamine metabolism and its importance in neoplastic growth and a target for chemotherapy.* Cancer Res, 1988. **48**(4): p. 759-774.

41. Cullis, P.M., et al., *Probing the mechanism of transport and compartmentalisation of polyamines in mammalian cells.* Chem Biol, 1999. **6**(10): p. 717-729.

42. Wolff, A.C., et al., *A Phase II study of the polyamine analog N1,N11-diethylnorspermine (DENSpm) daily for five days every 21 days in patients with previously treated metastatic breast cancer.* Clin Cancer Res, 2003. **9**(16 Pt 1): p. 5922-5928.

43. Wallace, H.M. and A.V. Fraser, *Inhibitors of polyamine metabolism: review article.* Amino Acids, 2004. **26**(4): p. 353-365.

44. Qu, N., et al., *Inhibition of human ornithine decarboxylase activity by enantiomers of difluoromethylornithine.* Biochemical Journal, 2003. **375**(Pt 2): p. 465-470.

45. Meyskens, F.L., Jr., et al., *Dose de-escalation chemoprevention trial of alpha-difluoromethylornithine in patients with colon polyps.* J Natl Cancer Inst, 1994. **86**(15): p. 1122-1130.

46. Koomoa, D.L., et al., *Ornithine decarboxylase inhibition by α-difluoromethylornithine activates opposing signaling pathways via phosphorylation of both Akt/protein kinase B and p27Kip1 in neuroblastoma.* Cancer Research, 2008. **68**(23): p. 9825-9831.

47. Alhonen-Hongisto, L., P. Seppänen, and J. Jänne, *Intracellular putrescine and spermidine deprivation induces increased uptake of the natural polyamines and methylglyoxal bis(guanylhydrazone).* Biochemical Journal, 1980. **192**(3): p. 941-945.

48. Byers, T.L. and A.E. Pegg, *Regulation of polyamine transport in Chinese hamster ovary cells.* Journal of Cellular Physiology, 1990. **143**(3): p. 460-467.

49. Seiler, N., *Thirty years of polyamine-related approaches to cancer therapy. retrospect and prospect. Part 2. Structural analogues and derivatives.* Current Drug Targets, 2003. **4**(7): p. 565-585.

50. Lessard, M., et al., *Hormonal and feedback regulation of putrescine and spermidine transport in human breast cancer cells.* Journal of Biological Chemistry, 1995. **270**(4): p. 1685-1694.

51. Seiler, N., J.G. Delcros, and J.P. Moulinoux, *Polyamine transport in mammalian cells. An update.* The International Journal of Biochemistry & Cell Biology, 1996. **28**(8): p. 843-861.

52. Wang, C., et al., *Molecular requirements for targeting the polyamine transport system. Synthesis and biological evaluation of polyamine-anthracene conjugates.* J Med Chem, 2003. **46**(13): p. 2672-2682.

53. Burns, M.R., et al., *Lipophilic lysine-spermine conjugates are potent polyamine transport inhibitors for use in combination with a polyamine biosynthesis inhibitor.* Journal of Medicinal Chemistry, 2009. **52**(7): p. 1983-1993.

54. Breitbeil, F., 3rd, et al., *Modeling the preferred shapes of polyamine transporter ligands and dihydromotuporamine-C mimics: shovel versus hoe.* J Med Chem, 2006. **49**(8): p. 2407-2416.

55. Mani, K., et al., *HIV-Tat protein transduction domain specifically attenuates growth of polyamine deprived tumor cells.* Mol Cancer Ther, 2007. **6**(2): p. 782-788.

56. Igarashi, K. and K. Kashiwagi, *Bacterial and eukaryotic transport systems*, in *Polyamine Cell Signaling*. 2006, Humana Press. p. 433-448.

57. Kashiwagi, K., et al., *Functions of potA and potD proteins in spermidine-preferential uptake system in Escherichia coli.* Journal of Biological Chemistry, 1993. **268**(26): p. 19358-19363.

58. Kashiwagi, K., et al., *Spermidine-preferential uptake system in Escherichia coli. ATP hydrolysis by PotA protein and its association with membrane.* J Biol Chem, 1995. **270**(43): p. 25377-25382.

59. Kakinuma, Y., et al., *Cloning of the gene encoding a putative serine/threonine protein kinase which enhances spermine uptake in Saccharomyces cerevisiae.* Biochemical and Biophysical Research Communications, 1995. **216**(3): p. 985-992

60. Uemura, T., K. Kashiwagi, and K. Igarashi, *Uptake of putrescine and spermidine by Gap1p on the plasma membrane in Saccharomyces cerevisias.* Biochem. Biophys. Res. Commun., 2005. **328**: p. 1028-1033.

61. Poulin, R., R.A. Casero, and D. Soulet, *Recent advances in the molecular biology of metazoan polyamine transport.* Amino acids, 2012. **42**(2-3): p. 711-723.

62. Belting, M., et al., *Glypican-1 is a vehicle for polyamine uptake in mammalian cells: a pivital role for nitrosothiol-derived nitric oxide.* Journal of Biological Chemistry, 2003. **278**(47): p. 47181-47189.

63. Roy, U.K., et al., *Activated K-RAS increases polyamine uptake in human colon cancer cells through modulation of caveolar endocytosis.* Mol Carcinog, 2008. **47**(7): p. 538-553.

64. Sharpe, J.G. and E.R. Seidel, *Polyamines are absorbed through a y+ amino acid carrier in rat intestinal epithelial cells.* Amino Acids, 2005. **29**(3): p. 245-253.

65. Heinick, A., et al., *Caenorhabditis elegans P_{5B}-type ATPase CATP-5 operates in polyamine transport and is crucial for norspermidine-mediated suppression of RNA interference.* FASEB J., 2010. **24**: p. 206–217.

66. Sarrazin, S., W.C. Lamanna, and J.D. Esko, *Heparan sulfate proteoglycans.* Cold Spring Harbor Perspectives in Biology, 2011. **3**(7).

67. Belting, M., S. Persson, and L.A. Fransson, *Proteoglycan involvement in polyamine uptake.* Biochem J, 1999. **338 (Pt 2)**: p. 317-323.

68. Welch, J.E., et al., *Single chain fragment anti-heparan sulfate antibody targets the polyamine transport system and attenuates polyamine-dependent cell proliferation.* International Journal of Oncology, 2008. **32**(4): p. 749-756.

69. Fredriksson, R., et al., *The solute carrier (SLC) complement of the human genome: Phylogenetic classification reveals four major families.* FEBS Letters, 2008. **582**(27): p. 3811-3816.

70. Daigle, N.D., et al., *Molecular characterization of a human cation-Cl− cotransporter (SLC12A8A, CCC9A) that promotes polyamine and amino acid transport.* Journal of Cellular Physiology, 2009. **220**(3): p. 680-689.

71. Aouida, M., R. Poulin, and D. Ramotar, *The human carnitine transporter SLC22A16 mediates high affinity uptake of the anticancer polyamine analogue bleomycin-A5.* Journal of Biological Chemistry, 2010. **285**(9): p. 6275-6284.

72. Busch, A.E., et al., *Electrogenic properties and substrate specificity of the polyspecific rat cation transporter rOCT1.* Journal of Biological Chemistry, 1996. **271**(51): p. 32599-32604.

73. Gründemann, D., et al., *Agmatine is efficiently transported by non-neuronal monoamine transporters extraneuronal monoamine transporter (EMT) and organic cation transporter 2 (OCT2).* Journal of Pharmacology and Experimental Therapeutics, 2003. **304**(2): p. 810-817.

74. Winter, T.N., W.F. Elmquist, and C.A. Fairbanks, *OCT2 and MATE1 provide bidirectional agmatine transport.* Molecular Pharmaceutics, 2011. **8**(1): p. 133-142.

75. Sala-Rabanal, M., et al., *Polyamine transport by the polyspecific organic cation transporters OCT1, OCT2 and OCT3.* Molecular pharmaceutics, 2013. **10**(4): p. 1450-1458.

76. Uemura, T., et al., *Identification and characterization of a diamine exporter in colon epithelial cells.* Journal of Biological Chemistry, 2008. **283**: p. 26428-26435.

77. Uemura, T., et al., *Polyamine transport is mediated by both endocytic and solute carrier transport mechanisms in the gastrointestinal tract.* Am J Physiol Gastrointest Liver Physiol, 2010. **299**(2): p. G517-522.

78. Abdulhussein, A.A. and H.M. Wallace, *Polyamines and membrane transporters.* Amino Acids, 2014. **46**(3): p. 655-660.

79. Christensen, H.N., *A transport system serving for mono- and diamino acids.* Proceedings of the National Academy of Sciences of the United States of America, 1964. **51**(2): p. 337-344.

80. Rojas, A.M. and R. Devés, *Mammalian amino acid transport system y+ revisited: specificity and cation dependence of the interaction with neutral amino acids.* The Journal of Membrane Biology, 1999. **168**(2): p. 199-208.

81. Fujita, M. and K. Shinozaki, *Identification of polyamine transporters in plants: paraquat transport provides crucial clues.* Plant and Cell Physiology, 2014. **55**(5): p. 855-861.

82. Fujita, M., et al., *Natural variation in a polyamine transporter determines paraquat tolerance in Arabidopsis.* Proceedings of the National Academy of Sciences, 2012. **109**(16): p. 6343-6347.

83. Li, J., et al., *PARAQUAT RESISTANT1, a Golgi-localized putative transporter protein, is involved in intracellular transport of paraquat.* Plant Physiology, 2013. **162**(1): p. 470-483.

84. Madan, M., et al., *ATP13A3 and caveolin-1 as potential biomarkers for difluoromethylornithine-based therapies in pancreatic cancers.* American Journal of Cancer Research, 2016. **6**(6): p. 1231-1252.

85. De La Hera, Diego P., et al., *Parkinson's disease-associated human P5B-ATPase ATP13A2 increases spermidine uptake.* Biochemical Journal, 2013. **450**(1): p. 47-53.

86. Soulet, D., et al., *A fluorescent probe of polyamine transport accumulates into intracellular acidic vesicles via a two-step mechanism.* Journal of Biological Chemistry, 2004. **279**(47): p. 49355-49366.

87. Kahana, C., *Antizyme and antizyme inhibitor, a regulatory tango.* Cellular and Molecular Life Sciences, 2009. **66**(15): p. 2479-2488.

88. Coffino, P., *Regulation of cellular polyamines by antizyme.* Nat Rev Mol Cell Biol, 2001. **2**(3): p. 188-194.

89. Kanerva, K., et al., *Ornithine decarboxylase antizyme inhibitor 2 regulates intracellular vesicle trafficking.* Experimental Cell Research, 2010. **316**(11): p. 1896-1906.

90. Cadigan, K.M. and R. Nusse, *Wnt signaling: a common theme in animal development.* Genes Dev, 1997. **11**(24): p. 3286-3305.

91. Johnson, R.L. and M.P. Scott, *New players and puzzles in the Hedgehog signaling pathway.* Curr Opin Genet Dev, 1998. **8**(4): p. 450-456.

92. Greenwald, I., *LIN-12/Notch signaling: lessons from worms and flies*. Genes Dev, 1998. **12**(12): p. 1751-1762.

93. Romero-Calderon, R. and D.E. Krantz, *Transport of polyamines in Drosophila S2 cells: kinetics, pharmacology and dependence on the plasma membrane proton gradient.* Biochem J, 2006. **393**(Pt 2): p. 583-589.

94. Tsen, C., et al., *A Drosophila model to identify polyamine-drug conjugates that target the polyamine transporter in an intact epithelium.* J Med Chem, 2008. **51**(2): p. 324-330.

95. Fristrom, D.K. and J.W. Fristrom, *The metamorphic development of the adult epidermis*, in *The Development of Drosophila melanogaster*. 1993, Cold Spring Harbor Laboratory Press. p. 843-897.

96. Beira, J.V. and R. Paro, *The legacy of Drosophila imaginal discs.* Chromosoma, 2016. **125**(4): p. 573-592.

97. von Kalm, L., D. Fristrom, and J. Fristrom, *The making of a fly leg: a model for epithelial morphogenesis.* Bioessays, 1995. **17**(8): p. 693-702.

98. Cohen, S.S., *A guide to the polyamines*. 1998, Oxford, UK: Oxford University Press. 543.

99. Oriol-Audit, C., *Polyamine-induced actin polymerization.* Eur J Biochem, 1978. **87**(2): p. 371-376.

100. Lopatin, A.N., E.N. Makhina, and C.G. Nichols, *Potassium channel block by cytoplasmic polyamines as the mechanism of intrinsic rectification.* Nature, 1994. **372**: p. 366-369.

101. Williams, K., et al., *Characterization of polyamines having agonist, antagonist, and inverse agonist effects at the polyamine recognition site of the nmda receptor.* Neuron, 1990. **5**(2): p. 199-208.

102. Matsufuji, S., et al., *Analyses of ornithine decarboxylase antizyme mRNA with a cDNA cloned from rat liver.* J Biochem, 1990. **108**(3): p. 365-371.

103. Igarashi, K. and K. Kashiwagi, *Polyamine transport in bacteria and yeast.* Biochem J, 1999. **344 Pt 3**: p. 633-642.

104. Igarashi, K., K. Ito, and K. Kashiwagi, *Polyamine uptake systems in Escherichia coli.* Res Microbiol, 2001. **152**(3-4): p. 271-278.

105. Poulin, R., et al., *Mechanism of the irreversible inactivation of mouse ornithine decarboxylase by alpha-difluoromethylornithine. Characterization of sequences at the inhibitor and coenzyme binding sites.* Journal of Biological Chemistry, 1992. **267**(1): p. 150-158.

106. Ask, A., L. Persson, and O. Heby, *Increased survival of L1210 leukemic mice by prevention of the utilization of extracellular polyamines. Studies using a polyamineuptake mutant, antibiotics and a polyamine-deficient diet.* Cancer Letters, 1992. **66**: p. 29-34.

107. Stabellini, G., et al., *Polyamine levels and ornithine decarboxylase activity in blood and erythrocytes in human diseases.* International journal of clinical pharmacology research, 2003. **23**(1): p. 17-22.

108. Sala, R., et al., *Two-way arginine transport in human endothelial cells: TNF-a stimulation is restricted to system y^+.* Am J Physiol Cell Physiol, 2002. **282**: p. C134–C143.

109. Hiasa, M., et al., *Identification of a mammalian vesicular polyamine transporter.* Sci Rep, 2014. **4**: p. 6836.

110. Isenring, P., et al., *Molecular characterization of a human cation-Cl(-) cotransporter (SLC12A8A, CCC9A) that promotes polyamine and amino acid transport.* Journal of Cellular Physiology, 2009. **220**(3): p. 680-689.

111. Fairbanks, C.A., T.N. Winter, and W.F. Elmquist, *OCT2 and MATE1 provide bidirectional agmatine transport.* Molecular Pharmaceutics, 2011. **8**(1): p. 133-142.

112. Kaur, N., et al., *A comparison of chloroambucil- and xylene-containing polyamines leads to improved ligands for accessing the polyamine transport system.* Journal of Medicinal Chemistry, 2008. **51**(5): p. 1393-1401.

113. Muth, A., et al., *Polyamine transport inhibitors: design, synthesis, and combination therapies with difluoromethylornithine.* J Med Chem, 2014. **57**(2): p. 348-363.

114. Metcalf, B.W., et al., *Catalytic irreversible inhibition of mammalian ornithine decarboxylase (EC41117) by substrate and product analogs.* Journal of the American Chemical Society, 1978. **100**(8): p. 2551-2553.

115. Jin, H.-T., et al., *Changes in blood polyamine levels in human acute pancreatitis.* Scandinavian Journal of Gastroenterology, 2009. **44**(8): p. 1004-1011.

116. Mandel, J.-L. and W.F. Flintoff, *Isolation of mutant mammalian cells altered in polyamine transport.* Journal of Cellular Physiology, 1978. **97**(3): p. 335-343.

117. Chen, Y., et al., *Combination therapy with α-difluoromethylornithine and a polyamine transport inhibitor against murine squamous cell carcinoma.* International Journal of Cancer Prevention, 2006. **118**(9): p. 2344–2349

118. Hayes, C.S., et al., *Polyamine-blocking therapy reverses immunosuppression in the tumor microenvironment.* Cancer Immunol. Res., 2014. **2**(3): p. 274-285.

119. Alexander, E.T., et al., *A novel polyamine blockade therapy activates an anti-tumor immune response.* Oncotarget, 2017. **8**(48): p. 84140-84152.

120. Maroni, G. and S.C. Stamey, *Use of blue food to select synchronous, late third instar larvae.* Dros. Inf. Serv., 1983. **59**: p. 142-143.

121. Fristrom, J.W., W.R. Logan, and C. Murphy, *The synthetic and minimal culture requirements for evagination of imaginal discs of Drosophila melanogaster in vitro.* Dev Biol, 1973. **33**(2): p. 441-456.

122. Brand, A.H. and N. Perrimon, *Targeted gene expression as a means of altering cell fates and generating dominant phenotypes.* Development, 1993. **118**(2): p. 401-415.

123. Lee, T. and L. Luo, *Mosaic analysis with a repressible cell marker for studies of gene function in neuronal morphogenesis.* Neuron, 1999. **22**(3): p. 451-61.

124. Mukherjee, A., et al., *The Drosophila Sox gene, fish-hook, is required for postembryonic development.* Developmental Biology, 2000. **217**(1): p. 91-106.

125. Wessells, R.J., et al., *Tissue-specific regulation of vein/EGF receptor signaling in Drosophila.* Developmental Biology, 1999. **216**(1): p. 243-259.

126. Guruharsha, K.G., et al., *A protein complex network of Drosophila melanogaster.* Cell, 2011. **147**(3): p. 690-703.

127. Rao, D.S., et al., *Huntingtin interacting protein 1 is a clathrin coat binding protein required for differentiation of late spermatogenic progenitors.* Molecular and Cellular Biology, 2001. **21**(22): p. 7796-7806.

128. Cheng, F., et al., *Nitric oxide-dependent processing of heparan sulfate in recycling s-nitrosylated Glypican-1 takes place in caveolin-1-containing endosomes.* Journal of Biological Chemistry, 2002. **277**(46): p. 44431-44439.

129. Rao, D.S., et al., *Huntingtin-interacting protein 1 is overexpressed in prostate and colon cancer and is critical for cellular survival.* The Journal of Clinical Investigation, 2002. **110**(3): p. 351-360.

130. Bradley, S.V., et al., *Aberrant huntingtin interacting protein 1 in lymphoid malignancies.* Cancer Research, 2007. **67**(18): p. 8923-8931.

131. Bradley, S.V., et al., *Huntingtin interacting protein 1 Is a novel brain tumor marker that associates with epidermal growth factor receptor.* Cancer Research, 2007. **67**(8): p. 3609-3615.

132. Belleannee, C., et al., *Purification and identification of sperm surface proteins and changes during epididymal maturation.* PROTEOMICS, 2011. **11**(10): p. 1952-1964.

133. Erez, O. and C. Kahana, *Screening for modulators of spermine tolerance identifies Sky1, the SR protein kinase of Saccharomyces cerevisiae, as a regulator of polyamine transport and ion homeostasis.* Molecular and Cellular Biology, 2001. **21**(1): p. 175-184.

134. Nikolakaki, E., et al., *Cloning and characterization of an alternatively spliced form of SR protein kinase 1 that interacts specifically with scaffold attachment factor-B.* Journal of Biological Chemistry, 2001. **276**(43): p. 40175-40182.

135. Hammerich-Hille, S., et al., *Low SAFB levels are associated with worse outcome in breast cancer patients.* Breast Cancer Research and Treatment, 2010. **121**(2): p. 503-509.

136. Dietzl, G., et al., *A genome-wide transgenic RNAi library for conditional gene inactivation in Drosophila.* Nature, 2007. **448**(7150): p. 151-156.

137. Marquez, R.M., et al., *Transgenic analysis of the smad family of TGF-β signal transducers in Drosophila melanogaster suggests new roles and new interactions between family members.* Genetics, 2001. **157**(4): p. 1639-1648.

138. Wang, M., O. Phanstiel, and L. von Kalm, *Evaluation of polyamine transport inhibitors in a Drosophila epithelial model suggests the existence of multiple transport systems.* Medical Sciences, 2017. **5**(4): p. 27.

139. Kashiwagi, K., et al., *Excretion and uptake of putrescine by the PotE protein in Escherichia coli.* Journal of Biological Chemistry, 1997. **272**(10): p. 6318-6323.

140. Uemura, T., K. Kashiwagi, and K. Igarashi, *Polyamine Uptake by DUR3 and SAM3 in Saccharomyces cerevisiae.* Journal of Biological Chemistry, 2007. **282**(10): p. 7733-7741.

141. Aouida, M., et al., *AGP2 encodes the major permease for high affinity polyamine import in Saccharomyces cerevisiae.* Journal of Biological Chemistry, 2005. **280**(25): p. 24267-24276.

142. Uemura, T., et al., *Uptake of GABA and putrescine by UGA4 on the vacuolar membrane in Saccharomyces cerevisiae.* Biochemical and Biophysical Research Communications, 2004. **315**(4): p. 1082-1087.

143. Tomitori, H., et al., *Identification of a gene for a polyamine transport protein in yeast.* Journal of Biological Chemistry, 1999. **274**(6): p. 3265-3267.

144. Tomitori, H., et al., *Multiple polyamine transport systems on the vacuolar membrane in yeast.* Biochemical Journal, 2001. **353**(Pt 3): p. 681-688.

145. Casero, R.A. and P.M. Woster, *Terminally alkylated polyamine analogues as chemotherapeutic agents.* Journal of Medicinal Chemistry, 2001. **44**(1): p. 1-26.

146. Derossi, D., G. Chassaing, and A. Prochiantz, *Trojan peptides: the penetratin system for intracellular delivery.* Trends in Cell Biology, 1998. **8**(2): p. 84-87.

147. Joliot, A. and A. Prochiantz, *Transduction peptides: from technology to physiology.* Nat Cell Biol, 2004. **6**(3): p. 189-196.

148. Hayes, C.S., M.R. Burns, and S.K. Gilmour, *Polyamine blockade promotes antitumor immunity.* Oncoimmunology, 2014. **3**: p. e27360.

APPENDIX A: RESULTS OF GENES TESTED FOR INVOLVEMENT IN POLYAMINE TRANSPORT USING WHOLE ANIMAL METHOD

Part I: Result of Testing Heparan Sulfate Proteoglycan Core Protein Genes for Involvement in Polyamine Transport Using Whole Animal Method

There are four heparan sulfate proteoglycan core protein genes in *Drosophila*: Dally, Dally-like, Perlecan and Syndecan. In this study both RNAi stocks, over-expression constructs and insertional mutants were tested if stocks are available.

1. *Dally RNAi Stocks: BL33952, V14136, BL28747*

1.1 BL33952: y^1scv^1; +; UAS-dally RNAi (TRiP, V20)

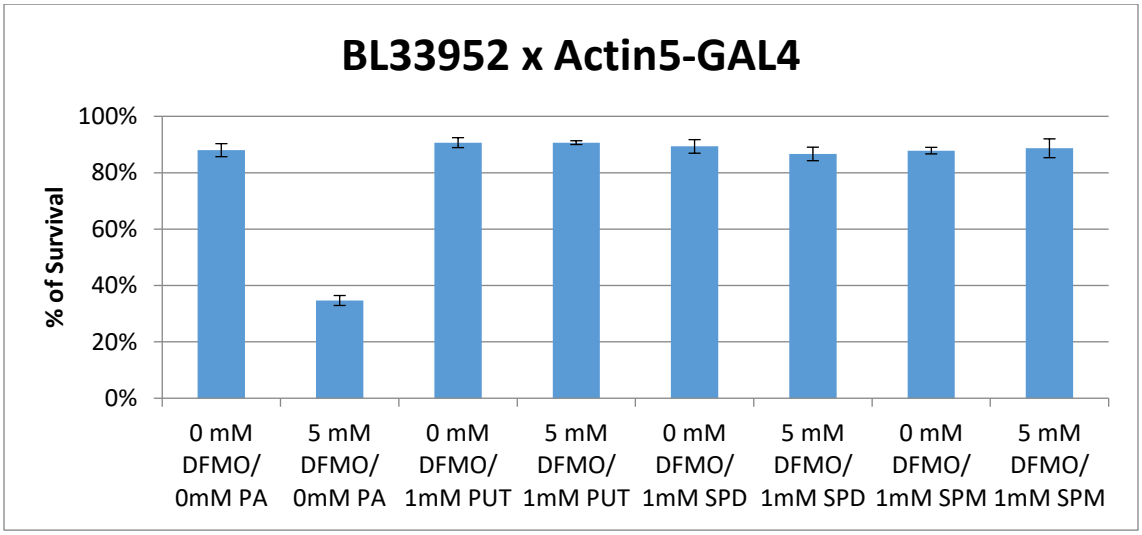

Figure 20 Rescue DFMO inhibition by native polyamines at 1mM in whole animals of Dally RNAi (BL33952) driven by Actin5-GAL4.

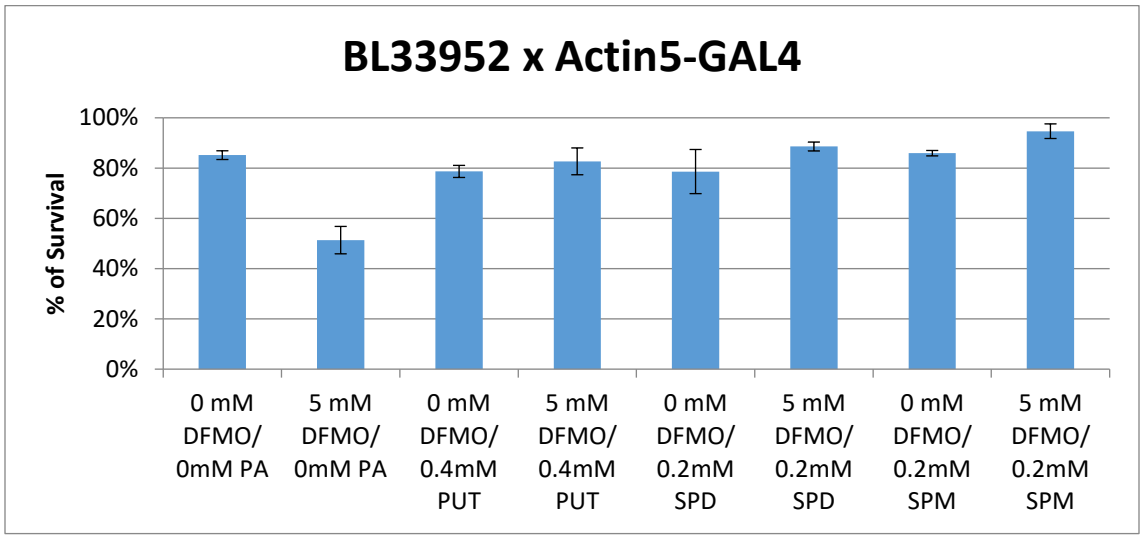

Figure 21 Rescue DFMO inhibition by native polyamines at minimum concentration in whole animals of Dally RNAi (BL33952) driven by Actin5-GAL4.

1.2 V14136: w^{1118}; +; UAS-dally RNAi (Vienna Stock, 1 Off-target)

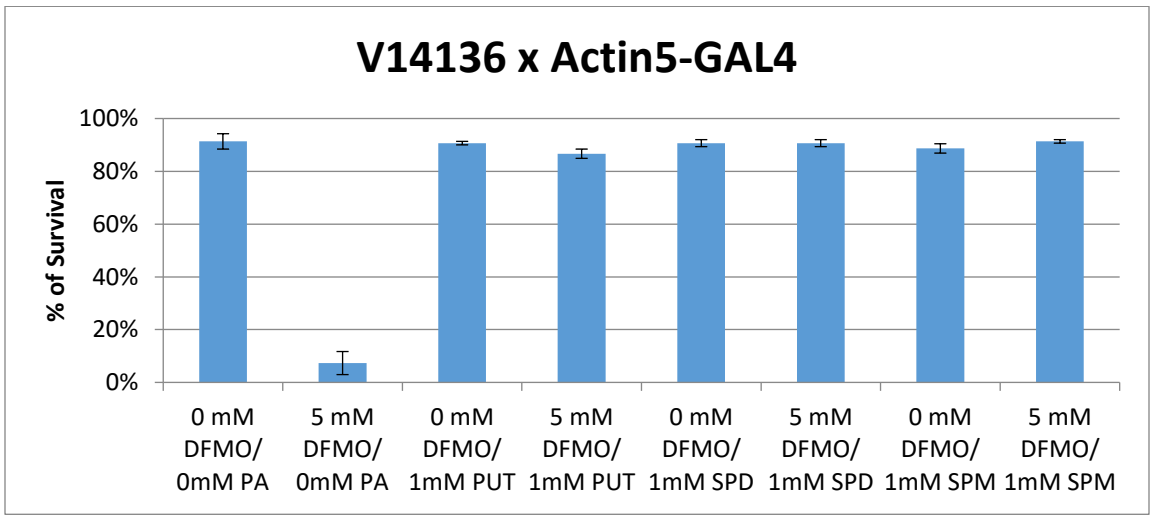

Figure 22 Rescue DFMO inhibition by native polyamines at 1mM in whole animals of Dally RNAi (V14136) driven by Actin5-GAL4.

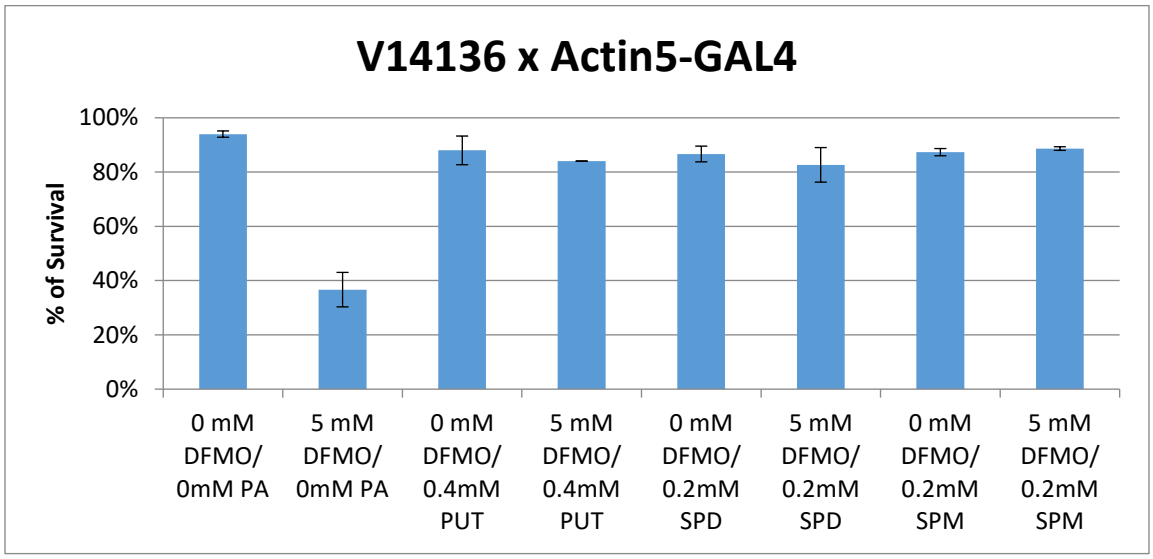

Figure 23 Rescue DFMO inhibition by native polyamines at minimum concentration in whole animals of Dally RNAi (V14136) driven by Actin5-GAL4.

1.3 BL28747: y^1v^1; +; UAS-dally RNAi (TRiP, V10)

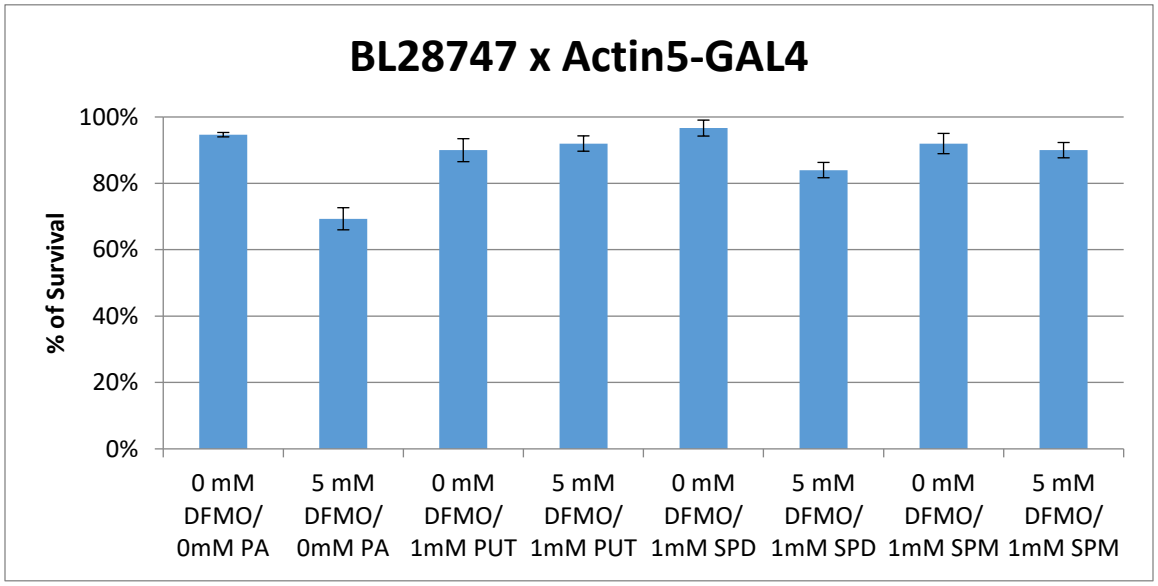

Figure 24 Rescue DFMO inhibition by native polyamines at 1mM in whole animals of Dally RNAi (BL28747) driven by Actin5-GAL4.

2 Dally-like Stocks: BL34089, BL34091, V10298, V10299

2.1 BL34089: y^1scv^1; +; UAS-dlp RNAi (TRiP, V20)

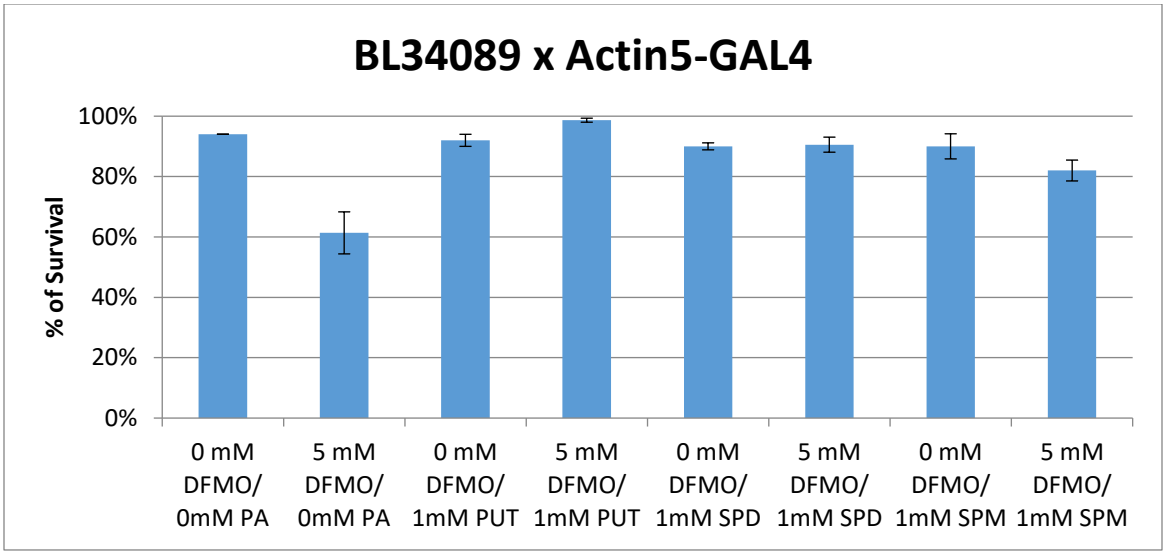

Figure 25 Rescue DFMO inhibition by native polyamines at 1mM in whole animals of Dally-like RNAi (BL34089) driven by Actin5-GAL4.

2.2 BL34091: y^1scv^1; +; UAS-dlp RNAi (TRiP, V20)

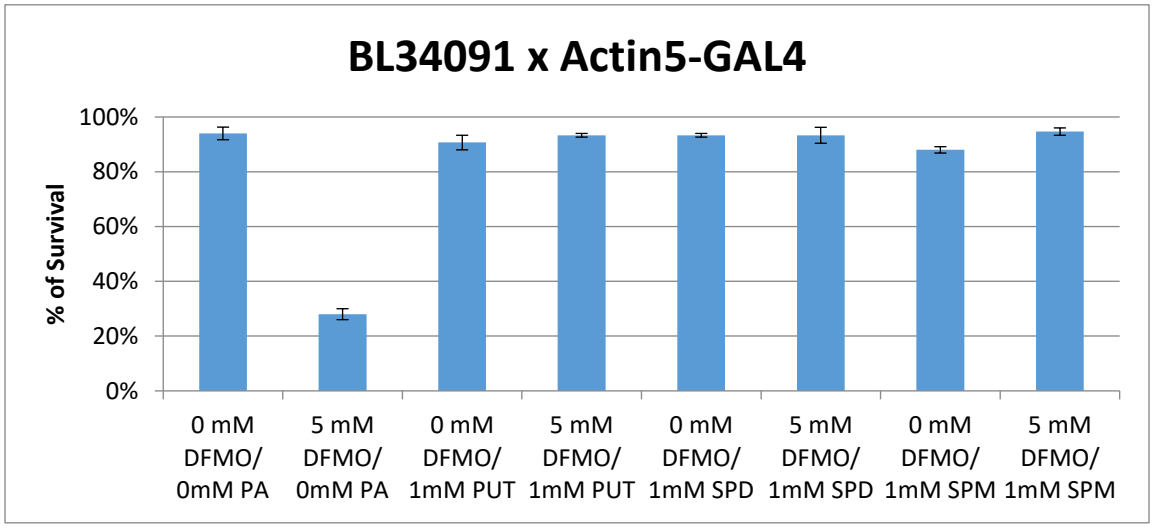

Figure 26 Rescue DFMO inhibition by native polyamines at 1mM in whole animals of Dally-like RNAi (BL34091) driven by Actin5-GAL4.

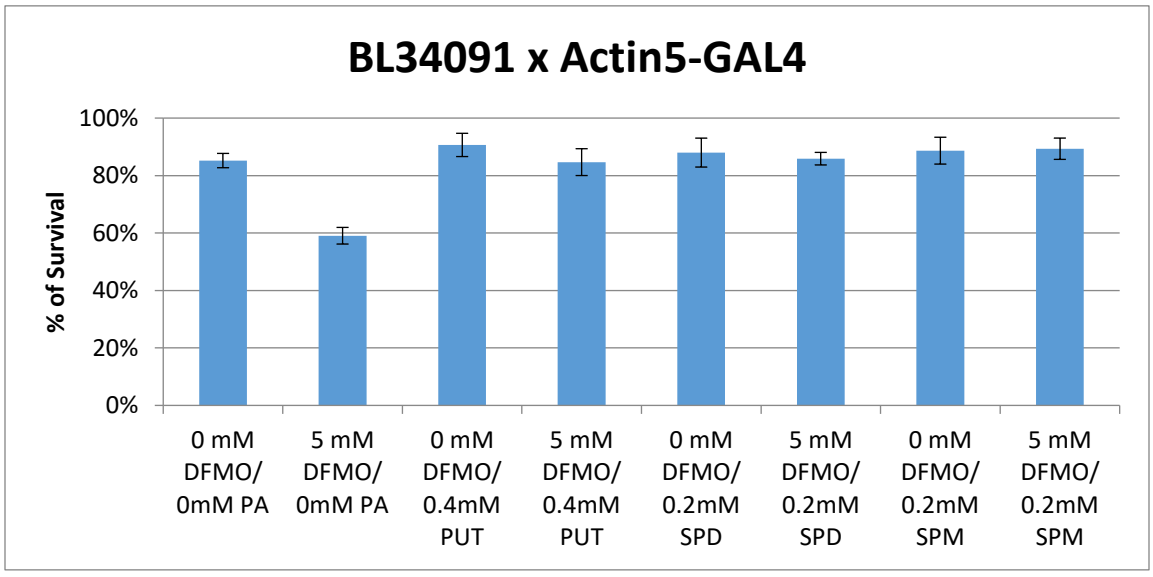

Figure 27 Rescue DFMO inhibition by native polyamines at minimum concentration in whole animals of Dally-like RNAi (BL34091) driven by Actin5-GAL4.

2.3 V10298: w^{1118}; +; UAS-dlp RNAi/ TM6B, Dfd-EYFP, Tb,Hu,Sb (Vienna Stock, 6 Off-targets)

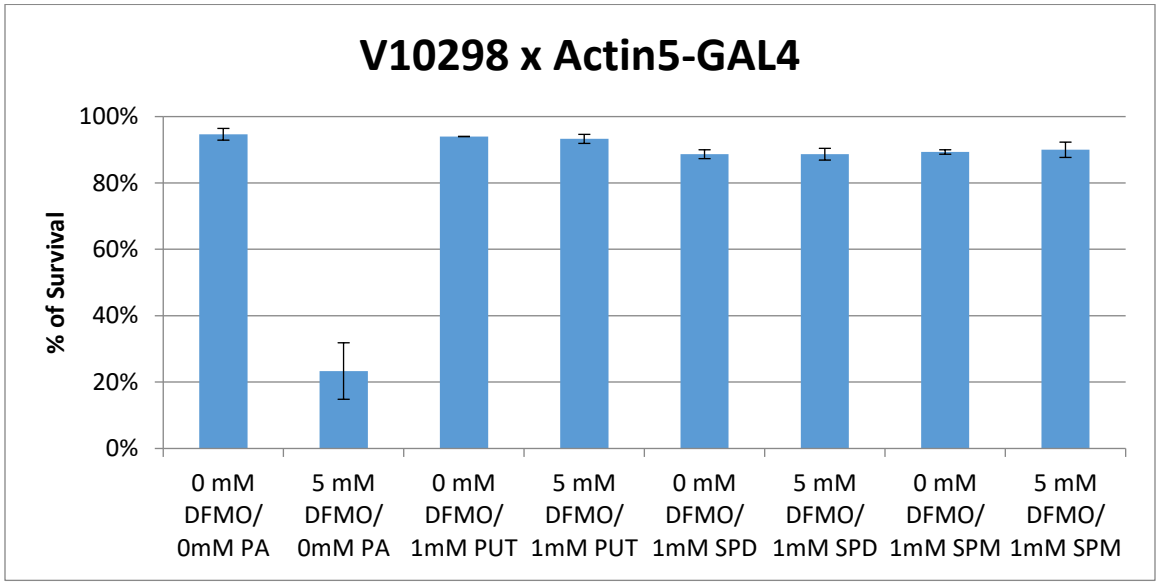

Figure 28 Rescue DFMO inhibition by native polyamines at 1mM in whole animals of Dally-like RNAi (V10298) driven by Actin5-GAL4 (pupa data).

2.4 V10299: w^{1118}; +; UAS-dlp RNAi (Vienna Stock, 6 Off-targets)

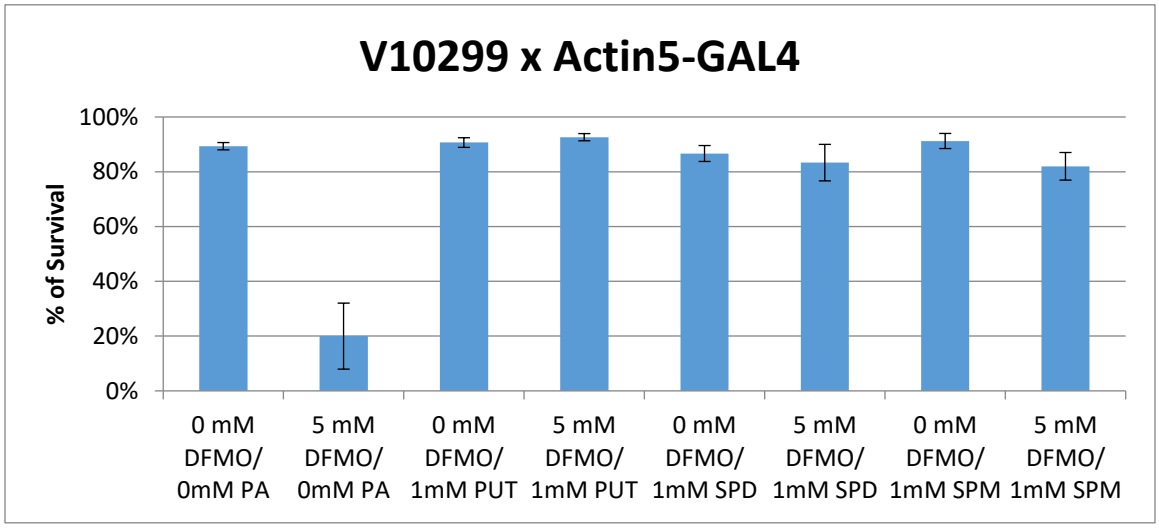

Figure 29 Rescue DFMO inhibition by native polyamines at 1mM in whole animals of Dally-like RNAi (V10299) driven by Actin5-GAL4 (pupa data).

3 Perlecan RNAi Stocks: BL29440, V24549

3.1 BL29440: y^1v^1;+; UAS-trol RNAi/TM6B,EYFP,Sb,Tb,Hu,ca (w floating, TRiP V10)

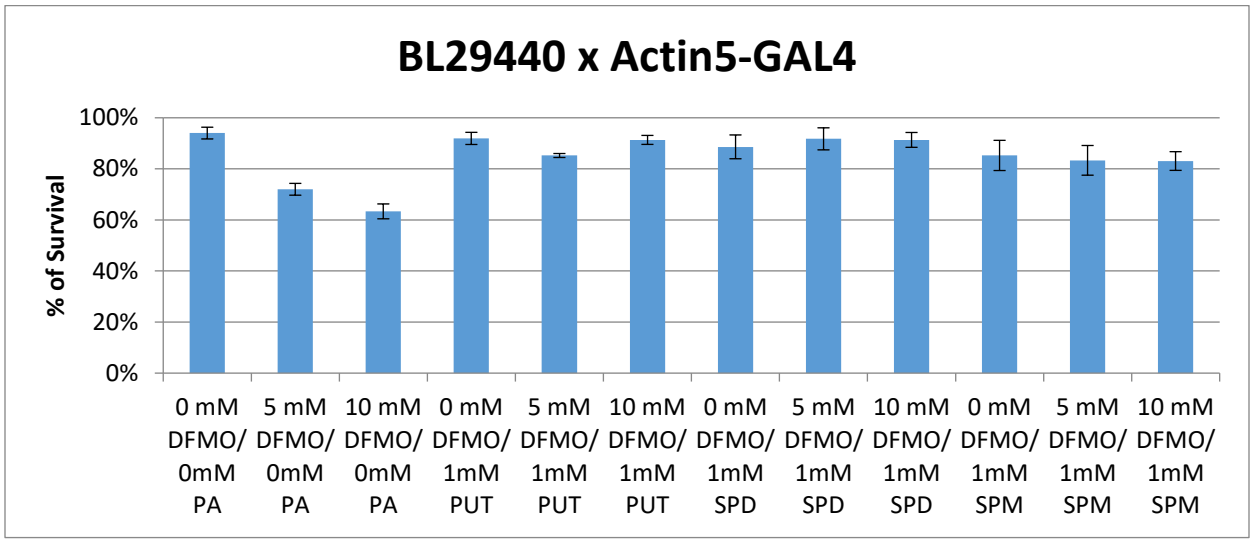

Figure 30 Rescue DFMO inhibition (both 5mM and 10mM) by native polyamines at 1mM in whole animals of Perlecan RNAi (BL29440) driven by Actin5-GAL4 (pupa data).

3.2 V24549: w^{1118}; UAS-trol RNAi (Vienna Stock)

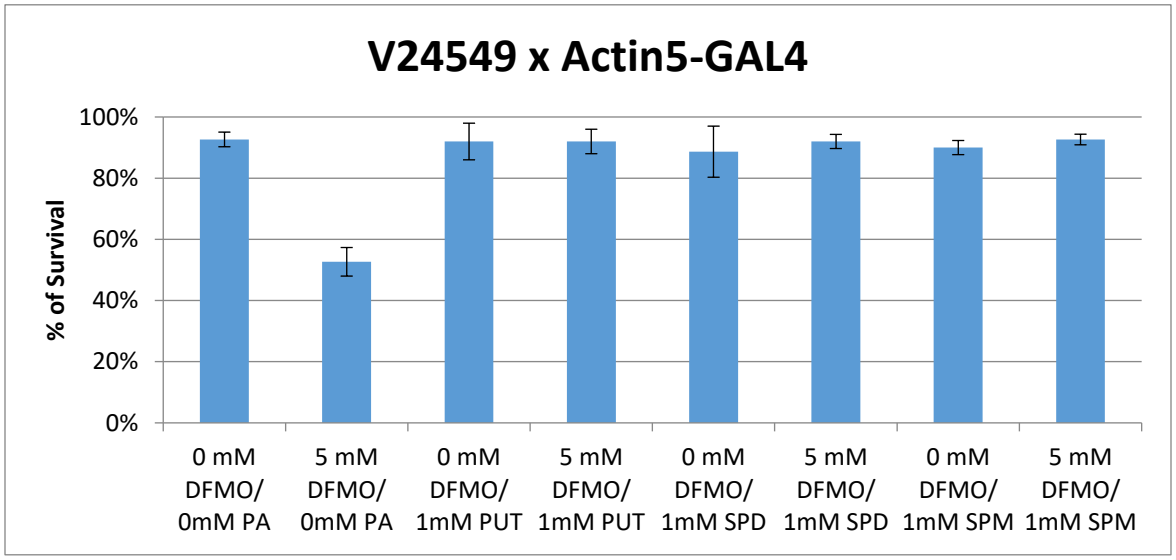

Figure 31 Rescue DFMO inhibition by native polyamines at 1mM in whole animals of Perlecan RNAi (V24549) driven by Actin5-GAL4 (pupa data).

4 Syndecan

4.1 RNAi Stock: V13322- w^{1118}; UAS-sdc RNAi (Vienna Stock)

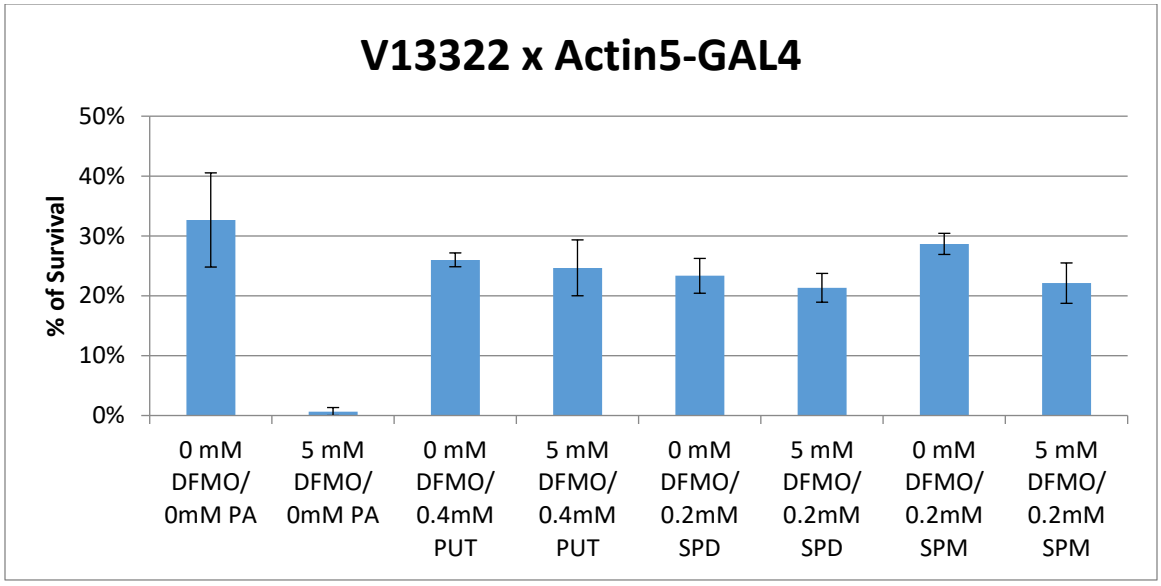

Figure 32 Rescue DFMO inhibition by native polyamines at minimum concentration in whole animals of Syndecan RNAi (V13322) driven by Actin5-GAL4 at 18^0C (pupa data).

4.2 Overexpression Stock: BL8564- yw;+; UAS-sdc (Bloomington Stock)

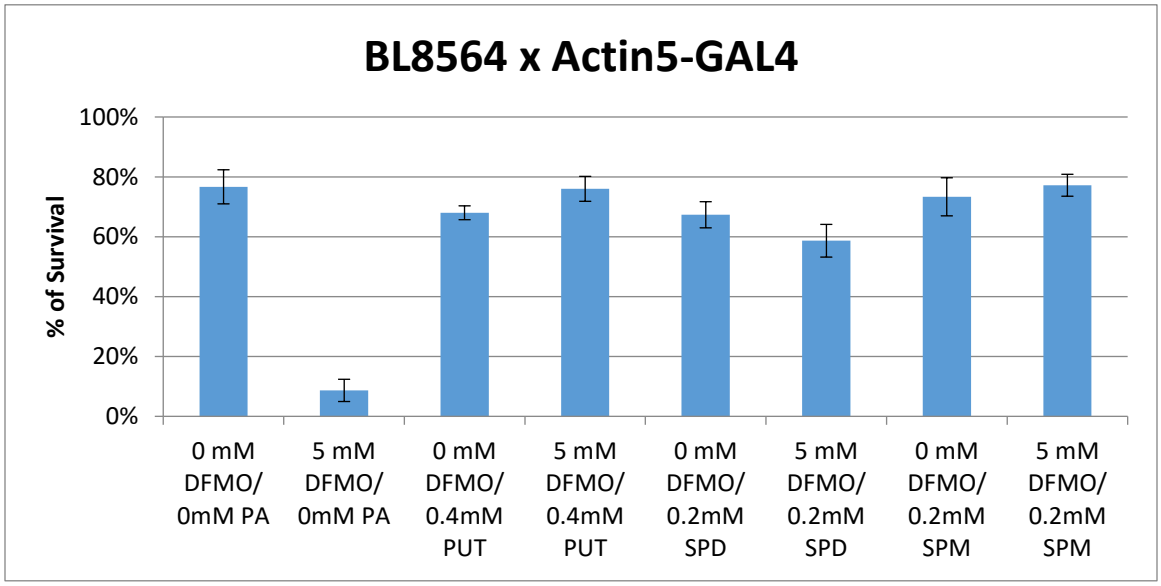

Figure 33 Rescue DFMO inhibition by native polyamines at minimum concentration in whole animals of Syndecan overexpression (BL8564) driven by Actin5-GAL4 (pupa data).

5 Mutants: BL23972, BL19695, BL36954, BL37444

5.1 BL23972: w^{1118}; $Sdc^{MB02461}$

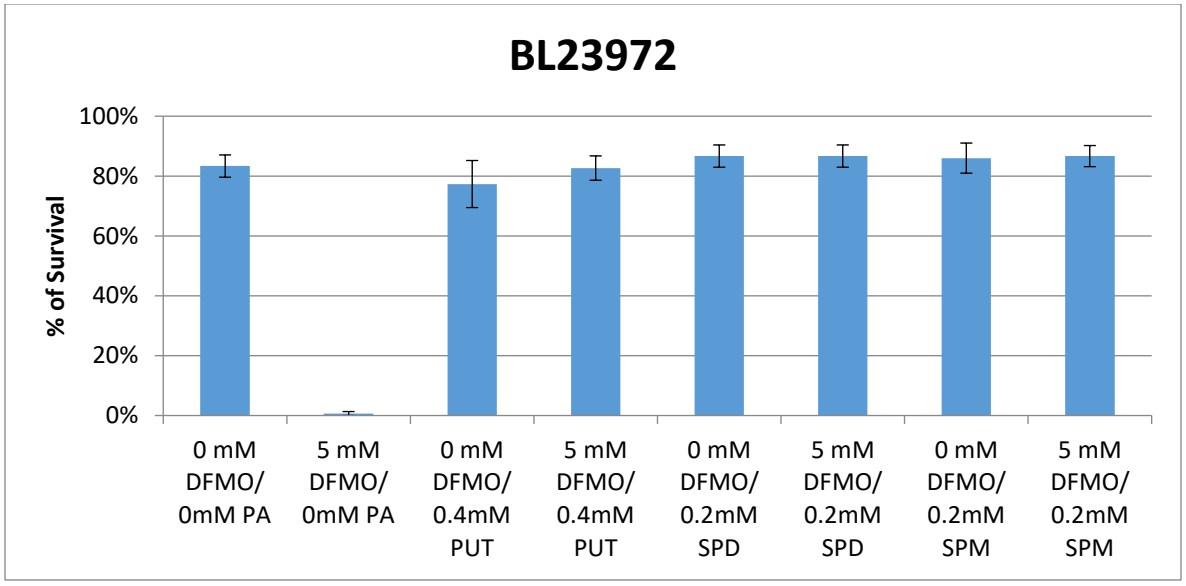

Figure 34 Rescue DFMO inhibition by native polyamines at minimum concentration in whole animals of Syndecan mutant (BL23972).

5.2 BL19695: $y^{1}w^{67c23}$; $Sdc^{EY04602}$/Cyo

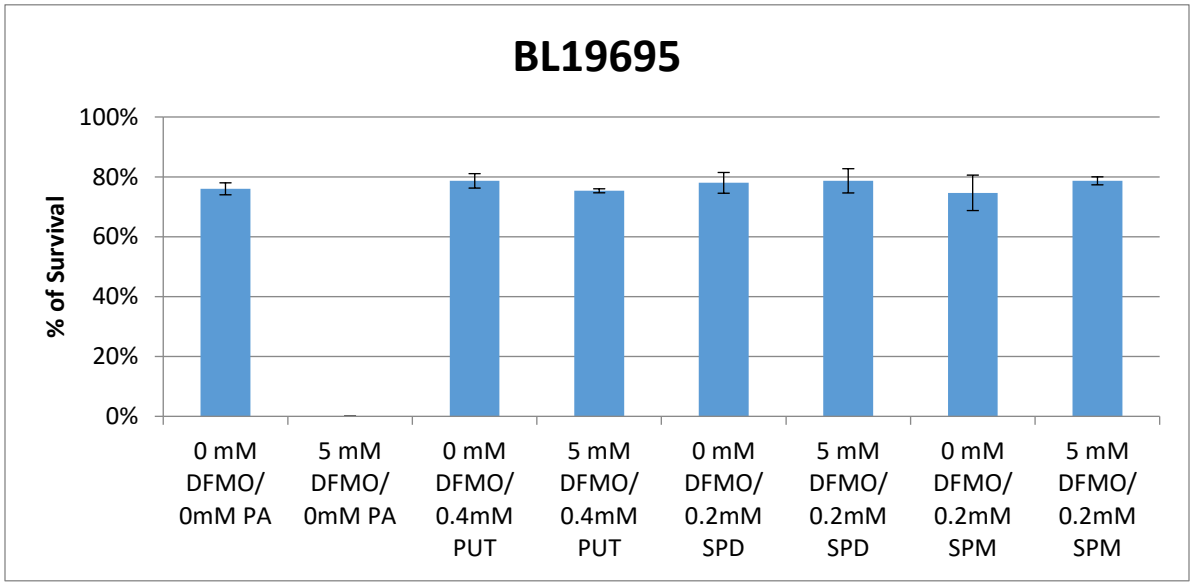

Figure 35 Rescue DFMO inhibition by native polyamines at minimum concentration in whole animals of Syndecan mutant (BL19695).

5.3 BL36954: yw; $Sdc^{M103925}$/SM6a

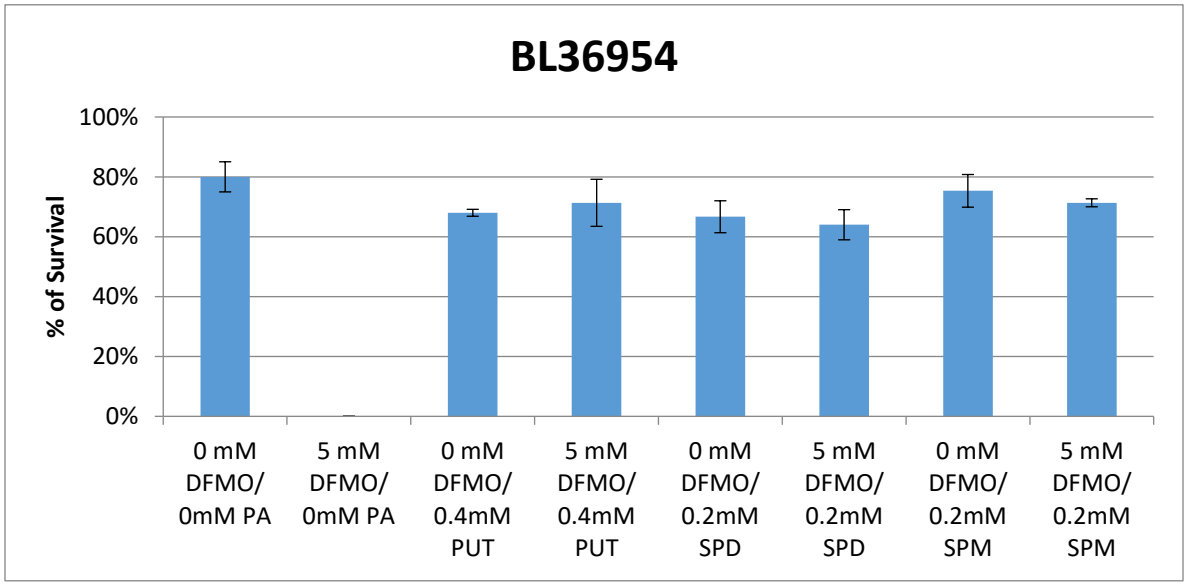

Figure 36 Rescue DFMO inhibition by native polyamines at minimum concentration in whole animals of Syndecan mutant (BL36954).

5.4 BL37444: y^1w; $Sdc^{M104345}$/SM6a

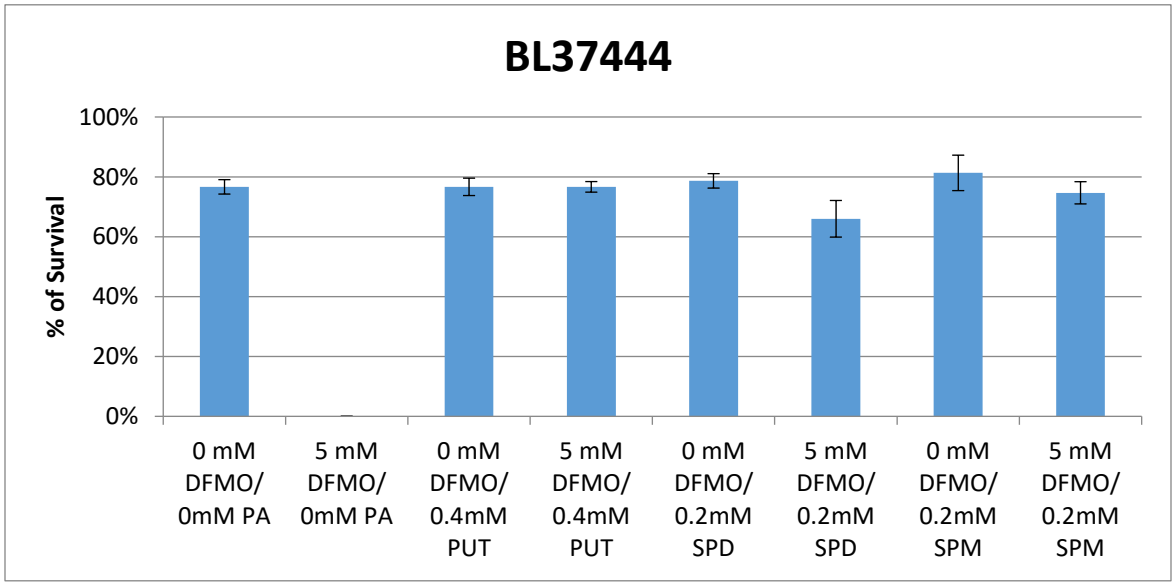

Figure 37 Rescue DFMO inhibition by native polyamines at minimum concentration in whole animals of Syndecan mutant (BL37444).

6 Dally/dally-like RNAi Stocks: BL33952/BL34089, BL33952/BL34091

6.1 BL33952/BL34089

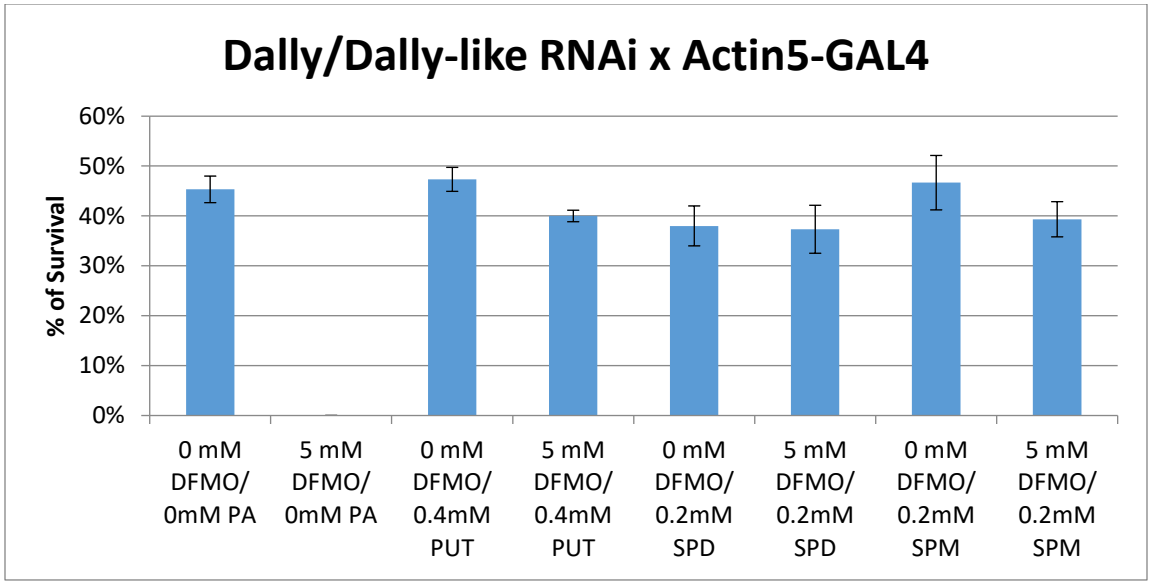

Figure 38 Rescue DFMO inhibition by native polyamines at minimum concentration in whole animals of Dally/Dally-like RNAi (BL33952/BL34089) driven by Actin5-GAL4.

6.2 BL33952/BL34091

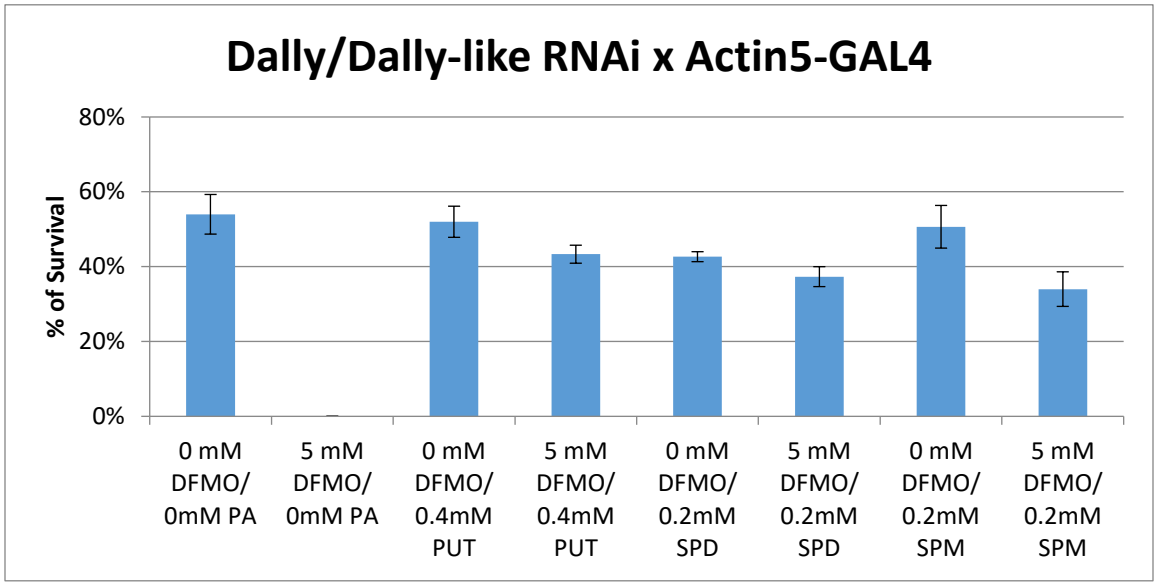

Figure 39 Rescue DFMO inhibition by native polyamines at minimum concentration in whole animals of Dally/Dally-like RNAi (BL33952/BL34091) driven by Actin5-GAL4.

7 Dally/Syndecan RNAi Stock: BL33952/V13322

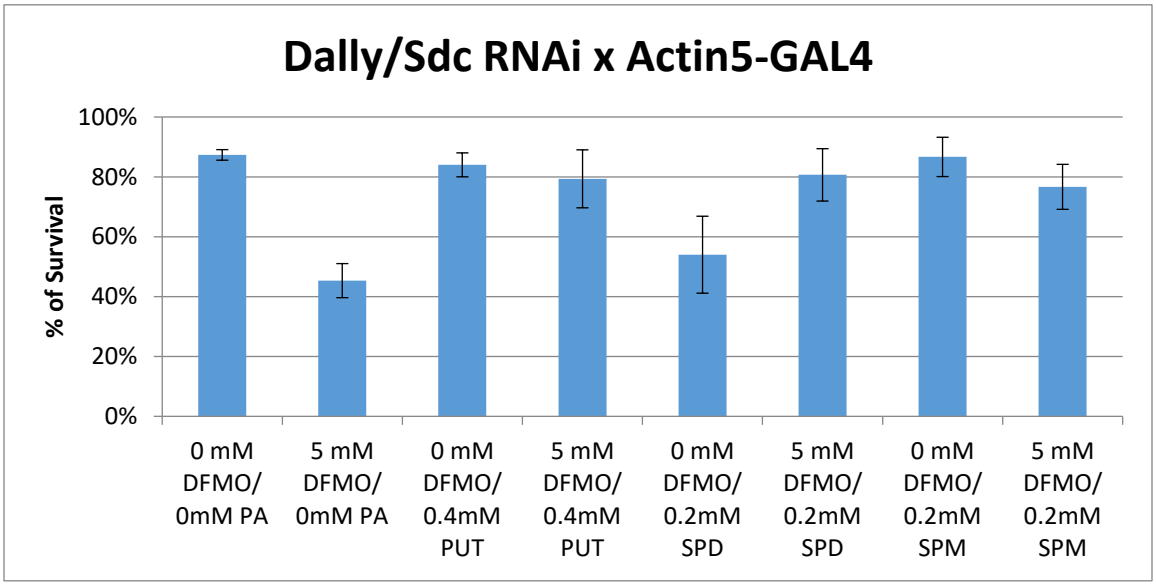

Figure 40 Rescue DFMO inhibition by native polyamines at minimum concentration in whole animals of Dally/Syndecan RNAi (BL33952/V13322) driven by Actin5-GAL4 at 18^0C (pupa data).

Part II: Result of Testing Heparan Sulfate Biosynthetic Enzyme Genes for Involvement in Polyamine Transport Using Whole Animal Method

There are six heparan sulfate biosynthetic enzymes in *Drosophila*: Sugarless, Slalom, Tout velu (ttv), Brother of Tout velu (bttv), Fringe Connection, Sulfateless, Hsepi (CG3194). In this study both RNAi stocks, over-expression constructs and insertional mutants were tested if stocks are available.

1. *Sugarless RNAi Stock: V29434- w^{1118}; UAS-sugarless RNAi (Vienna Stock)*

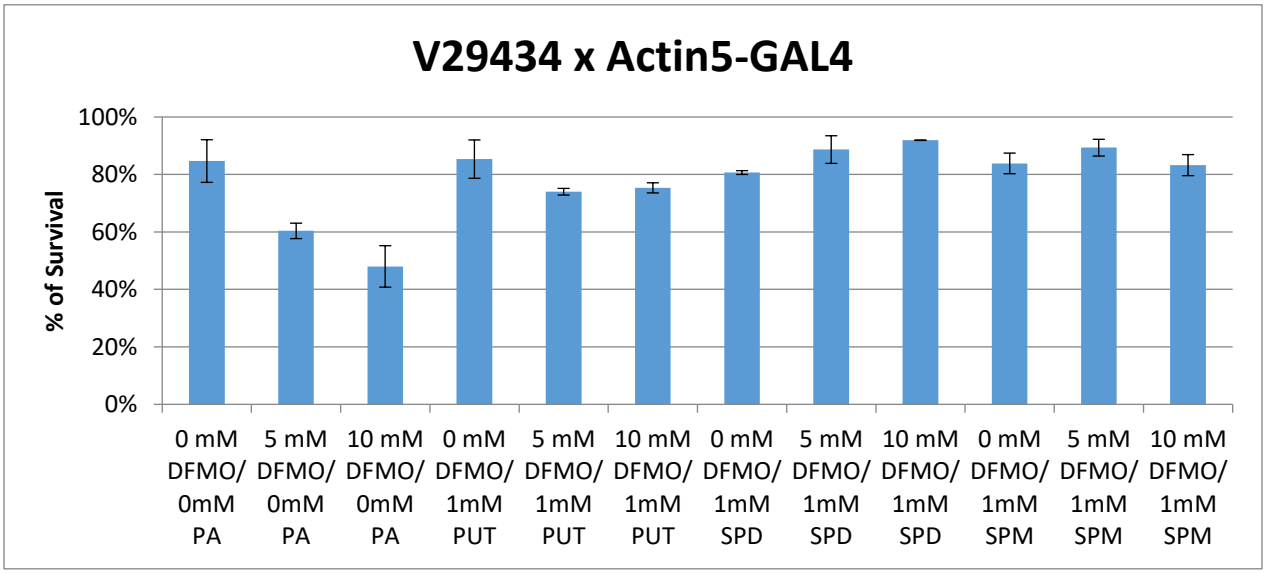

Figure 41 Rescue DFMO inhibition (both 5mM and 10mM) by native polyamines at 1mM in whole animals of Surgarless RNAi (V29434) driven by Actin5-GAL4 (pupa data).

2. Slalom RNAi Stocks: V12148, V12149

2.1 V12148: w^{1118};+;UAS-slalom RNAi (Vienna Stock, 1 Off-target)

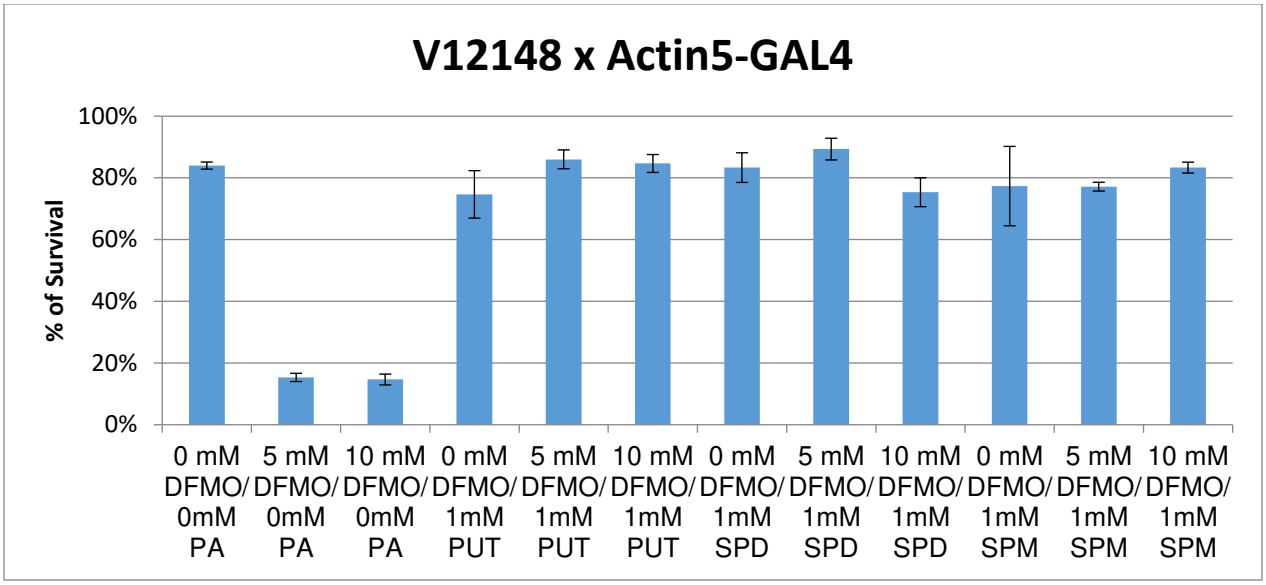

Figure 42 Rescue DFMO inhibition (both 5mM and 10mM) by native polyamines at 1mM in whole animals of Slalom RNAi (V12148) driven by Actin5-GAL4 (pupa data).

2.2 V12149: w^{1118};+;UAS-slalom RNAi/_TM6B,Tb,Sb,EYFP (Vienna Stock, 1 Off-target)

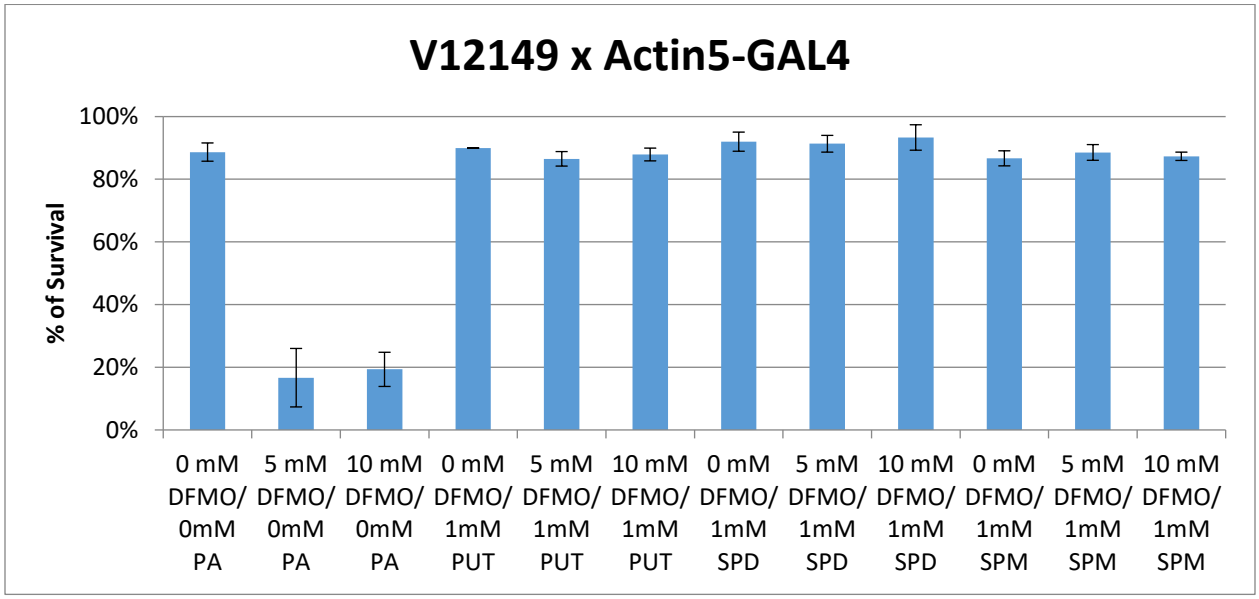

Figure 43 Rescue DFMO inhibition (both 5mM and 10mM) by native polyamines at 1mM in whole animals of Slalom RNAi (V12149) driven by Actin5-GAL4 (pupa data).

3. *Tout Velu RNAi Stock: V4871- w^{1118};+;UAS-ttv RNAi (Vienna Stock)*

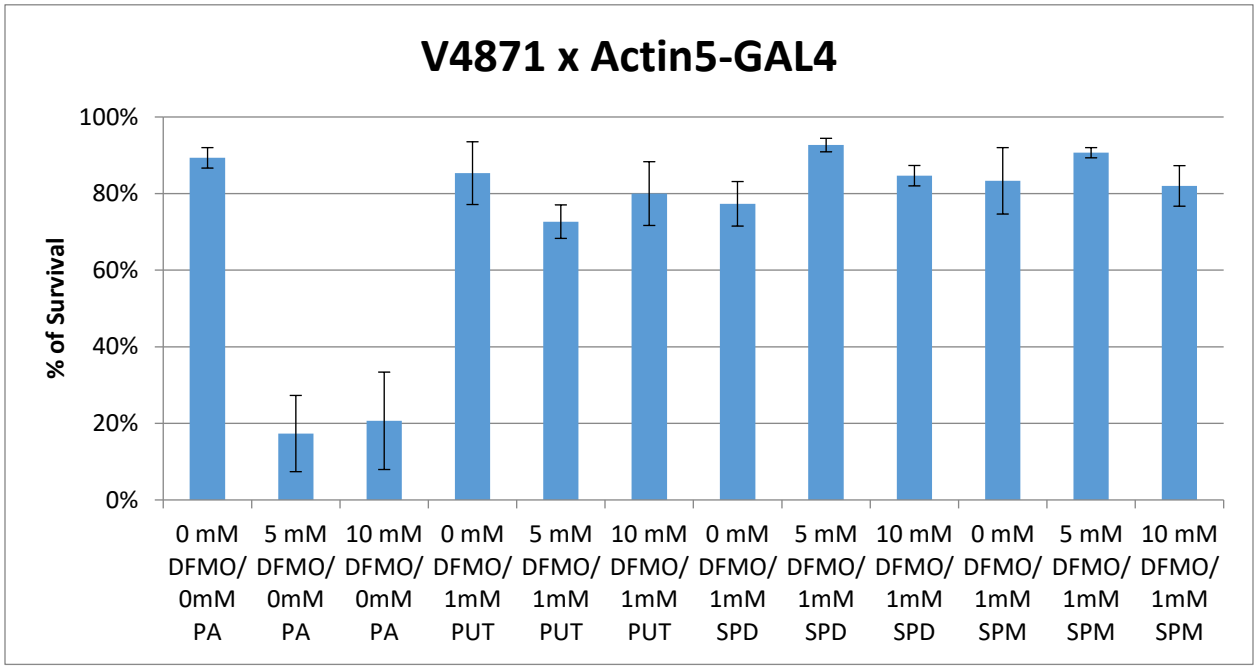

Figure 44 Rescue DFMO inhibition (both 5mM and 10mM) by native polyamines at 1mM in whole animals of ttv RNAi (V4871) driven by Actin5-GAL4 (pupa data).

4. *Brother of Tout Velu RNAi Stock: V3718- w^{1118};UAS-bttv RNAi (Vienna Stock)*

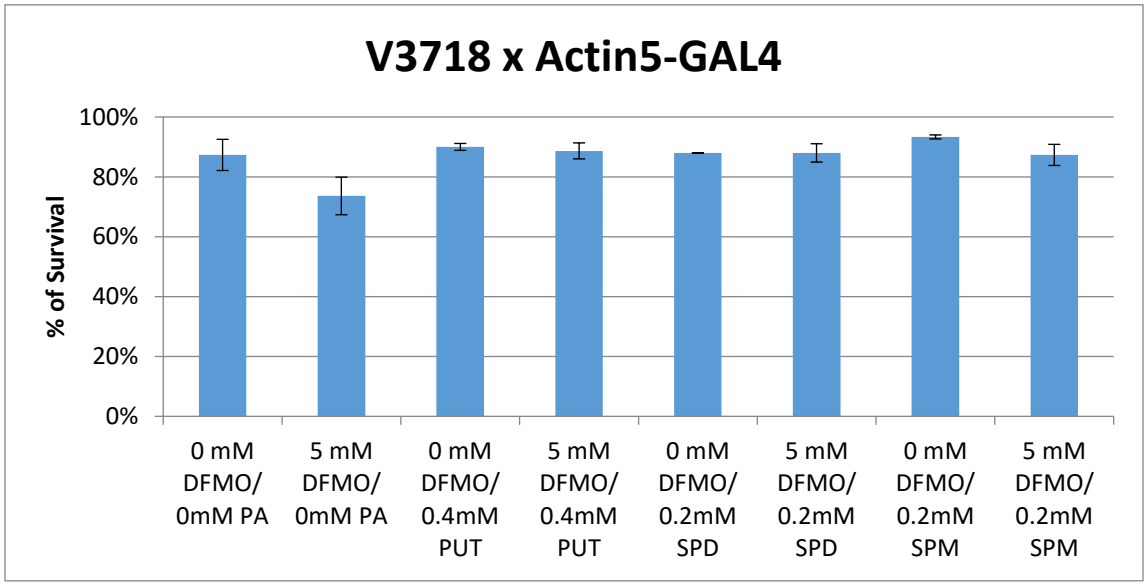

Figure 45 Rescue DFMO inhibition by native polyamines at minimum concentration in whole animals of bttv RNAi (V3718) driven by Actin5-GAL4 (pupa data).

5. Fringe Connection RNAi Stocks: V47542, V47543

5.1 V47542: w;UAS-frc RNAi/Cyo, EYFP (Vienna Stock)

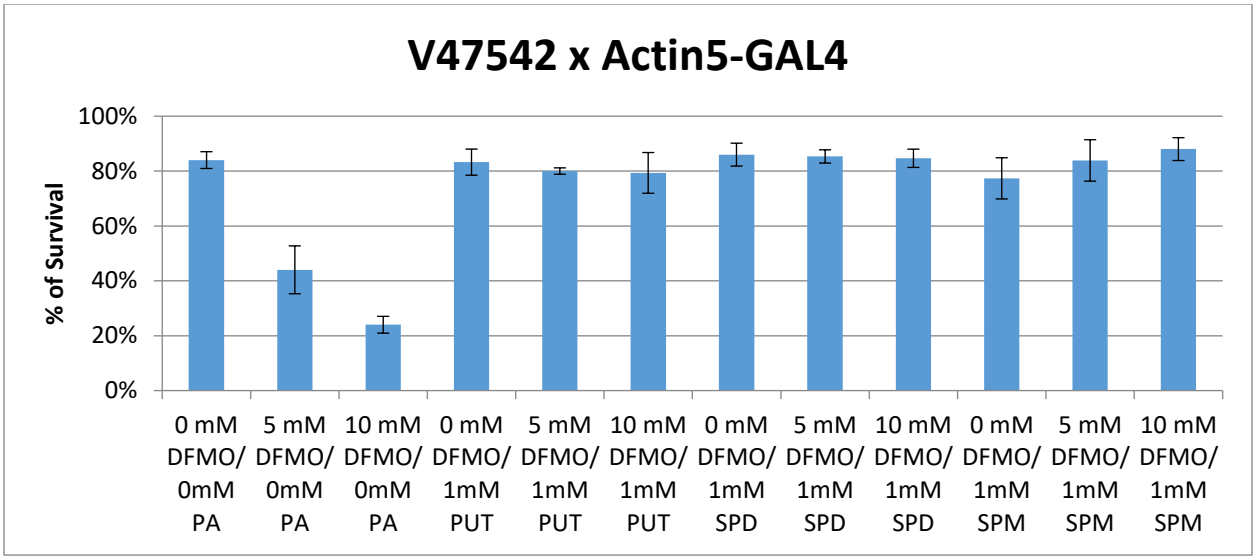

Figure 46 Rescue DFMO inhibition (both 5mM and 10mM) by native polyamines at 1mM in whole animals of Fringe Connection RNAi (V47542) driven by Actin5-GAL4.

5.2 V47543: w^{1118};+;UAS-frc RNAi (Vienna Stock)

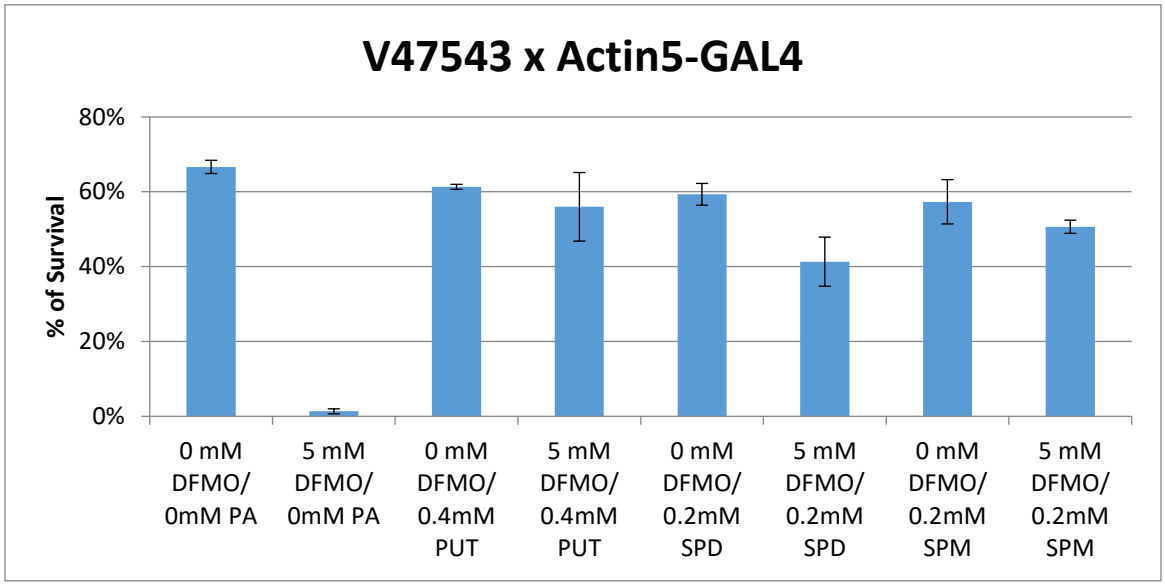

Figure 47 Rescue DFMO inhibition by native polyamines at minimum concentration in whole animals of Fringe Connection RNAi (V47543) driven by Actin5-GAL4.

6. Sulfateless RNAi Stocks: V5070, BL34601

6.1 V5070: w^{1118};+;UAS-sulfateless RNAi (Vienna Stock)

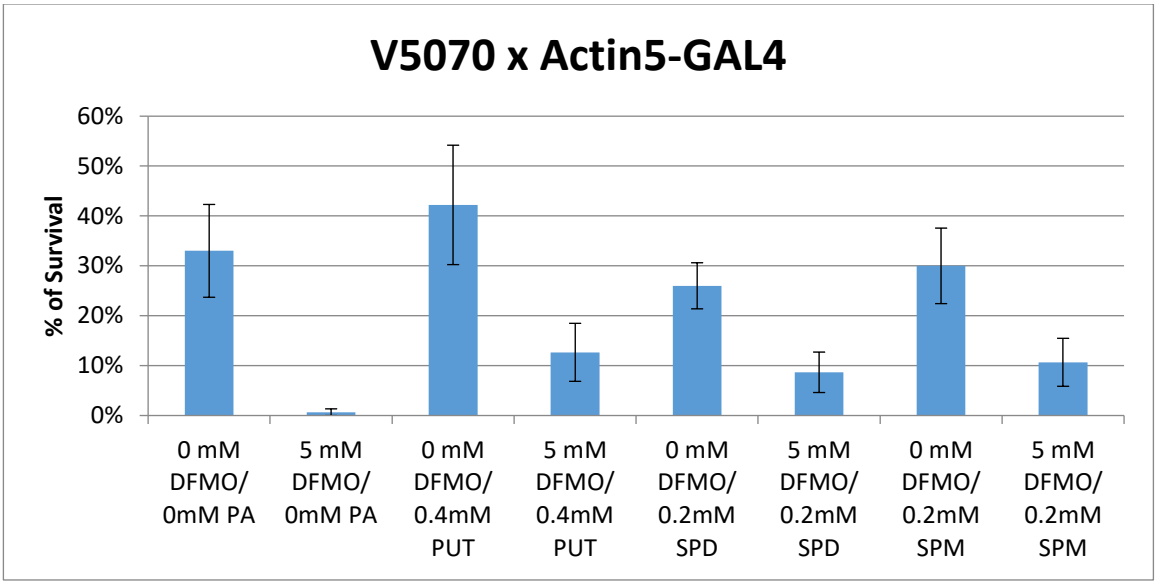

Figure 48 Rescue DFMO inhibition by native polyamines at minimum concentration in whole animals of Sulfateless RNAi (V5070) driven by Actin5-GAL4 (pupa data).

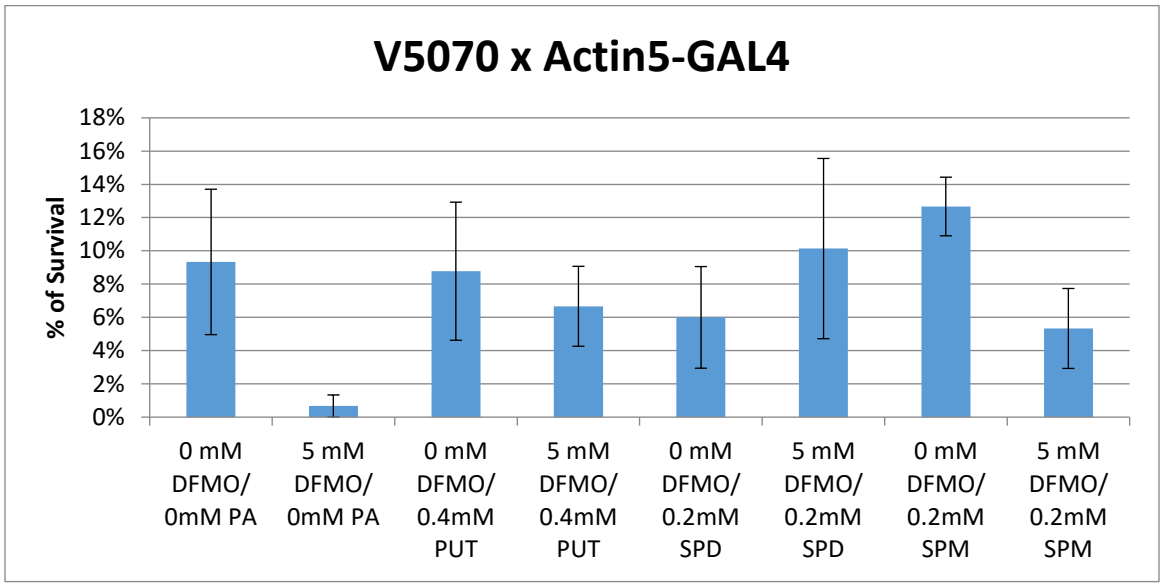

Figure 49 Rescue DFMO inhibition by native polyamines at minimum concentration in whole animals of Sulfateless RNAi (V5070) driven by Actin5-GAL4 (pupa data)-Repeat.

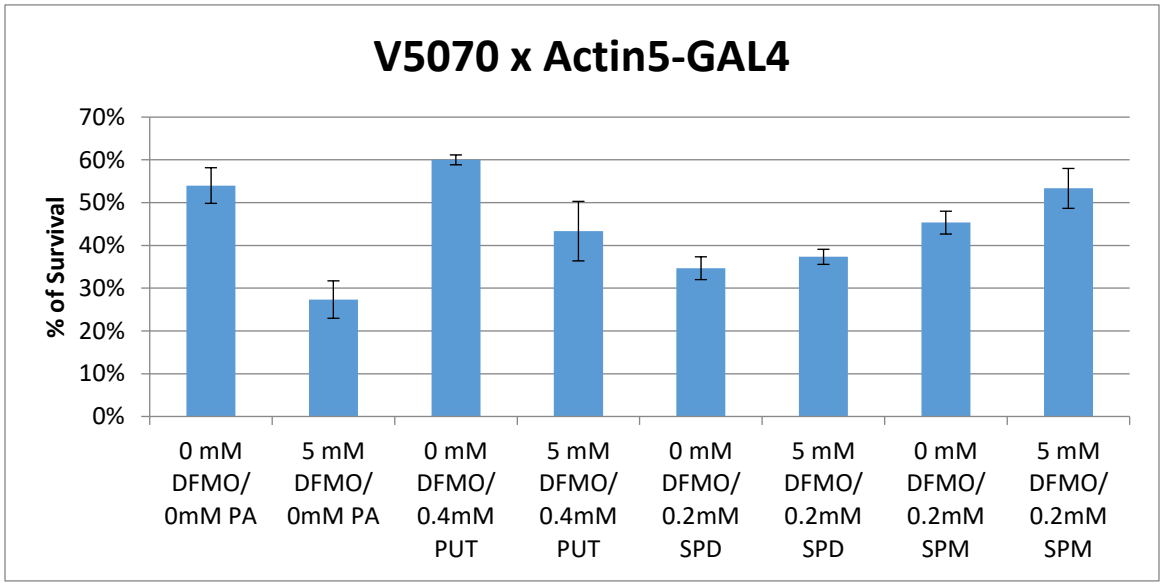

Figure 50 Rescue DFMO inhibition by native polyamines at minimum concentration in whole animals of Sulfateless RNAi (V5070) driven by Actin5-GAL4 (pupa data) at 18^0C.

6.2 BL34601: y^1scv^1;+;UAS-sulfateless RNAi (TRiP)

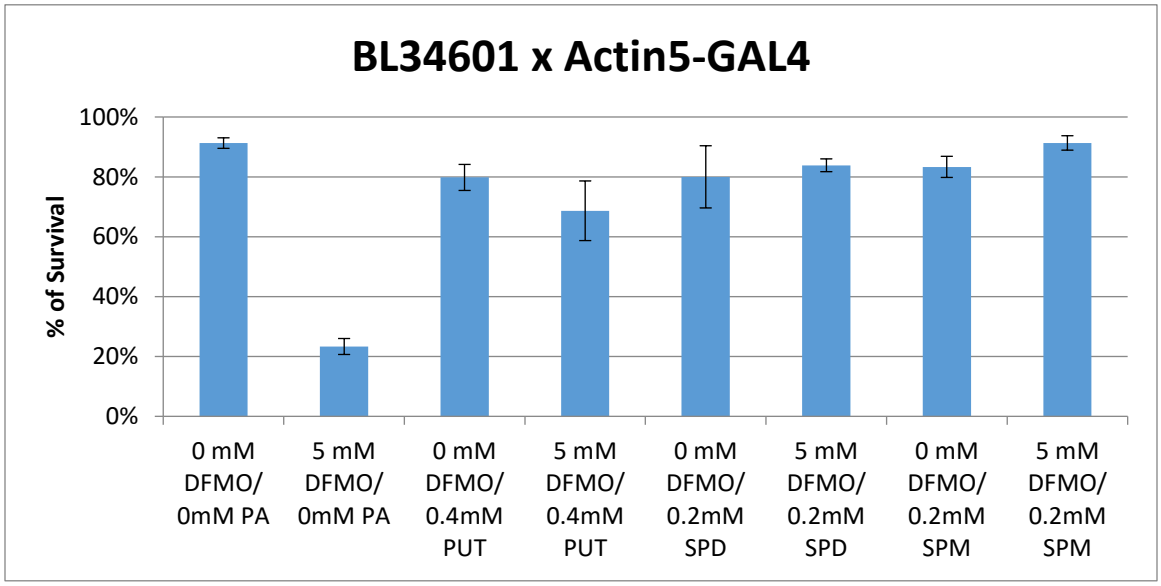

Figure 51 Rescue DFMO inhibition by native polyamines at minimum concentration in whole animals of Sulfateless RNAi (BL34601) driven by Actin5-GAL4 (pupa data).

7. *Hsepi Mutant: BL13498- y^1w^{67c23}; Hsepi [KG02877]*

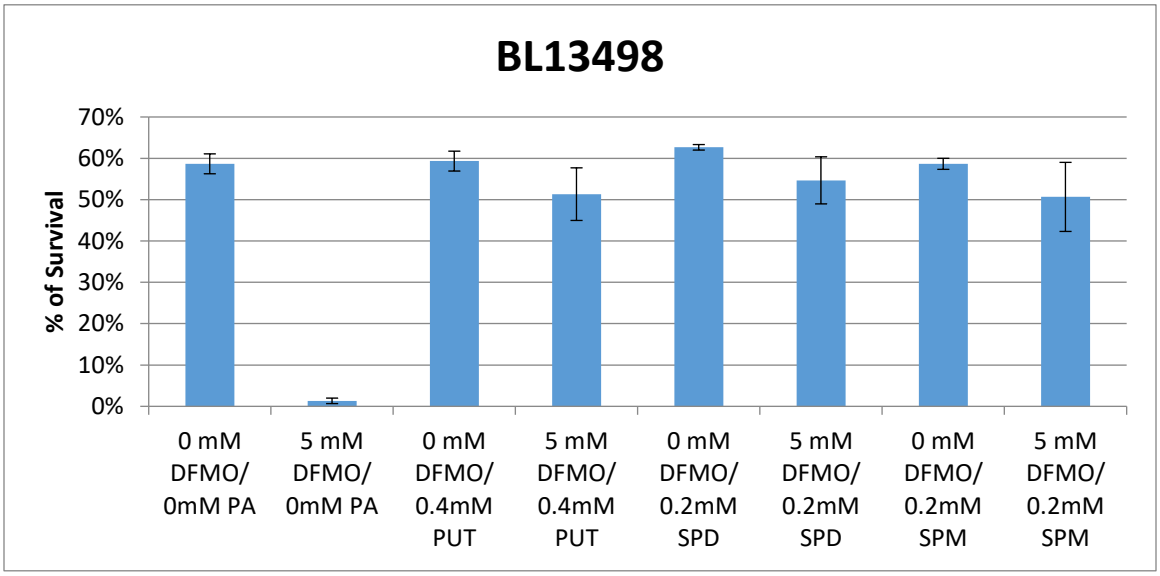

Figure 52 Rescue DFMO inhibition by native polyamines at minimum concentration in whole animals of Hsepi mutant (BL13498).

Part III: Result of Testing Nitric Oxide Synthase (NOS), Scaffold Attachment Factor B (SafB) and Huntingtin Interacting Protein (Hip1) Genes for Involvement in Polyamine Transport Using Whole Animal Method

Three other genes were tested for involvement in polyamine transport in *Drosophila*: Nitric oxide synthase (NOS), Scaffold attachment factor B (SafB), Huntingtin interacting protein (Hip1). In this study both RNAi stocks and insertional mutants were tested if stocks are available.

1. Nitric Oxide Synthase (NOS)

1.1 RNAi Stock: BL28792: y^1v^1;+; NOS RNAi

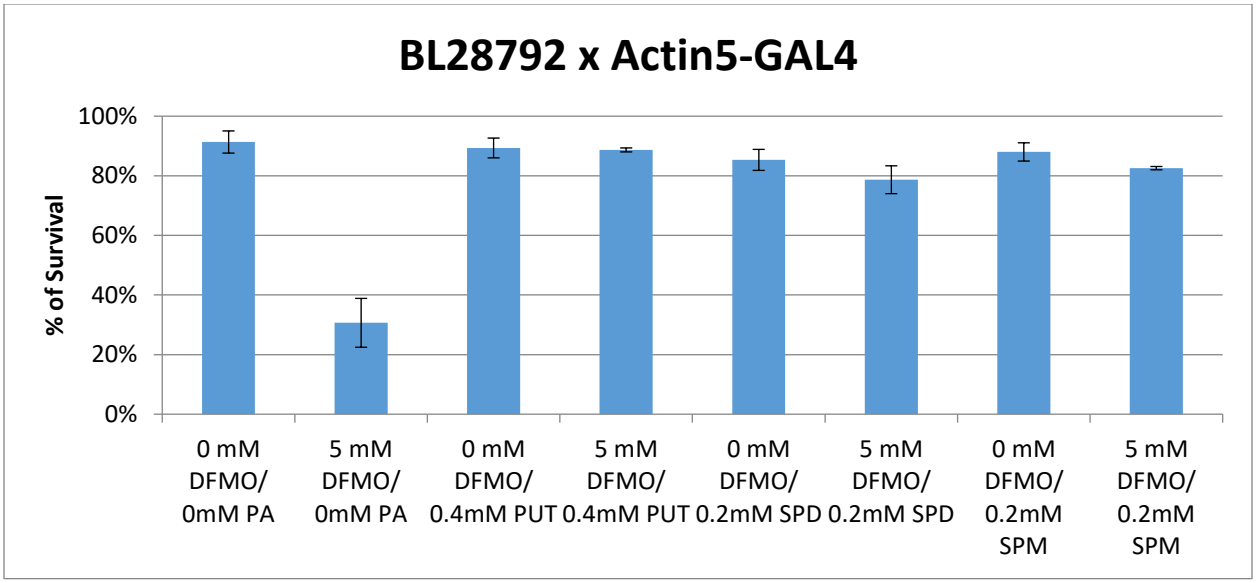

Figure 53 Rescue DFMO inhibition by native polyamines at minimum concentration in whole animals of NOS RNAi (BL28792) driven by Actin5-GAL4 (pupa data).

1.2 Mutant: BL18555- w^{1118}; NOS^{f02469}

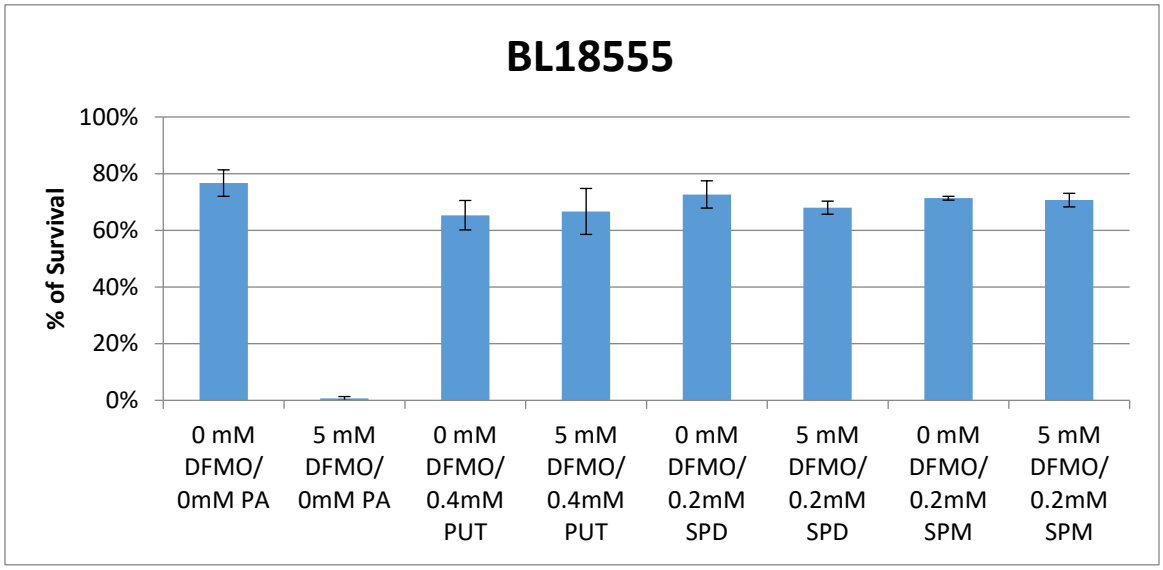

Figure 54 Rescue DFMO inhibition by native polyamines at minimum concentration in whole animals of NOS mutant (BL18555).

2. *Huntingtin Interacting Protein (Hip1)*

2.1 RNAi Stocks: BL32504, BL38377

i. BL32504- y^1scv^1;+; Hip1 RNAi

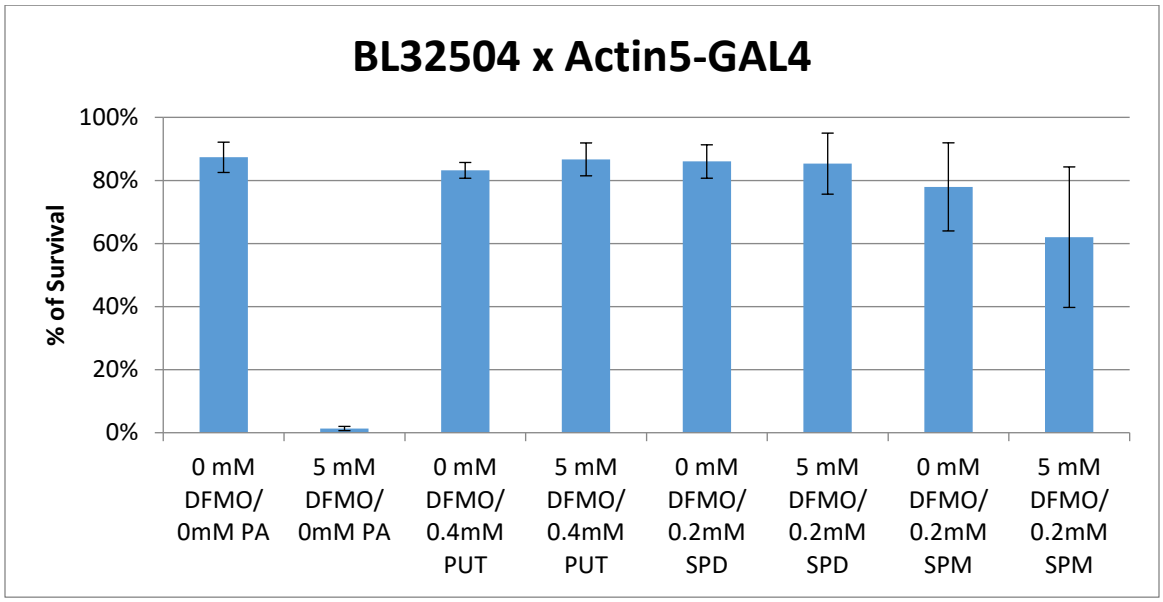

Figure 55 Rescue DFMO inhibition by native polyamines at minimum concentration in whole animals of Hip1 RNAi (BL32504) driven by Actin5-GAL4.

ii. BL38377- y^1v^1;+; Hip1 RNAi

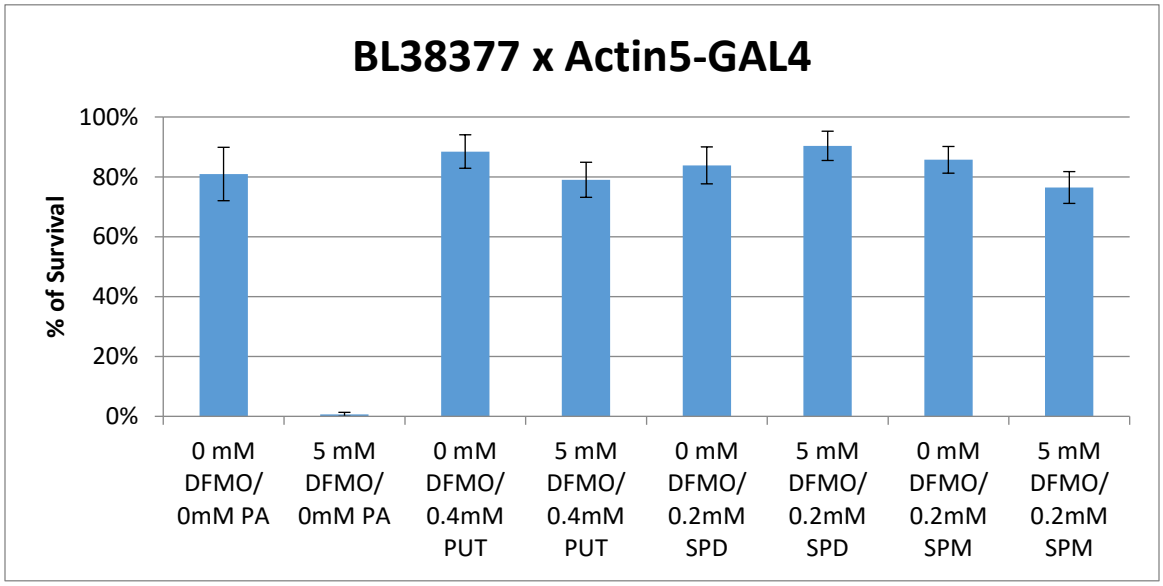

Figure 56 Rescue DFMO inhibition by native polyamines at minimum concentration in whole animals of Hip1 RNAi (BL38377) driven by Actin5-GAL4.

2.2 Hip1 Mutant: BL42355- y^1w; Hip1 [M105905]

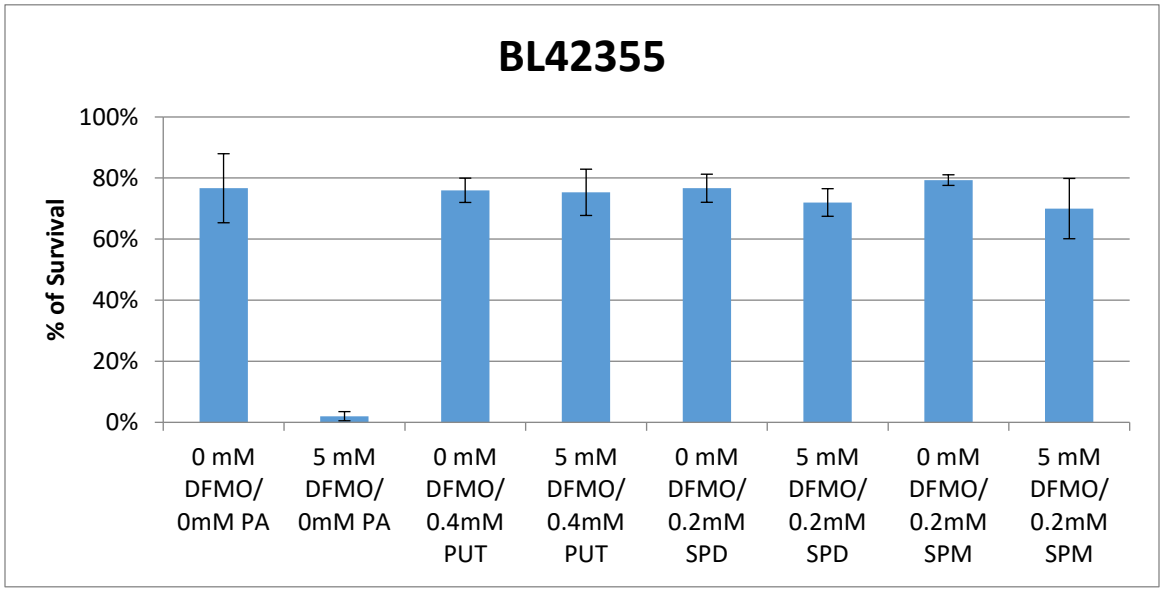

Figure 57 Rescue DFMO inhibition by native polyamines at minimum concentration in whole animals of Hip1 mutant (BL42355).

3. *SafB Mutant: BL32026- w^{1118}; +; Saf-$B^{[G16146]}$*

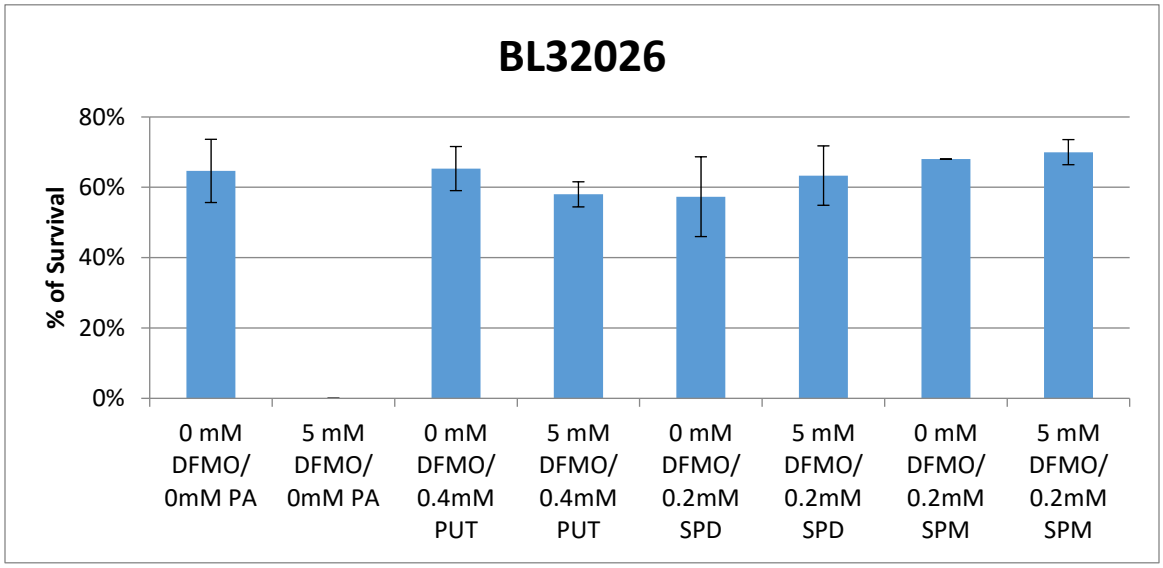

Figure 58 Rescue DFMO inhibition by native polyamines at minimum concentration in whole animals of SafB mutant (BL32026).

APPENDIX B: COPYRIGHT PERMISSION

Cambridge University Press License

This Agreement between Minpei Wang ("You") and Cambridge University Press ("Cambridge University Press") consists of your license details and the terms and conditions provided by Cambridge University Press and Copyright Clearance Center.

License Number 4135700494812

License date Jun 24, 2017

Licensed Content Publisher Cambridge University Press

Licensed Content Publication Expert Reviews in Molecular Medicine

Licensed Content Title Polyamines and cancer: implications for chemotherapy and chemoprevention

Licensed Content Author Shannon L. Nowotarski, Patrick M. Woster, Robert A. Casero

Licensed Content Date Sep 29, 2012

Licensed Content Volume 15

Licensed Content Issue undefined

Start page 3

End page undefined

Type of Use Dissertation/Thesis

Requestor type Not-for-profit

Portion Text extract

Number of pages requested 1

Order reference number

Territory for reuse World

Title of your thesis / dissertation A CHEMICAL AND GENETIC APPROACH TO STUDY THE POLYAMINE TRANSPORT SYSTEM IN *DROSOPHILA*

Expected completion date Apr 2017

Estimated size(pages) 150

Requestor Location Minpei Wang 2660 Stanmore Ct. ORLANDO, FL 32817 United States

Attn: Minpei Wang

Publisher Tax ID GB823847609

Billing Type Invoice

Billing Address Minpei Wang 2660 Stanmore Ct. ORLANDO, FL 32817 United States

Attn: Minpei Wang

Total 0.00 USD

Springer License I

This Agreement between Minpei Wang ("You") and Springer ("Springer") consists of your license details and the terms and conditions provided by Springer and Copyright Clearance Center.

License Number 4023990003169

License date Jan 07, 2017

Licensed Content Publisher Springer

Licensed Content Publication Amino Acids

Licensed Content Title Recent advances in the molecular biology of metazoan polyamine transport

Licensed Content Author R. Poulin

Licensed Content Date Jan 1, 2011

Licensed Content Volume Number 42

Licensed Content Issue Number 2

Type of Use Thesis/Dissertation

Portion Figures/tables/illustrations

Number of figures/tables/illustrations 1

Author of this Springer article No

Order reference number

Original figure numbers Figure 1

Title of your thesis / dissertation A CHEMICAL AND GENETIC APPROACH TO STUDY THE POLYAMINE TRANSPORT SYSTEM IN *DROSOPHILA*

Expected completion date Apr 2017

Estimated size (pages) 150

Requestor Location Minpei Wang 2660 Stanmore Ct. ORLANDO, FL 32817 Unite States

Attn: Minpei Wang

Billing Type Invoice

Billing Address Minpei Wang 2660 Stanmore Ct. ORLANDO, FL 32817 Unite States

Attn: Minpei Wang

Total 0.00 USD

Springer License II

This Agreement between Minpei Wang ("You") and Springer ("Springer") consists of your license details and the terms and conditions provided by Springer and Copyright Clearance Center.

License Number 4023980987690

License date Jan 07, 2017

Licensed Content Publisher Springer

Licensed Content Publication Amino Acids

Licensed Content Title Polyamines and membrane transporters

Licensed Content Author Ahmed A. Abdulhussein

Licensed Content Date Jan 1, 2013

Licensed Content Volume Number 46

Licensed Content Issue Number 3

Type of Use Thesis/Dissertation

Portion Figures/tables/illustrations

Number of figures/tables/illustrations 1

Author of this Springer article No

Order reference number

Original figure numbers table 1

Title of your thesis / dissertation A CHEMICAL AND GENETIC APPROACH TO STUDY THE POLYAMINE TRANSPORT SYSTEM IN *DROSOPHILA*

Expected completion date Apr 2017

Estimated size(pages) 150

Requestor Location Minpei Wang 2660 Stanmore Ct ORLANDO, FL 32817 United States

Attn: Minpei Wang

Billing Type Invoice

Billing Address Minpei Wang 2660 Stanmore Ct ORLANDO, FL 32817 United States

Attn: Minpei Wang

Total 0.00 USD